Université du Sud Toulon - Var

HABILITATION A DIRIGER DES RECHERCHES

Discipline : Mathématiques

Analyse et approximation numérique de quelques modèles macroscopiques de trafic routier

soutenue publiquement le 15 mai 2009

par

Paola Goatin

après avis des rapporteurs :

M. Constantine DAFERMOS	Professeur, Brown University
M. Thierry GALLOUËT	Professeur, Université de Provence Aix-Marseille I
M. Michel RASCLE	Professeur, Université de Nice Sophia Antipolis

et devant le jury composé de :

M. Thierry GALLOUËT	Professeur, Université de Provence Aix-Marseille I
M. Cédric GALUSINSKI	Professeur, Université du Sud Toulon - Var
M. Jean-Patrick LEBACQUE	Ingénieur général des Ponts et Chaussées, INRETS-GRETIA
M. Philippe G. LEFLOCH	Directeur de recherche, CNRS
M. Michel RASCLE	Professeur, Université de Nice Sophia Antipolis

Remerciements

J'exprime ma plus grande gratitude à Constantine Dafermos, Thierry Gallouët et Michel Rascle, qui ont accepté d'être rapporteurs de cette habilitation. Je les remercie très sincèrement pour le temps qu'ils m'ont consacré et pour l'intêret qu'ils ont montré pour mon travail de recherche. Je remercie aussi vivement Cédric Galusinski, Jean-Patrick Lebacque et Philippe LeFloch d'avoir accepté de faire partie du jury.

Mes remerciements vont ensuite à mes collaborateurs, qui m'ont beaucoup appris au fil des années. Parmi eux, je voudrais mentionner Rinaldo Colombo, Christophe Chalons, Nicolas Seguin, Benedetto Piccoli et Boris Andreianov, sans lesquels ce travail n'aurait pas vu le jour. Travailler à leur côtés (ou à distance!) est toujours un grand plaisir et une source de motivation et d'enrichissement.

Je voudrais inclure dans ces remerciements l'ensemble des membres du Laboratoire IMATH, qui m'ont accueillie dans leur équipe et m'ont toujours apporté leur soutien. Une pensée particulière s'adresse a mes collègues et au personnel de l'ISITV, qui m'ont énormément aidée durant ces années, qui par sa collaboration directe, qui par ses conseils, qui par son aide administrative ou technique.

Je suis très reconnaissante envers Jean-Antoine Désidéri, qui m'a encouragée à passer cette habilitation et a été à l'origine de ma délégation à l'INRIA Sophia Antipolis - Méditerranée. L'accueil de l'équipe OPALE m'a fait bénéficier de conditions de travail idéales, et ce mémoire lui doit beaucoup.

Enfin, un grand "GRAZIE" va à Michele, qui n'a jamais cessé de m'apporter son soutien et son aide précieux.

Table des matières

1

Introduction

Ce mémoire présente une partie de mon activité de recherche postérieure à la thèse, soutenue en 2000. Plus particulièrement, je décris ici les résultats obtenus à partir de 2004, en tant que Maître de Conférences à l'Institut des Sciences de l'Ingénieur de Toulon et du Var et membre de l'actuel Institut de mathématiques de Toulon et du Var.

Mon travail de recherche est centré autour des solutions faibles des systèmes hyperboliques de lois de conservation. Je me suis intéressée à l'existence, l'unicité et la stabilité des solutions du problème de Cauchy et aux limites, avec applications à la dynamique des fluides et des matériaux compressibles, le trafic routier et la théorie mathématique du contrôle.
De 2000 à 2003, j'ai eu des contrats postdoctoraux (CNRS et Communauté Européenne) au Centre de Mathématiques Appliquées de l'Ecole Polytechnique, sous la direction de P.G. LeFloch. Pendant cette période, j'ai étudié la stabilité en norme $\mathbf{L^1}$ des solutions entropiques des systèmes de lois de conservation [A8, A10], ainsi que certains systèmes avec termes source et résonants [A6, A7, A9].
J'ai commencé à m'intéresser à la modélisation du trafic routier lors du séjour de R.M. Colombo en qualité de professeur invité à l'Université de Toulon en 2004. Ce mémoire est une synthèse des résultats que j'ai obtenus dans ce domaine.

L'intérêt des mathématiciens appliqués pour la dynamique du trafic routier et pédestre a considérablement augmenté ces dernières années. La modélisation associée peut se faire à différentes échelles : on distingue ainsi des modèles de description microscopiques (particulaires), mésoscopiques (cinétiques) et macroscopiques (dynamique des fluides). Les modèles macroscopiques de trafic routier représentent une application de la théorie des lois de conservation. Dans ce contexte, plusieurs modèles ont été proposés. Je me suis principalement intéressée au modèle de trafic routier avec transition de phase introduit par R.M. Colombo [40] dans le but de retrouver les relations observées expérimentalement entre le flux et la densité. Le modèle consiste en une loi de conservation scalaire qui décrit l'écoulement "fluide", et un système de deux lois de conservation (il s'agit d'un système de Temple) pour décrire le comportement "congestionné". Le couplage est obtenu par l'introduction d'une transition de phase entre la phase fluide et la phase

congestionnée.

Dans [A4] nous montrons un résultat de stabilité pour le problème de Cauchy et pour le problème aux limites, pour toute donnée à variation totale bornée. Du point de vue théorique, il s'agit du premier exemple d'un résultat de bonne position globale pour des lois de conservation avec transition de phase, qui est indépendant du nombre de transitions dans la solution. Ce résultat est également important du point de vue des applications aux problèmes de contrôle et d'optimisation.

Le même modèle peut être utilisé sur un réseau représentant un ensemble de routes avec des jonctions. Ce problème fait l'objet d'une étude en collaboration avec R.M. Colombo et B. Piccoli [P1]. Dans ce cas, le problème consiste à définir correctement le solveur de Riemann au niveau des jonctions, de façon à obtenir l'unicité de la solution. En utilisant la méthode de suivi de fronts, nous démontrons l'existence globale des solutions.

En m'inspirant du modèle de Colombo, j'ai proposé dans [A5] un couplage du modèle 2×2 de Aw et Rascle [8] et du modèle LWR [86, 91], en introduisant une transition de phase entre le flux fluide et le flux congestionné. Ceci permet un meilleur accord avec les données expérimentales, et présente l'avantage de corriger certains défauts du modèle 2×2 d'origine [8]. D'autres couplages et une description générale des modèles avec transition de phase sont présentés dans [P3].

D'un point de vue numérique, la présence des transitions de phase rend difficile l'utilisation des méthodes classiques, comme par exemple la méthode de Godunov. Dans les faits, puisque le domaine du modèle n'est pas convexe (il n'est même pas connexe), l'étape de projection inhérente à la méthode de Godunov donne généralement des valeurs qui n'appartiennent pas au domaine. En collaboration avec C. Chalons [A1], nous avons modifié l'algorithme habituel de façon à contourner ce problème. Plus précisément, on introduit des cellules modifiées en suivant les fronts des transitions de phase. Ainsi, on effectue l'étape de projection sur des valeurs qui appartiennent à une seule et même phase. Le retour aux cellules initiales se fait par une stratégie d'échantillonnage. Une extension à l'ordre deux en temps et en espace est également proposée.

Dans le même esprit, dans [A2] nous avons proposé un algorithme de type Transport-équilibre pour assurer une bonne approximation des discontinuités de contact du modèle Aw-Rascle. L'objectif est de supprimer les oscillations importantes générées par la méthode de Godunov à proximité de ces discontinuités. Pour cela, nous traitons séparément les discontinuités de contact en utilisant une stratégie d'échantillonnage a la Glimm, et continuons à utiliser le schéma de Godunov pour les autres ondes. Comme cela est attendu, l'algorithme obtenu n'est pas conservatif, mais les tests effectués semblent montrer que la convergence vers la solution exacte est garantie. Par ailleurs, ce qui nous paraît à la fois très intéressant et nouveau dans ce contexte, c'est la possibilité de démontrer une propriété de consistance forte de la méthode, ainsi que la validité d'un principe du maximum sur les deux invariants de Riemann.

Un autre problème issu de la modélisation du trafic routier, intéressant dans un cadre plus général, est l'étude d'une loi de conservation scalaire (ou plus généralement d'un système de lois de conservation) soumise à une contrainte unilatérale en un point (comme dans le cas d'un péage) ou sur un intervalle (comme dans le cas d'une limite

de flux ou de vitesse). Dans [A3], un premier résultat d'existence et de stabilité par rapport à la donnée initiale est obtenu par la méthode de suivi de fronts dans un cadre **BV**. Le point fondamental de cette construction est le choix d'un solveur de Riemann non classique et la disponibilité d'un critère d'entropie. Ensuite, nous construisons une approximation du problème par des lois de conservation avec flux discontinu en temps et en espace, comme dans [76, 77, 37]. Par un passage à la limite, nous retrouvons la solution faible entropique du problème originel. Cela renforce le premier résultat.
Des lois de conservation avec contraintes unilatérales ont déjà été étudiées dans la littérature (voir [16], et ses références), mais avec des motivations et des résultats différents. A notre connaissance, le problème que nous avons proposé n'avait jamais été étudié.

La construction d'un schéma numérique pour le problème avec contrainte a fait l'objet d'une étude en collaboration avec B. Andreianov et N. Seguin [P4]. Nous montrons d'abord que le problème peut être interprété du point de vue de la théorie des lois de conservation avec flux discontinu développée par Adimurthi et al. [3] et Bürger et al. [26]. Cela nous permet de reformuler la définition de solution entropique par des conditions qui s'avèrent plus adaptées à l'étude de la convergence des schémas numériques. Par ailleurs, nous étendons les résultats d'existence et d'unicité au cadre $\mathbf{L}^\infty$.
Le schéma numérique pour le problème avec contrainte est construit à partir d'un schéma volumes finis monotone général. La convergence est démontrée en utilisant une notion nouvelle de solution processus [61].

Les problèmes avec contrainte unilatérale trouvent une application dans la modélisation du trafic routier et les mouvements de foule. Des travaux sont en cours dans cette direction en collaboration avec R.M. Colombo et M.D. Rosini. Les premiers résultats sont présentés dans [P2].

La plupart des résultats analytiques présentés dans ce mémoire ont été obtenus en appliquant la méthode du suivi des fronts. Cette technique, qui permet de construire des solutions approchées constantes par morceaux, a été introduite dans les papiers de Dafermos [52] pour les équations scalaires, et DiPerna [57] pour les systèmes 2×2. Bressan [20] et Risebro [92] ont généralisé cette technique aux systémes $n \times n$. La méthode du suivi des fronts génère des approximations très précises, et permet de bien capturer les caractéristiques des solutions.

L'étude de la stabilité des solutions a été conduit selon l'approche du *semigroupe* introduit par Bressan dans [21], puis développé dans nombreuses publications, en particulier dans [23, 24].

Afin de permettre une plus grande accessibilité pour tous les rapporteurs, les autres chapitres de ce mémoire ont été rédigés en anglais.

1.1 Liste des travaux posterieurs à la thèse

Publications dans des revues avec comité de lecture

[A1] C. Chalons et **P. Goatin**, *"Godunov scheme and sampling technique for computing phase transitions in traffic flow modeling"*, Interfaces and Free Boundaries, 10 (2) (2008), 195-219.

[A2] C. Chalons et **P. Goatin**, *"Transport-Equilibrium schemes for computing contact discontinuities in traffic flow modeling"*, Comm. Math. Sci. 5 (3) (2007), 533-551.

[A3] R.M. Colombo et **P. Goatin**, *"A well posed conservation law with a variable unilateral constraint"*, J. Differential Equations 234 (2007), 654-675.

[A4] R.M. Colombo, **P. Goatin** et F. Priuli, *"Global well posedness of a traffic flow model with phase transitions"*, Nonlinear Anal. Ser. A: Theory, Methods & Applications 66 (2007) 11, 2413-2426.

[A5] **P. Goatin**, *" The Aw-Rascle vehicular traffic flow model with phase transitions"*, Math. Comput. Modeling. 44 (2006), 287-303.

[A6] **P. Goatin** et P.G. LeFloch, *" The Riemann problem for a class of resonant hyperbolic systems of balance laws"*, Ann. Inst. H. Poincaré (C) Nonlinear Analysis 21 (2004) 6, 881-902.

[A7] **P. Goatin** et L.Gosse, *"Decay of positive waves for $n \times n$ hyperbolic systems of balance laws"*, Proc. AMS. 132 (2004) 6, 1627-1637.

[A8] **P. Goatin** et P.G. LeFloch, *" L^1 continuous dependence for the Euler equations of compressible fluids dynamics"*, Comm. Pure Appl. Anal. 2 (2003) 1, 107-137.

[A9] **P. Goatin**, *"One sided estimates and uniqueness for hyperbolic systems of balance laws"*, Math. Models Methods Appl. Sci. 13 (2003) 4, 527-543.

[A10] **P. Goatin** et P.G. LeFloch, *"Sharp L^1 continuous dependence of solutions of bounded variation for hyperbolic systems of conservation laws"*, Arch. Rational Mech. Anal. 157 (2001) 1, 35-73.

Actes de congrès avec comité de lecture

[C1] **P. Goatin**, *"Traffic flow model with phase transitions on road networks"*, Netw. Heterog. Media, à paraître.

[C2] **P. Goatin**, *"Analysis and numerical approximation of a traffic flow model with phase transitions"*, Oberwolfach Reports, Vol. 5 (1) (2008), 537–540.

[C3] C. Chalons et **P. Goatin**, *"Computing phase transitions arising in traffic flow modeling"*, "Hyperbolic problems: theory, numerics, applications. Proceedings of the eleventh international conference in Lyon, July 2006", Springer (2008), 559–566.

[C4] **P. Goatin**, *"Modeling a bottleneck by the Aw-Rascle model with phase transitions"*, Traffic and Granular Flow '05, Springer (2007), 587–593.

[C5] R.M. Colombo et **P. Goatin**, *"Traffic flow models with phase transitions"*, Flow Turbulence Combust. 76 (2006), 383–390.

Preprints

[P1] R.M. Colombo, **P. Goatin** et B. Piccoli, *"Road network with phase transitions"*, soumis.

[P2] R.M. Colombo, **P. Goatin** et M.D. Rosini, *"Conservation laws with unilateral constraints in traffic modeling"*, soumis à Communications to SIMAI Congress.

[P3] S. Blandin, D. Work, **P. Goatin**, B. Piccoli et A. Bayen, *"A general phase transition model for vehicular traffic"*, soumis.

[P4] B. Andreianov, **P. Goatin** et N. Seguin, *"Finite volume schemes for locally constrained conservation laws"*, soumis.

2

Vehicular traffic flow models with phase transitions

Macroscopic traffic flow models are derived from fluid dynamics, and are intended to describe the evolution of macroscopic variables such as the density and the mean velocity of vehicles. To this aim, the road is represented by an (infinite) line, and car's size is assumed negligible compared to the road length.

The first model of this type was proposed by Lighthill and Whitham [86], and independently by Richards [91], and it is known as the LWR model. It consists in a scalar equation that expresses the conservation of the number of cars:

$$\partial_t \rho + \partial_x f(\rho) = 0, \tag{2.1}$$

where $\rho = \rho(t, x)$ is the mean traffic density, usually intended as the number of vehicles per unit length, and $f(\rho)$ is the traffic flow, i.e. the number of vehicles per time unit. In scalar models, also called first order models, the flux is assumed to depend only on the density, and can be expressed as

$$f(\rho) = \rho v(\rho),$$

where the mean velocity v is a non-negative, non-increasing function, but more complex closure relations, involving the density gradient, can be considered (see [15] and references therein). However, this phenomenological relation is valid in steady state conditions, and it is not realistic in more complicate situations. In particular, as shown in Fig. 2.1, the fundamental diagram of equation (2.1) in the (ρ, f)-plane does not qualitatively match the experimental data at high traffic densities (we refer the reader to the paper of Helbing [71, Section II] for a description of the features recovered by a detailed analysis of the fundamental diagram). The experimental data suggest that a realistic traffic flow model should exhibit two qualitative different behaviors:

1. for low densities, the flow is *free* and can be described by a scalar model of LWR type;

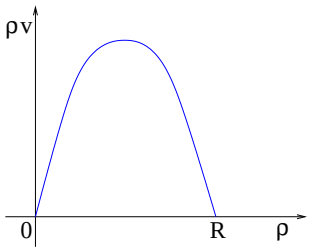

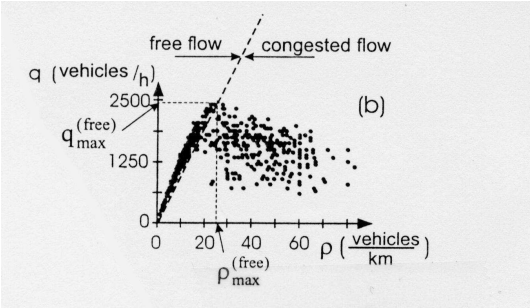

Figure 2.1: Left: standard flow for the LWR model. Right: experimental data, taken from [81]; q denotes the flux ρv.

2. when density increases, the flow becomes *congested* and covers a 2-dimensional domain in the fundamental diagram: a "second order" model (with two equations) seems more appropriate to describe this dynamic.

A first prototype of second order models was proposed by Payne [90] and Whitham [101]:

$$\begin{cases} \partial_t \rho + \partial_x(\rho v) = 0\,, \\ \partial_t(\rho v) + \partial_x(\rho v^2 + p(\rho))) = 0\,, \end{cases} \tag{2.2}$$

where $p(\rho)$ is a "pressure" term in analogy to the equations of gas dynamics. The main drawback of this model is that it does not satisfy the two principles usually required for a traffic flow model, that are:

a) drivers react to what happens in front of them, thus no information travels faster than cars;

b) density ρ and velocity v must stay non-negative and bounded.

It appears that the Payne-Whitham model (2.2) may display negative velocities. Moreover, the eigenvalues of the system (2.2) are $\lambda_{1,2} = v \pm \sqrt{p'(\rho)}$, so part of the informations travels with speed always bigger than the cars' one (we refer the reader to Daganzo's paper [54]). These failures have been corrected by Aw and Rascle [8], by replacing the spatial derivative ∂_x of the pressure in the second equation by the convective derivative $\partial_t + v\partial_x$, getting

$$\begin{cases} \partial_t \rho + \partial_x(\rho v) = 0\,, \\ \partial_t(\rho(v + p(\rho)) + \partial_x(\rho v(v + p(\rho))) = 0\,. \end{cases} \tag{2.3}$$

Thus, the quantity $p(\rho)$ plays the role of an "anticipation factor" that takes into account the reactions of the drives to what happens in front of them. Nevertheless, as pointed out by the authors, the Aw-Rascle model is not well-posed near the vacuum $\rho = 0$. This fact is intended to reproduce instabilities that might appear in real situations at low car densities, but it is a source of difficulties from the mathematical point of view. Global

well posedness is needed for analytical and numerical results.
Another second order model has been proposed by Colombo in [39]:

$$\begin{cases} \partial_t \rho + \partial_x(\rho v) = 0\,, \\ \partial_t q + \partial_x((q-Q)v) = 0\,, \end{cases} \tag{2.4}$$

where q is a sort of "weighted momentum" in analogy to gas dynamics, Q is a parameter depending on the road under consideration and a closure law for $v = v(\rho, q)$ is given. This model displays a maximal car density, that is the only positive density at which velocity is zero. In other words, whenever a queue at zero speed forms, the maximal density is reached. Viceversa, cars cannot stop if maximal density is not reached.

In order to describe the different behaviors observed between free and congested traffic, some models with phase transitions have been introduced [59, 40, 68, 19]. In this Chapter, I describe the models that I have studied and the analytical results that I have obtained.

A *phase transition* is a discontinuity separating a state of free traffic from one in the congested phase.

In the following I will denote by Ω_f (respectively Ω_c) the domain of free (respectively congested) data, and I will use the unified notation

$$\partial_t \mathbf{u} + \partial_x \mathbf{f}(\mathbf{u}) = 0\,, \qquad \mathbf{u} \in \Omega = \Omega_f \cup \Omega_c\,, \tag{2.5}$$

for the models of phase transitions under consideration, with

$$\begin{cases} \mathbf{u} = \mathbf{u}_f \quad \text{and} \quad \mathbf{f}(\mathbf{u}) = \mathbf{f}_f(\mathbf{u}_f)\,, & \text{if} \quad \mathbf{u} \in \Omega_f\,, \\ \mathbf{u} = \mathbf{u}_c \quad \text{and} \quad \mathbf{f}(\mathbf{u}) = \mathbf{f}_c(\mathbf{u}_c)\,, & \text{if} \quad \mathbf{u} \in \Omega_c\,. \end{cases}$$

It is important to keep in mind that $\mathbf{u}$ and $\mathbf{f}(\mathbf{u})$ have not the same meaning in the free phase and in the congested phase.

2.1 The scalar model

In [59] the authors select a variation of the *"Edie formulation"* [60] as the best among several traffic models, see also [88] or [102, Model B]. Essentially, it consists of the Lighthill-Whitham [86] and Richards [91] (LWR) model with a fundamental diagram as in Fig. 2.2. Then, the conservation of the total number of vehicles along any road segment reads

$$\partial_t \rho + \partial_x \left(\rho\, v(\rho)\right) = 0\,, \tag{2.6}$$

where the speed v and the flow ρv are defined on a *disconnected* set, its two connected components being two disjoint intervals representing the free and the congested phases.

Proposition 2.1.1 *Let $\Omega_f = [0, \check{R}]$, $\Omega_c = [\hat{R}, R]$, with $0 < \check{R} < \hat{R} < R$, and $v\colon \Omega_f \cup \Omega_c \mapsto \mathbb{R}$ be smooth, decreasing and such that $v(R) = 0$. Then, for all $\rho_o \in \mathbf{L^1}(\mathbb{R}; \Omega_f \cup \Omega_c)$, (2.6) admits a unique weak entropy solution $\rho \in \mathbf{C^0}\left(\mathbb{R}^+; \mathbf{L^1}(\mathbb{R}; \Omega_f \cup \Omega_c)\right)$ attaining ρ_o as initial datum and which is non expansive with respect to the $\mathbf{L^1}$ norm.*

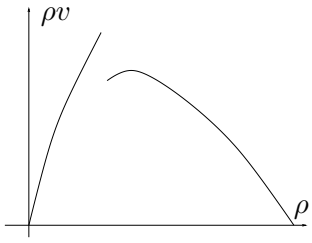

Figure 2.2: The fundamental diagram in the Edie hypothesis, see [59, 60].

Above, R is the maximal car density, which corresponds to a traffic jam. Note that the invariance of $\Omega_f \cup \Omega_c$ implies that density and speed remain positive and bounded. The proof of Proposition 2.1.1 follows from the slightly more general Proposition 2.1.2 below.

Let $f\colon \Omega \mapsto \mathbb{R}$ be smooth with $\Omega = \Omega_f \cup \Omega_c$. The case of more than two phases is entirely similar. The standard Kružkov Theorem, see for instance [22, § 6.2 and 6.3] is directly extended to the present situation.

Proposition 2.1.2 *Let $f\colon \Omega \mapsto \mathbb{R}$ be locally Lipschitz. Then,*

1. *for all $u_0 \in \mathbf{L^1}(\mathbb{R};\Omega) \cap \mathbf{BV}(\mathbb{R};\Omega)$, the Cauchy problem (2.6) with initial datum u_0 admits a weak entropy solution $u\colon \mathbb{R}^+ \times \mathbb{R} \mapsto \mathbb{R}$ with*

$$\mathbf{TV}\left(u(t,\cdot)\right) \leq \mathbf{TV}(u_0) \quad \text{and} \quad \|u(t,\cdot)\|_{\mathbf{L}^\infty} \leq \|u_0\|_{\mathbf{L}^\infty} \quad \forall t \geq 0\,;$$

2. *if u_0 and w_0 are in $\mathbf{L^1}(\mathbb{R};\Omega) \cap \mathbf{BV}(\mathbb{R};\Omega)$, then for all $t \geq 0$*

$$\|u(t,\cdot) - w(t,\cdot)\|_{\mathbf{L^1}} \leq \|u_0 - w_0\|_{\mathbf{L^1}}\,;$$

Proof. It is straightforward to extend the proof in [22] to the present situation. Indeed, assume for simplicity that $\Omega_f = [a,b]$ and $\Omega_c = [c,d]$, with $-\infty < a \leq b < c \leq d < +\infty$, the other cases being entirely analogous. Consider the following extension $\bar{f}$ of f to the whole $\mathbb{R}$:

$$\bar{f}(u) = \begin{cases} f(a) & \text{if } u \in \,]-\infty, a[\\ f(u) & \text{if } u \in [a,b] \\ \dfrac{c-u}{c-b} f(b) + \dfrac{u-b}{c-b} f(c) & \text{if } u \in \,]b,c[\\ f(u) & \text{if } u \in [c,d] \\ f(d) & \text{if } u \in \,]d, +\infty[\end{cases}$$

Then, it is immediate to prove that if $u_0 \in \mathbf{L^1}(\mathbb{R},\Omega) \cap \mathbf{BV}(\mathbb{R},\Omega)$, then the weak entropy solution $u = u(t,x)$ of

$$\begin{cases} \partial_t u + \partial_x \bar{f}(u) = 0 \\ u(0,x) = u_0(x) \end{cases}$$

attains values in Ω. Indeed, if $u_0(\mathbb{R}) \subseteq [a,d]$, then also $u(t,\mathbb{R}) \in [a,d]$ for all $t \geq 0$ by the *"maximum principle"* [22, (iv), Theorem 6.3, Chapter 6]. Moreover, $u(t,x)$ is the limit of piecewise constant solutions $u^\nu(t,x)$ to conservation laws

$$\begin{cases} \partial_t u + \partial_x \bar{f}^\nu(u) = 0 \\ u(0,x) = u_0^\nu(x) \end{cases}$$

with $\bar{f}^\nu$ being a piecewise linear and continuous approximation of $\bar{f}$ and u_0^ν a piecewise constant approximation of u_0, see [22, § 6.1 and § 6.2]. For all ν, $\bar{f}^\nu$ can be chosen so that $\bar{f}^\nu(u) = \bar{f}(u)$ for $u \in [b,c]$. Hence, if $u_0^\nu(\mathbb{R})$ does not intersect $]b,c[$, also $u^\nu(t)$ does not attain values in $]b,c[$. □

I recall that in the present section we used Liu's entropy condition, see [53, § 8.4].

2.2 The 2×2 model of Colombo

In this section, I consider the model introduced in [40]. It consists of a scalar LWR model coupled with the 2×2 system (2.4) presented in [39]. The former applies to the states of free flow, while the latter to the congested states. More precisely, the model in [40] reads

$$\begin{array}{ll} \text{Free flow: } (\rho,q) \in \Omega_f & \text{Congested flow: } (\rho,q) \in \Omega_c \\ \partial_t \rho + \partial_x(\rho v) = 0 & \partial_t \rho + \partial_x(\rho v) = 0 \\ q = \rho V & \partial_t q + \partial_x((q-Q)v) = 0 \\ v = v_f(\rho) = \left(1 - \frac{\rho}{R}\right) V & v = v_c(\rho,q) = \left(1 - \frac{\rho}{R}\right) \frac{q}{\rho} \,. \end{array} \tag{2.7}$$

Using the notation (2.5), we set

$$\begin{cases} \mathbf{u} = (\rho,q) \quad \text{and} \quad \mathbf{f}(\mathbf{u}) = (\rho v_f(\rho), q v_f(\rho)) \,, & \text{if} \quad (\rho,q) \in \Omega_f \,, \\ \mathbf{u} = (\rho,q) \quad \text{and} \quad \mathbf{f}(\mathbf{u}) = (\rho v_c(\rho,q), (q-Q) v_c(\rho,q)) \,, & \text{if} \quad (\rho,q) \in \Omega_c \,. \end{cases}$$

Here, R is the maximal traffic density, V is the maximal traffic speed and Q is a parameter of the road under consideration related to the phenomenon of *wide jams*, see [40, 80]. The weighted linear momentum q is originally motivated by gas dynamics. It approximates the real flux ρv for ρ small compared to R.

It is assumed that if the initial data are entirely in the free (resp. congested) phase, then the solution will remain in the free (resp. congested) phase for all time. Thus Ω_f and Ω_c are chosen to be invariant sets for the corresponding equations. The resulting domain is given by $\Omega_f \cup \Omega_c$, where

$$\begin{aligned} \Omega_f &= \{(\rho,q) \in [0,R] \times [0,+\infty[\,:\, v_f(\rho) \geq V_f,\, q = \rho V\} \\ \Omega_c &= \left\{(\rho,q) \in [0,R] \times [0,+\infty[\,:\, v_c(\rho,q) \leq V_c,\, \tfrac{q-Q}{\rho} \in \left[\tfrac{Q^- - Q}{R}, \tfrac{Q^+ - Q}{R}\right]\right\} \,, \end{aligned}$$

where V_f and V_c are the threshold speeds, i.e. above V_f the flow is free, and below V_c the flow is congested. The parameters $Q^- \in \,]0,Q]$ and $Q^+ \in [Q,+\infty[$ depend on the environmental conditions and determine the width of the congested region.

Fig. 2.3, left, shows that the shape of the invariant domain is in good agreement with experimental data in Fig. 2.1, right. Following [48], throughout the present chapter we assume that the various parameters are strictly positive and satisfy:

$$V > V_f > V_c\,, \quad \frac{Q^+ - Q}{RV} < 1\,, \quad V_f = \frac{V - Q^+/R}{1 - (Q^+ - Q)/(RV)}\,. \tag{2.8}$$

I recall here the basic informations on the 2×2 system on the right hand side of (2.7):

$$\begin{array}{ll}
r_1(\rho, q) = \begin{bmatrix} \rho \\ q - Q \end{bmatrix}\,, & r_2(\rho, q) = \begin{bmatrix} R - \rho \\ \frac{R}{\rho} q \end{bmatrix}\,, \\
\lambda_1(\rho, q) = \left(\frac{2}{R} - \frac{1}{\rho}\right) \cdot (Q - q) - \frac{Q}{R}\,, & \lambda_2(\rho, q) = v_c(\rho, q)\,, \\
\nabla\lambda_1 \cdot r_1 = 2\dfrac{Q - q}{R}\,, & \nabla\lambda_2 \cdot r_2 = 0\,, \\
\mathcal{L}_1(\rho; \rho_o, q_o) = Q + \dfrac{q_o - Q}{\rho_o}\rho\,, & \mathcal{L}_2(\rho; \rho_o, q_o) = \dfrac{\rho}{\rho_o}\dfrac{R - \rho_o}{R - \rho} q_o\,, \\
w_1 = v_c(\rho, q)\,, & w_2 = \dfrac{q - Q}{\rho}\,,
\end{array} \tag{2.9}$$

where r_i is the i-th right eigenvector, λ_i the corresponding eigenvalue and $\mathcal{L}_i$ is the i-Lax curve. In the Riemann coordinates (w_1, w_2), $\Omega_c = [0, V_c] \times [W_2^-, W_2^+]$, where

$$W_2^- = \frac{Q^- - Q}{R}\,, \quad W_2^+ = \frac{Q^+ - Q}{R}\,.$$

For $(\rho, q) \in \Omega_f$, we extend the corresponding Riemann coordinates (w_1, w_2) as follows. Let $\tilde{u} = (\tilde{\rho}, \tilde{\rho}V)$ be the point in Ω_f with $\tilde{\rho} = Q/(V - W_2^-)$, see Fig. 2.3, left. Define

$$w_1 = V_f \quad \text{and} \quad w_2 = \begin{cases} V - Q/\rho & \text{if } \rho \geq \tilde{\rho}\,, \\ v_f(\tilde{\rho}) - v_f(\rho) + V - Q/\tilde{\rho} & \text{if } \rho < \tilde{\rho}\,, \end{cases} \tag{2.10}$$

so that, in the Riemann coordinates, $\Omega_f = \{V_f\} \times [W_o, W_2^+]$, with $W_o = W_2^- + v_f(\tilde{\rho}) - V$ (see Fig. 2.3, right).

Note that the 2×2 system describing the congested flow is hyperbolic, the second characteristic field is linearly degenerate but the first has an inflection point along the curve $q = Q$.

2.2.1 The Riemann problem

For sake of completeness and future reference, I recall in this section the description of the classical Riemann solver for (2.7), i.e. the self-similar solution of the Cauchy problem

$$\begin{cases} \partial_t \mathbf{u} + \partial_x \mathbf{f}(\mathbf{u}) = 0\,, \\ \mathbf{u}_0(x) = \begin{cases} \mathbf{u}^l\,, & \text{if } x < 0\,, \\ \mathbf{u}^r\,, & \text{if } x > 0\,. \end{cases} \end{cases} \tag{2.11}$$

If the initial data $\mathbf{u}^l$, $\mathbf{u}^r$ belong to the same set Ω_f or Ω_c, standard Lax solutions to the corresponding Riemann problem can be considered. Otherwise, following [40], admissible solutions are defined as follows.

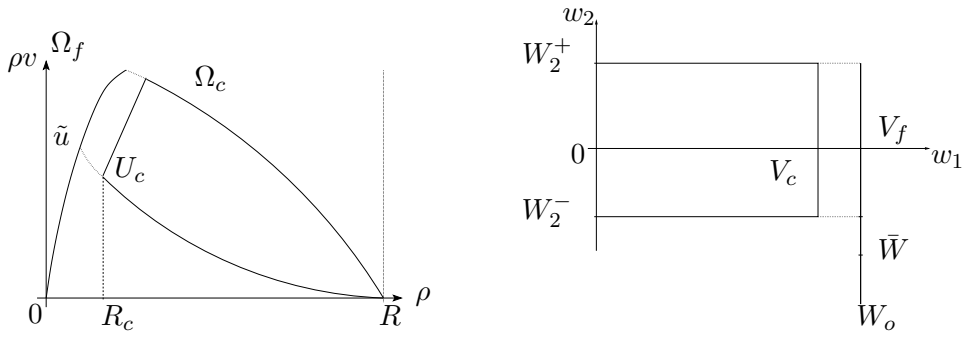

Figure 2.3: Notation used in Section 2.2. The continuous curves that border Ω_c are $\rho v = (1-\rho/R)(Q+\rho(Q^{\pm}-Q)/R)$.

Definition 2.2.1 *If $\mathbf{u}^l \in \Omega_f$ and $\mathbf{u}^r \in \Omega_c$, then an* **admissible solution** *to* (2.11) *is a self-similar function $\mathbf{u} : \mathbb{R}^+ \times \mathbb{R} \mapsto \Omega_f \cup \Omega_c$ such that, for some $\Lambda \in \mathbb{R}$, we have:*

1. *$\mathbf{u}(t,]-\infty, \Lambda t[) \subseteq \Omega_f$ and $\mathbf{u}(t,]\Lambda t, +\infty[) \subseteq \Omega_c$;*
2. *the functions*

$$\mathbf{u}^-(t,x) = \begin{cases} \mathbf{u}(t,x) & \text{if } x < \Lambda t\,, \\ \mathbf{u}(t,\Lambda t-) & \text{if } x > \Lambda t\,, \end{cases} \tag{2.12}$$

$$\mathbf{u}^+(t,x) = \begin{cases} \mathbf{u}(t,\Lambda t+) & \text{if } x < \Lambda t\,, \\ \mathbf{u}(t,x) & \text{if } x > \Lambda t\,, \end{cases} \tag{2.13}$$

$$\tag{2.14}$$

   are Lax solutions to corresponding Riemann problems for (2.7) *left, right, respectively;*

3. *the Rankine-Hugoniot condition*

$$\rho(t,\Lambda t+)\, v_c(\rho,q)(t,\Lambda t+) - \rho(t,\Lambda t-)\, v_f\left(\rho(t,\Lambda t-)\right) = \Lambda\left(\rho(t,\Lambda t+) - \rho(t,\Lambda t-)\right)$$

   holds for all $t > 0$.

If $\mathbf{u}^l \in \Omega_c$ and $\mathbf{u}^r \in \Omega_f$, the conditions are obtained by interchanging the roles of Ω_f, Ω_c and v_f, v_c.

Notice that condition 3 above ensures that the total number of car is conserved across phase transitions.

Definition 2.2.1 does not assure uniqueness. We are then led to introduce the notion of consistency [40].

Definition 2.2.2 *Let $\mathcal{R} : (\mathbf{u}^l, \mathbf{u}^r) \mapsto \mathcal{R}(\mathbf{u}^l, \mathbf{u}^r)$ denote a Riemann solver, i.e. $(t, x) \mapsto \mathcal{R}(\mathbf{u}^l, \mathbf{u}^r)(x/t)$ is a self-similar solution of (2.11). $\mathcal{R}$ is* **consistent** *if the following two conditions hold for all $\mathbf{u}^l,\ \mathbf{u}^m,\ \mathbf{u}^r \in \Omega_f \cup \Omega_c$, and $\bar{\lambda} \in \mathbb{R}$:*

$$\textbf{(C1)} \quad \left.\begin{array}{ll} \mathcal{R}(\mathbf{u}^l, \mathbf{u}^m)(\bar{\lambda}) & = \mathbf{u}^m \\ \mathcal{R}(\mathbf{u}^m, \mathbf{u}^r)(\bar{\lambda}) & = \mathbf{u}^m \end{array}\right\} \quad \Rightarrow \quad \mathcal{R}(\mathbf{u}^l, \mathbf{u}^r)(\lambda) = \begin{cases} \mathcal{R}(\mathbf{u}^l, \mathbf{u}^m)(\lambda)\,, & \text{if } \lambda < \bar{\lambda}\,, \\ \mathcal{R}(\mathbf{u}^m, \mathbf{u}^r)(\lambda)\,, & \text{if } \lambda \geq \bar{\lambda}\,, \end{cases}$$

$$\textbf{(C2)} \quad \mathcal{R}(\mathbf{u}^l, \mathbf{u}^r)(\bar{\lambda}) = \mathbf{u}^m \quad \Rightarrow \quad \begin{cases} \mathcal{R}(\mathbf{u}^l, \mathbf{u}^m)(\lambda) = \begin{cases} \mathcal{R}(\mathbf{u}^l, \mathbf{u}^r)(\lambda)\,, & \text{if } \lambda \leq \bar{\lambda}\,, \\ \mathbf{u}^m\,, & \text{if } \lambda > \bar{\lambda}\,, \end{cases} \\ \mathcal{R}(\mathbf{u}^m, \mathbf{u}^r)(\lambda) = \begin{cases} \mathbf{u}^m\,, & \text{if } \lambda < \bar{\lambda}\,, \\ \mathcal{R}(\mathbf{u}^l, \mathbf{u}^r)(\lambda)\,, & \text{if } \lambda \geq \bar{\lambda}\,. \end{cases} \end{cases}$$

Essentially, **(C1)** states that whenever two solutions to two Riemann problems can be placed side by side, then their juxtaposition is again a solution to a Riemann problem. **(C2)** is the vice-versa.

To describe the Riemann solver, we have to consider several different cases:

(A) The data in (2.11) are in the same phase, i.e. they are either both in Ω_f or both in Ω_c. Then the solution is the standard Lax solution to (2.7), left, respectively right, and no phase boundary is present.

(B) $\mathbf{u}^l \in \Omega_c$ and $\mathbf{u}^r \in \Omega_f$. We consider the points $\mathbf{u}^c \in \Omega_c$ and $\mathbf{u}^m \in \Omega_f$ implicitly defined by

$$\begin{aligned} \left(1 - \frac{\rho^c}{R}\right)\left(Q + w_2(\mathbf{u}^l)\rho^c\right) &= \rho^c V_c\,, \\ \left(1 - \frac{\rho^m}{R}\right)\left(Q + w_2(\mathbf{u}^l)\rho^m\right) &= \rho^m V\left(1 - \frac{\rho^m}{R}\right). \end{aligned}$$

If $w_2(\mathbf{u}^l) > 0$, the solution is made of a 1-rarefaction from $\mathbf{u}^l$ to $\mathbf{u}^c$, a phase transition from $\mathbf{u}^c$ to $\mathbf{u}^m$ and a Lax wave from $\mathbf{u}^m$ to $\mathbf{u}^r$. If $w_2(\mathbf{u}^l) \leq 0$, we have a shock-like phase transition from $\mathbf{u}^l$ to $\mathbf{u}^m$ and a Lax wave from $\mathbf{u}^m$ to $\mathbf{u}^r$.

(C) $\mathbf{u}^l \in \Omega_f$ and $\mathbf{u}^r \in \Omega_c$ with $w_2(\mathbf{u}^l) \in [W_2^-, W_2^+]$. Consider the points $\mathbf{u}^c$ and $\mathbf{u}^m \in \Omega_c$ implicitly defined by

$$\begin{aligned} \left(1 - \frac{\rho^c}{R}\right)\left(Q + w_2(\mathbf{u}^l)\rho^c\right) &= \rho^c V_c\,, \\ \left(1 - \frac{\rho^m}{R}\right)\left(Q + w_2(\mathbf{u}^l)\rho^m\right) &= \rho^m w_1(\mathbf{u}^r)\,. \end{aligned}$$

If $w_2(\mathbf{u}^l) > 0$, the solution is made of a shock-like phase transition from $\mathbf{u}^l$ to $\mathbf{u}^m$ and a 2-contact discontinuity from $\mathbf{u}^m$ to $\mathbf{u}^r$. If $w_2(\mathbf{u}^l) \leq 0$, the solution displays a phase transition from $\mathbf{u}^l$ to $\mathbf{u}^c$, a 2-rarefaction from $\mathbf{u}^c$ to $\mathbf{u}^m$ and a 2-contact discontinuity from $\mathbf{u}^m$ to $\mathbf{u}^r$.

(D) $\mathbf{u}^l \in \Omega_f$ with $w_2(\mathbf{u}^l) < W_2^-$ and $\mathbf{u}^r \in \Omega_c$. Let $\mathbf{u}^m \in \Omega_c$ be the point on the lower boundary of Ω_c implicitly defined by

$$\left(1 - \frac{\rho^m}{R}\right)\left(Q + W_2^- \rho^m\right) = \rho^m w_1(\mathbf{u}^r)\,,$$

and consider the speed of the phase boundary joining $\mathbf{u}^l \in \Omega_f$ to $\mathbf{u}^m \in \Omega_c$

$$\Lambda(\mathbf{u}^l, \mathbf{u}^m) = \frac{\rho^l v_f(\rho^l) - \rho^m w_1(\mathbf{u}^r)}{\rho^l - \rho^m}.$$

Let $\mathbf{U}_c = (R_c, Q^-) \in \Omega_c$ be the point whose Riemann coordinates are (V_c, W_2^-), see Fig. 2.3. If $\lambda_1(\mathbf{U}_c) \geq \Lambda(\mathbf{u}^l, \mathbf{U}_c)$, the solution is a phase transition from $\mathbf{u}^l$ to $\mathbf{U}_c$, a 1-rarefaction from $\mathbf{U}_c$ to $\mathbf{u}^m$ and a 2-contact discontinuity from $\mathbf{u}^m$ to $\mathbf{u}^r$. Otherwise:

- If $\lambda_1(\mathbf{u}^m) \leq \Lambda(\mathbf{u}^l, \mathbf{u}^m)$, the solution is a phase transition from $\mathbf{u}^l$ to $\mathbf{u}^m$ followed by a 2-contact discontinuity from $\mathbf{u}^m$ to $\mathbf{u}^r$.
- If $\lambda_1(\mathbf{u}^m) > \Lambda(\mathbf{u}^l, \mathbf{u}^m)$, let $\mathbf{u}^c = (\rho^c, q^c) \in \Omega_c$ be implicitly defined by

  $$\lambda_1(\mathbf{u}^c) = \Lambda(\mathbf{u}^l, \mathbf{u}^c)\,,$$

  i.e. ρ^c is the bigger root of the equation

  $$(Q - Q^-)\rho^2 - 2\rho^l(Q - Q^-)\rho + R^2(\rho^l v_f(\rho^l) - Q) + \rho^l R(2Q - Q^-) = 0$$

  and $q^c = Q - \rho^c(Q - Q^-)/R$. Then the solution shows a phase transition from $\mathbf{u}^l$ to $\mathbf{u}^c$, an attached 1-rarefaction from $\mathbf{u}^c$ to $\mathbf{u}^m$ and a 2-contact discontinuity from $\mathbf{u}^m$ to $\mathbf{u}^r$.

2.3 The Aw-Rascle model with phase transitions

The model under consideration has been introduced in [68]. The LWR equation and the Aw-Rascle model (2.3) describe the *free* flow and the *congested* phase, respectively. More precisely, the model in conservative variables reads

$$\begin{array}{ll}
\text{Free flow:} & \text{Congested flow:} \\
(\rho, y) \in \Omega_f & (\rho, y) \in \Omega_c \\
\partial_t \rho + \partial_x(\rho v) = 0 & \partial_t \rho + \partial_x(\rho v) = 0 \\
y = \rho V & \partial_t y + \partial_x(y v) = 0 \\
v = v_f(\rho) = (1 - \rho/R)V & y = \rho(v + p(\rho)), \quad p(\rho) = V_{ref} \ln(\rho/R),
\end{array} \tag{2.15}$$

i.e., using the notation (2.5),

$$\begin{cases}
\mathbf{u} = (\rho, y) \quad \text{and} \quad \mathbf{f}(\mathbf{u}) = (\rho v_f(\rho), y v_f(\rho))\,, & \text{if} \quad (\rho, y) \in \Omega_f\,, \\
\mathbf{u} = (\rho, y) \quad \text{and} \quad \mathbf{f}(\mathbf{u}) = (\rho v, y v)\,, & \text{if} \quad (\rho, y) \in \Omega_c\,.
\end{cases}$$

As before, R is the maximal possible car density, V is the maximal speed allowed and V_{ref} a given reference velocity. The 2×2 hyperbolic system describing the congested phase has the first characteristic field which is genuinely non-linear, and the second is linearly degenerate. The variables are the car density ρ and the car speed v or, equivalently, the conservative variables ρ and $y := \rho v + \rho p(\rho)$. In [8], the "pressure" function p is assumed increasing and plays the role of an *anticipation factor*, taking into account drivers' reactions to the state of traffic in front of them. Here we take $p(\rho) = V_{ref} \ln(\rho/R)$ as in [7, 9], because this choice allows to define a unique Riemann solver without any further assumption on the parameters R and V. However, under suitable assumptions, the model allows more general pressures (see [68] for further details).

I recall at this point the main features of the two models used in (2.15). In the free phase the characteristic speed is $\lambda(\rho) = V(1 - 2\rho/R)$, while the informations on the Aw-Rascle system are collected in the following table (see [8] for a more detailed study of the model):

$$\begin{array}{ll} r_1(\rho, v) = \begin{bmatrix} 1 \\ -p'(\rho) \end{bmatrix}, & r_2(\rho, v) = \begin{bmatrix} 1 \\ 0 \end{bmatrix}, \\ \lambda_1(\rho, v) = v - \rho\, p'(\rho)\,, & \lambda_2(\rho, v) = v\,, \\ \nabla\lambda_1 \cdot r_1 = -2\, p'(\rho) - \rho\, p''(\rho)\,, & \nabla\lambda_2 \cdot r_2 = 0\,, \\ \mathcal{L}_1(\rho; \rho_o, v_o) = v_o + p(\rho_o) - p(\rho)\,, & \mathcal{L}_2(\rho; \rho_o, v_o) = v_o\,, \\ w_1 = v\,, & w_2 = v + p(\rho)\,, \end{array} \tag{2.16}$$

where r_i is the i-th right eigenvector, λ_i the corresponding eigenvalue and $\mathcal{L}_i$ is the i-Lax curve. Shock and rarefaction curves coincide, hence the system belongs to the Temple class [96].

The invariant domain for (2.15) is shown in Fig. 2.4, left. Its shape agrees with the experimental data in Fig. 2.1, right, better than the scalar fundamental diagram in Fig. 2.1, left. In the (ρ, v) coordinates, it is given by

$$\Omega_f = \{(\rho, v) \in [0, R_f] \times [V_f, V] : \; v = v_f(\rho)\}\,,$$

$$\Omega_c = \{(\rho, v) \in [0, R] \times [0, V_c] : \; p(r) \le v + p(\rho) \le p(R)\}\,.$$

where $V_f > V_c$ are the threshold speeds, i.e. above V_f the flow is free and below V_c the flow is congested. The parameter $r \in \,]0, R]$ is fixed depending on the environmental conditions and determines the width of the congested region. The maximal free-flow density R_f must satisfy $V_f + p(R_f) = p(R)$ (that is $V_f + V_{ref} \ln(R_f/R) = 0$ with our choice of the pressure). In order to get this condition, we are led to assume $V_{ref} < V$. It is easy to check that the *capacity drop* in the passage from the free phase to the congested phase [81] is then automatically satisfied. In order to resume, we have the following order relation between the speed parameters:

$$V > V_{ref} > V_f > V_c.$$

Using Riemann coordinates (w_1, w_2), $\Omega_c = [0, V_c] \times [p(r), p(R)]$. For $(\rho, v) \in \Omega_f$, I extend the corresponding Riemann coordinates (w_1, w_2) as in Sec. 2.2: Let $\tilde{u} = (\tilde{\rho}, v_f(\tilde{\rho}))$

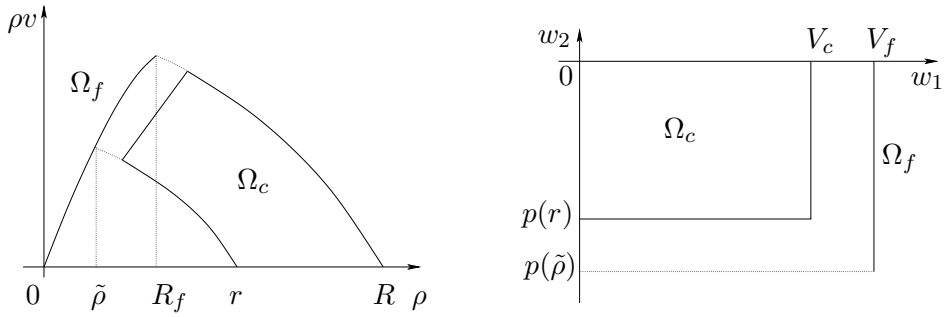

Figure 2.4: Notation used in Section 2.3.

be the point in Ω_f implicitly defined by $v_f(\tilde{\rho}) + p(\tilde{\rho}) = p(r)$. We define

$$w_1 = V_f\,, \qquad w_2 = \begin{cases} v_f(\rho) + p(\rho)\,, & \text{if } \rho \geq \tilde{\rho}\,, \\ v_f(\rho) + p(\tilde{\rho})\,, & \text{if } \rho < \tilde{\rho}\,, \end{cases} \tag{2.17}$$

so that, in Riemann coordinates, $\Omega_f = \{V_f\} \times [p(\tilde{\rho}), p(R)]$ (Fig. 2.4, right).

A detailed description of the Riemann solver and further analytical results are given in [68].

Remark. Coupling the Aw-Rascle model with the LWR equation allows to correct some drawbacks of the original Aw-Rascle model. First of all, model (2.15) is well-posed and stable near the vacuum, which is not the case for the Aw-Rascle system. Second, as noted in [8, Sec. 5], when there is a rarefaction wave connecting a state $(\rho_-, \rho_- v_-)$ to the vacuum, the maximal velocity v reached by the cars with our choice of pressure is $v_{max} = +\infty$, i.e. the maximal speed reached by the cars on an empty road is infinite, which is clearly unrealistic. With other choices of the pressure, the maximal speed depends on the initial data ρ_-, v_-. On the contrary, the solution given by model (2.15) reaches the maximal velocity V independently from the choice of the pressure and the initial data.

2.4 Well posedness for the Cauchy problem

When considering the Cauchy problem, (2.5) is supplemented with a given value of the solution at time $t = 0$. More precisely, we assume that the initial datum $\mathbf{u}_0 \in \Omega$ is given and we set

$$\mathbf{u}(0, \cdot) = \mathbf{u}_0. \tag{2.18}$$

Definition 2.4.1 *Fix $M > 0$. A map $S\colon \mathbb{R}^+ \times \mathcal{D} \mapsto \mathcal{D}$ is an M-*Riemann Semigroup *(M-RS) if the following holds:*

(RS1) $\mathcal{D} \supseteq \left\{\mathbf{u} \in \mathbf{L^1}\left(\mathbb{R}; \Omega_f \cup \Omega_c\right) : \mathbf{TV}(\mathbf{u}) \leq M\right\}$*;*

(RS2) $S_0 = \mathrm{Id}$ *and* $S_{t_1} \circ S_{t_2} = S_{t_1 + t_2}$*;*

(RS3) there exists an $L = L(M)$ such that for t_1, t_2 in $\mathbb{R}^+$ and $\mathbf{u}_1, \mathbf{u}_2$ in $\mathcal{D}$,

$$\|S_{t_1}\mathbf{u}_1 - S_{t_2}\mathbf{u}_2\|_{\mathbf{L^1}} \leq L \cdot (\|\mathbf{u}_1 - \mathbf{u}_2\|_{\mathbf{L^1}} + |t_1 - t_2|)\,;$$

(RS4) if $\mathbf{u} \in \mathcal{D}$ is piecewise constant, then for t small, $S_t\mathbf{u}$ coincides with the gluing of solutions to Riemann problems.

Properties *(RS1)–(RS4)* provide the natural extension of [22, Definition 9.1] to the present case.

The following theorem states the existence of an M-RS generated by the Cauchy problem for (2.5), (2.18). It has been published in [48].

Theorem 2.4.2 *For any positive M, the system* (2.5) *generates an M-RS $S\colon \mathbb{R}^+ \times \mathcal{D} \mapsto \mathcal{D}$. Moreover*

(CP1) for all $\mathbf{u}_0 \in \mathcal{D}$, the orbit $t \mapsto S_t\mathbf{u}_0$ is a weak entropic solution to (2.5), (2.18)*;*

(CP2) any two M–RS coincide up to the domain;

(CP3) the solutions yielded by S can be characterized as viscosity solutions, in the sense of [22, Theorem 9.2].

(CP4) $\mathcal{D} \subseteq \left\{\mathbf{u} \in \mathbf{L^1}(\mathbb{R}; \Omega_f \cup \Omega_c) : \mathbf{TV}(\mathbf{u}) \leq \widehat{M}\right\}$ for a positive $\widehat{M} = \widehat{M}(M)$.

Sketch of the proof. I give the proof for model (2.7), but it remains valid with minor changes when applied to (2.15). The proof follows [18] and is achieved through the construction of exact weak solutions to (2.7) that are only approximately entropic, built by means of wave-front tracking. For $\nu \in \mathbb{N}$, we introduce a mesh Ω^ν in Ω. In Riemann coordinates, let

$$\Omega_c^\nu = \left\{\left(i2^{-\nu}V_c, W_2^- + j2^{-\nu}(W_2^+ - W_2^-)\right) \in \Omega_c\colon i, j = 0, \ldots, 2^\nu\right\}$$

where W_2^- and W_2^+ are as in Fig. 2.3, right. Now, let

$$\begin{aligned}
I_1^\nu &= \left\{W_2^- + j2^{-\nu}(W_2^+ - W_2^-)\colon j = 0, \ldots, 2^\nu\right\} \\
I_2^\nu &= \left\{w \in [W_o, W_2^-]\colon \begin{array}{l} w = V - Q/\rho \text{ where } \bar{\Lambda}(\rho', \rho) = \bar{\lambda}_1(\rho') \\ \text{for some } (\rho', \mathcal{L}_1(\rho'; R, Q^-)) \in \Omega_c^\nu \end{array}\right\} \\
\bar{W} &= \min I_2^\nu \\
I_3^\nu &= \begin{cases} \{W_o\} & \text{if } \bar{W} - W_o < 2^{-\nu} \\ \left\{W_o + j2^{-\nu}(\bar{W} - W_o)\colon j = 0, \ldots, 2^\nu\right\} & \text{if } \bar{W} - W_o > 2^{-\nu} \end{cases} \\
\Omega_f^\nu &= \{V_f\} \times (I_1^\nu \cup I_2^\nu \cup I_3^\nu) \\
\Omega^\nu &= \Omega_f^\nu \cup \Omega_c^\nu\,.
\end{aligned}$$

We note that, since we are dealing with a Temple class system, the Riemann problem (2.11) with data in Ω^ν admits a piecewise constant weak solution attaining values

in Ω^ν. Nevertheless, these solutions may well be non entropic, since rarefaction waves are replaced by shock fans.

An approximate solution $u^\nu = u^\nu(t,x)$ to the Cauchy problem for (2.5)-(2.18) is now constructed by means of the standard wave front tracking technique, see [18, 22]. Recall that u^ν can be defined up to any positive time provided the number of interaction points is finite on any compact subset of $\mathbb{R}^+ \times \mathbb{R}$ and the range of u^ν remains in Ω^ν.

The latter requirement is met, as pointed out above. The former is obtained through suitable interaction estimates, that also ensure the existence of a bound on $\mathbf{TV}\left(u^\nu(t,\cdot)\right)$ uniform in ν and t.

To this aim, we assign a *strength* to each simple wave. Let u^l, u^r be the states on the sides of the wave and call (w_1^l, w_2^l), (w_1^r, w_2^r) the corresponding Riemann coordinates, see (2.9), (2.10). Then, the strength of the wave is

$$\tau = \left| w_1^r - w_1^l \right| + \left| w_2^r - w_2^l \right| . \tag{2.19}$$

Note that only in case **(D)** in Sec. 2.2.1 these summands are both non zero. Let $\tau_{i,\alpha}$ be the strength of the wave of the i-th family exiting from the α-th point of jump x_α in $u^\nu(t,\cdot)$. With this choice, we define the usual Glimm functionals

$$V^\nu(t) = \sum_{i,\alpha} |\tau_{i,\alpha}| \,, \qquad Q^\nu(t) = \sum_{\alpha,\beta\colon\, x_\alpha < x_\beta} |\tau_{2,\alpha}\tau_{1,\beta}| \,. \tag{2.20}$$

It is immediate to prove that along any approximate solution, the maps $t \mapsto V^\nu(t)$ and $t \mapsto Q^\nu(t)$ are both non increasing and, at each interaction, at least one of them decreases by at least $2^{-\nu}$. Hence there is a finite number of interactions on all $\mathbb{R}^+ \times \mathbb{R}$.

We prove the $\mathbf{L^1}$ Lipschitz continuous dependence using pseudo-polygonals, as in [23, 4, 18]. We introduce a class of curves (pseudo-polygonals) that connect any two initial data in $\mathcal{D}^\nu_M = \{u\colon \mathbb{R} \to \Omega^\nu : V^\nu(u) \leq M\}$.

Let $]a,b[$ be an open interval and $\mathbf{PC}$ denote the set of piecewise constant functions with a finite number of jumps. An *elementary path* is a map $\gamma\colon\,]a,b[\mapsto \mathbf{PC}$ of the form

$$\gamma(\theta) = \sum_{\alpha=1}^{N} u^\alpha \cdot \chi_{[x^\theta_{\alpha-1}, x^\theta_\alpha[} \,, \quad x^\theta_\alpha = x_\alpha + \xi_\alpha \theta \,,$$

with $x^\theta_{\alpha-1} \leq x^\theta_\alpha$ for all $\theta \in]a,b[$ and $\alpha = 1, \ldots, N$.

A continuous map $\gamma\colon\,]a,b[\mapsto \mathcal{D}^\nu_M$ is a pseudo-polygonal if there exist countably many disjoint open intervals $J_h \subseteq]a,b[$ such that $]a,b[\setminus \bigcup_h J_h$ is countable and the restriction of γ to each J_h is an elementary path. Moreover, any two elements of $\mathcal{D}^\nu_M$ can be joined by a pseudo-polygonal γ entirely contained in $\mathcal{D}^\nu_M$.

As shown in [18, 22, 23], the semigroup S^ν defined by $S^\nu_t = u^\nu(t,\cdot)$ preserves the pseudo-polygonals in the sense that if γ is a pseudo-polygonal then $S^\nu_t \circ \gamma$ is also a pseudo-polygonal, for all $t \geq 0$.

Define the length of a curve $\gamma \subseteq \mathcal{D}^\nu_M$ of approximate solutions as $\|\gamma\|_\nu = \int_a^b \Upsilon^\nu\left[\gamma(\theta)\right] \, d\theta$, where $\Upsilon^\nu = \sum_{i,\alpha} |\sigma_{i,\alpha}\xi_{i,\alpha}W_{i,\alpha}|$, $W_{i,\alpha}$ being a suitable weight and $\sigma_{i,\alpha}$ being the strength

of a jump measured in the conserved coordinates. Suitable interaction estimates, see [48, Prop. 4.4], ensure that one can define weights $W_{i,\alpha}$ such that $W_{i,\alpha} \in [1, W]$ and the map $t \mapsto \Upsilon^\nu(u(t,\cdot))$ is non increasing. The first requirement implies that the metric

$$d^\nu_\eta(u,w) = \inf\left\{\|\gamma\|_\nu \colon \gamma \text{ pseudo-polygonal joining } u \text{ to } w\right\}$$

is equivalent to the $\mathbf{L^1}$-distance uniformly in ν, see also [4, 18, 22]; the latter ensures that the ν-approximate semigroup S^ν is non expansive with respect to d^ν_η. This finally ensures that the approximate semigroup is Lipschitz in the $\mathbf{L^1}$ norm, uniformly with respect to ν. □

Remark. From the analytical point of view, this is a first example of a system of conservation laws developing phase transitions whose well posedness is proved *globally*, i.e., for all initial data attaining values in a given set and with bounded total variation. In the literature, several results deal with the solution to Riemann problems in presence of phase transitions, see for instance [51, 84, 85]. Other works prove the global in time well posedness of the Cauchy problem, but with initial data that are perturbations of a given phase boundary, see for instance [41, 42]. On the contrary, here the number of phase boundaries that are present in the data and in the solution is not *a priori* fixed.

Note that it is not possible to extend the result to initial data in $\mathbf{L}^\infty(\mathbb{R})$, due to the presence of a linearly degenerate field, see [25].

From the traffic point of view, well posedness allows to consider various control and optimization problems, see [50].

Observe that the description of several realistic situations requires suitable source terms in the right hand sides of models (2.7), (2.15). The techniques in [9, 43] can then be applied.

2.5 Road networks

In this section I illustrate the extension to road networks of the existence theory for systems with phase transitions reported above. The results have been obtained in collaboration with R.M. Colombo and B. Piccoli, and are contained in [47]. They are detailed for system (2.7), but they remain valid for (2.15).

There are now many available results for the LWR model or the Aw-Rascle model on networks, see [13, 35, 36, 63, 64, 65, 72, 73, 74]. However, this is the first result for a phase transition model applied to a network. The interest in such a theory is motivated also by other applications: data networks [56], supply chains [55, 70], air traffic management [14] and gas pipelines [11, 44, 45].

Our main result is the existence of weak solutions on the whole network for initial data in $\mathbf{BV}$ under a technical assumption. More precisely the latter asks for traffic to keep away from the zero velocity, see assumption **(H)** in Section 2.5.5. Our construction is based on the wave-front tracking method, for reference see [22, 53, 75].

More precisely, first we consider Riemann problems at nodes, which are Cauchy problems with constant initial data on each road. Notice that the conservation of cars

alone is not sufficient to single out a unique solution. Thus, one has to prescribe solutions for every initial data and we call the relative map a *Riemann solver at nodes*. Then, it is possible to construct approximate solutions using classical self-similar entropic solutions for Riemann problems inside roads and an assigned Riemann solver at junctions. To pass to the limit we rely on a **BV** estimate on the density flux variation, and assumption **(H)** is necessary to get **BV** bounds also on the density itself and the linearized momentum.

Following [67], we define three properties **(Pr1)**, **(Pr2)** and **(Pr3)** of a Riemann solver (see Definition 2.5.7), which guarantee the needed bounds and thus the existence of solutions to the Cauchy problem. These key properties are in particular satisfied by the Riemann solver $\mathcal{R}_J$ introduced in Section 2.5.4. The latter is defined generalizing to the phase transition model the Riemann solver previously presented for the LWR scalar model in [36]. It prescribes a fixed distribution of traffic in outgoing roads, and then the maximization of the flux through the junction.

The definition of $\mathcal{R}_J$ for the case of the phase transition model is a nontrivial extension of the Riemann solver for the LWR model. In particular, the set of attainable states on a road, entering or exiting a junction, gives rise to non-convex sets of possible density fluxes. In order to have the continuous dependence of solutions, we have to get convexity removing the *metastable* states from the attainable set. This choice is consistent with the idea that these states should appear in a transient situation, which should not happen at a junction.

2.5.1 Basic definitions

A road network is a couple $(\mathcal{I}, \mathcal{J})$, where $\mathcal{I}$ is a finite collection of unidirectional roads and $\mathcal{J}$ is the set of junctions. Each road is modelled by real intervals $I_i =]a_i, b_i[$, $i = 1, \dots, N$, whereas each junction J consists of two sets $Inc(J) \subset \{1, \dots, N\}$ and $Out(J) \subset \{1, \dots, N\}$ corresponding to incoming and outgoing roads of J.

Given a junction J, a Riemann problem at J is a Cauchy problem with initial data constant on each incoming and outgoing road. As for classical Riemann problems on a real line, we look for self-similar, centered solutions, which are the building blocks to construct solutions to Cauchy problems.
We follow the same procedure used in Sec. 2.2.1 for classical Riemann problems on the real line: we first define *admissible solutions at the junction*, state a *consistency* property and then select a *Riemann solver*.

Definition 2.5.1 *Consider a junction J and assume for simplicity $Inc(J) = \{1, \dots, n\}$, $Out(J) = \{n+1, \dots, n+m\}$. If $\mathbf{u}_{i,0} \in \Omega_f \cap \Omega_c$ for $i = 1, \dots, n+m$, then an **admissible solution** to*

$$\begin{cases} \partial_t \mathbf{u}_i + \partial_x \mathbf{f}(\mathbf{u}_i) = 0\,, \\ \mathbf{u}_i(0,x) = \mathbf{u}_{i,0} \end{cases} \qquad i = 1, \dots, n+m\,. \tag{2.21}$$

is a self-similar function $\mathbf{u}\colon \mathbb{R}\times[0,+\infty[\mapsto (\Omega_f \cup \Omega_c)^{n+m}$ such that, for some $\hat{\mathbf{u}}_1, \dots \hat{\mathbf{u}}_{n+m} \in \Omega_f \cap \Omega_c$, we have:

1. *for all $i \in \{1, \dots, n\}$, $(\mathcal{R}(\mathbf{u}_{i,0}, \hat{\mathbf{u}}_i))(x/t) = \hat{\mathbf{u}}_i$ for $x \geq 0$ and $\mathbf{u}_i(t,x) = (\mathcal{R}(\mathbf{u}_{i,0}, \hat{\mathbf{u}}_i))(x/t)$, for $x \leq 0$;*

2. *for all* $i \in \{n+1, \dots, n+m\}$, $(\mathcal{R}(\hat{\mathbf{u}}_i, \mathbf{u}_{i,0}))(x/t) = \hat{\mathbf{u}}_i$ *for* $x \leq 0$ *and* $\mathbf{u}_i(t,x) = (\mathcal{R}(\hat{\mathbf{u}}_i, \mathbf{u}_{i,0}))(x/t)$, *for* $x \geq 0$;

3. $\displaystyle\sum_{i=1}^{n} \mathbf{f}_1(\hat{\mathbf{u}}_i) = \sum_{j=n+1}^{n+m} \mathbf{f}_1(\hat{\mathbf{u}}_j)$, *where* $\mathbf{f}_1$ *is the first component of* $\mathbf{f}$.

In other words, Definition 2.5.1 states that an admissible solution:

1. consists of waves with negative speed in incoming roads;
2. consists of waves with positive speed in outgoing roads;
3. conserves the number of cars at J.

The above definition assigns a key role to the traces $\hat{\mathbf{u}}_i$ of admissible solutions at the junction. Once these values are known, the whole solution is uniquely determined by points 1 and 2 in Definition 2.5.1. Therefore, following [66, Def. 4.2.2], in the case of the Riemann problem at a junction (2.21) we call *Riemann Solver at* J the map

$$\begin{array}{rccc} \mathcal{R}_J\colon & (\Omega_f \cup \Omega_c)^{n+m} & \longrightarrow & (\Omega_f \cup \Omega_c)^{n+m} \\ & (\mathbf{u}_{1,0}, \dots, \mathbf{u}_{n+m,0}) & \longmapsto & (\hat{\mathbf{u}}_1, \dots, \hat{\mathbf{u}}_{n+m}) \end{array}$$

assigning to the initial data in (2.21) the trace $\hat{\mathbf{u}}_1, \dots, \hat{\mathbf{u}}_{n+m}$ of the admissible solution at the junction.

We give the following

Definition 2.5.2 *We define a Riemann solver at a Junction* $\mathcal{R}_J$ *to be* ***consistent*** *at* J *if*

$$\textbf{\textit{(CC)}} \qquad \mathcal{R}_J\left(\mathcal{R}_J(\mathbf{u}_{1,0}, \dots, \mathbf{u}_{n+m,0})\right) = \mathcal{R}_J(\mathbf{u}_{1,0}, \dots, \mathbf{u}_{n+m,0})$$

for every $(\mathbf{u}_{1,0}, \dots, \mathbf{u}_{n+m,0}) \in (\Omega_f \cup \Omega_c)^{n+m}$.

Below, I assume that, besides (2.8), also

$$\left(1 - \frac{Q^+}{RV}\right) \cdot \left(\frac{Q^+}{Q} - 1\right) < 1 \tag{2.22}$$

holds. Notice that condition (2.22) is fulfilled for Q^+ sufficiently large. It ensures that $\sup_{\Omega_f \cup \Omega_c} \lambda_1 < 0$, hence all waves of the first family in the congested region move with negative speed.

2.5.2 Incoming roads: attainable values at the junction

To respect condition 1 of Definition 2.5.1, only waves with negative speed can be produced on incoming roads. Thus we determine all states which can be connected to an initial state (to the right) by waves with negative speed. In particular, we determine the maximum flux $\gamma_i^{\max}$ that can be reached from an initial datum $\mathbf{u}_{i,0} = (\rho_{i,0}, q_{i,0})$ by means of waves with negative speed only.

We start describing the sets of fluxes corresponding to states that can be connected to $\mathbf{u}_{i,0}$ on the right using non positive waves only. We use the notations introduced in Sec. 2.2.1, cases **(B)-(D)**, where we set $\mathbf{u}_{i,0} = \mathbf{u}^l$. Moreover, we introduce the velocities V_1 and V_2 defined as follows:

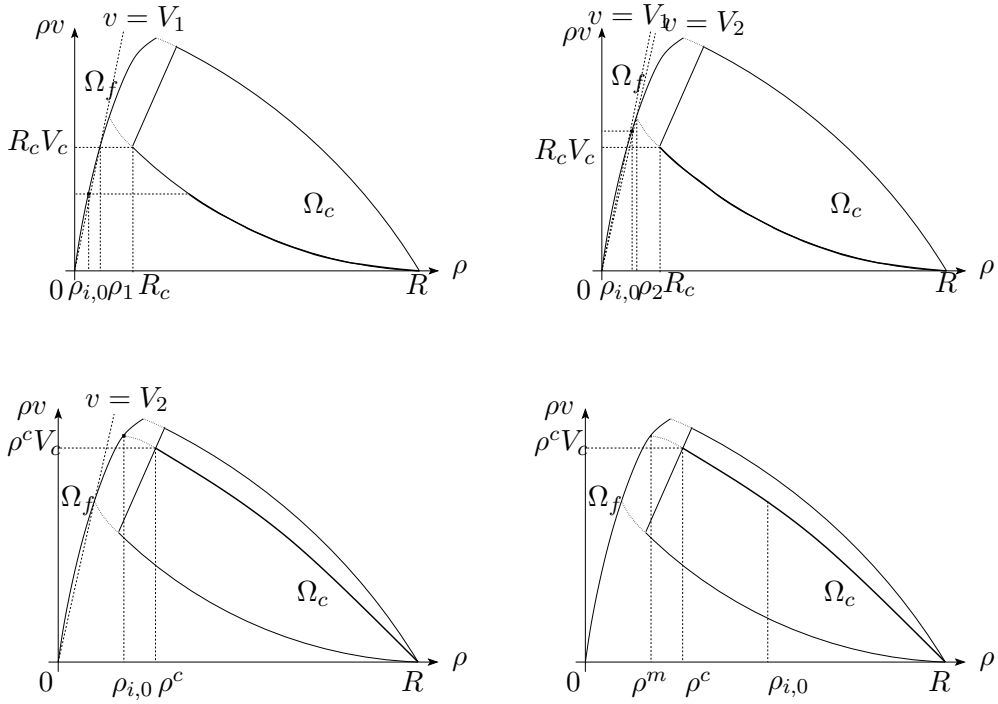

Figure 2.5: Notations used in the definition of $\mathcal{O}_i$, $i = 1, \dots, n$.

- $V_1 := v_f(\rho_1)$, where $\rho_1 \in \Omega_f$ is the smaller root of the equation $\rho_1 v_f(\rho_1) = R_c V_c$;
- $V_2 := v_f(\rho_2)$, where $\rho_2 \in \Omega_f$ is the smaller root of the equation

$$\left(1 - \frac{\rho_2}{R}\right)\left(Q + \frac{Q_- - Q}{R}\rho_2\right) = \rho_2 V \left(1 - \frac{\rho_2}{R}\right).$$

We refer the reader to Fig. 2.5 for a more intuitive explication of the notations. The sets of reachable fluxes are then given by:

$$\mathcal{O}_i = \begin{cases} [0, \rho_{i,0} v_f(\rho_{i,0})] & \text{if } \mathbf{u}_{i,0} \in \Omega_f, v_f(\rho_{i,0}) \geq V_1\,, \\ [0, R_c V_c] \cup \{\rho_{i,0} v_f(\rho_{i,0})\} & \text{if } \mathbf{u}_{i,0} \in \Omega_f, V_2 \leq v_f(\rho_{i,0}) \leq V_1 (\text{Case } \textbf{(D)}, \text{ Sec. 2.2.1})\,, \\ [0, \rho^c V_c] \cup \{\rho_{i,0} v_f(\rho_{i,0})\} & \text{if } \mathbf{u}_{i,0} \in \Omega_f, v_f(\rho_{i,0}) \leq V_2 (\text{Case } \textbf{(C)}, \text{ Sec. 2.2.1})\,, \\ [0, \rho^c V_c] \cup \{\rho^m v_f(\rho^m)\} & \text{if } \mathbf{u}_{i,0} \in \Omega_c (\text{Case } \textbf{(B)}, \text{ Sec. 2.2.1})\,, \end{cases} \tag{2.23}$$

for $i = 1, \dots, n$. We observe that the sets $\mathcal{O}_i$ are non convex. Thus we remove the *metastable* states from the attainable sets and we define the corresponding maximum fluxes as follows:

$$\gamma_i^{\max} = \begin{cases} \rho_{i,0} v_f(\rho_{i,0}) & \text{if } \mathbf{u}_{i,0} \in \Omega_f, v_f(\rho_{i,0}) \geq V_1\,, \\ R_c V_c & \text{if } \mathbf{u}_{i,0} \in \Omega_f, V_2 \leq v_f(\rho_{i,0}) \leq V_1 (\text{Case } \textbf{(D)}, \text{ Sec. 2.2.1})\,, \\ \rho^c V_c & \text{if } \mathbf{u}_{i,0} \in \Omega_f, v_f(\rho_{i,0}) \leq V_2 (\text{Case } \textbf{(C)}, \text{ Sec. 2.2.1})\,, \\ \rho^c V_c & \text{if } \mathbf{u}_{i,0} \in \Omega_c (\text{Case } \textbf{(B)}, \text{ Sec. 2.2.1})\,. \end{cases} \tag{2.24}$$

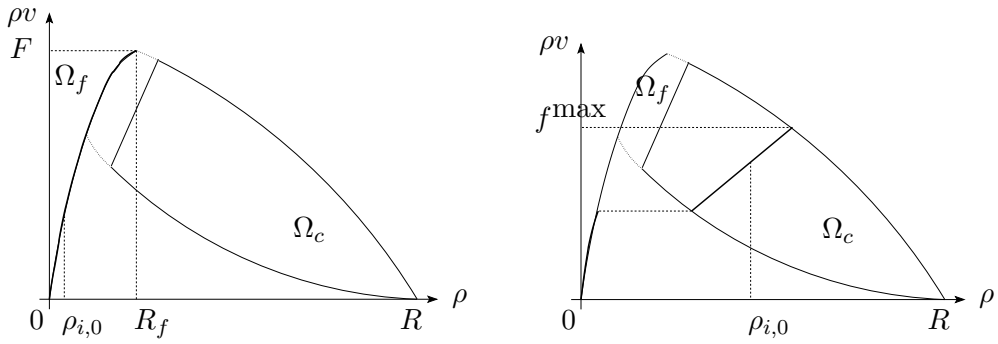

Figure 2.6: Notations used in the definition of $\mathcal{O}_j$, $j = n+1, \ldots, n+m$.

Proposition 2.5.3 *Given an initial datum $\mathbf{u}_{i,0}$ on an incoming road and $\hat{\gamma} \in [0, \gamma_i^{max}]$, there exists a unique $\hat{\mathbf{u}}_i$ such that the Riemann problem $(\mathbf{u}_{i,0}\hat{\mathbf{u}}_i)$ is solved by waves with negative speed and $\mathbf{f}_1(\hat{\mathbf{u}}_i) = \hat{\gamma}$.*

2.5.3 Outgoing roads: maximal flux at the junction

To respect condition 2 of Definition 2.5.1 only waves with positive speed can be produced on outgoing roads. Thus we determine all states, and the corresponding set of fluxes, which can be connected to an initial state $\mathbf{u}_{j,0}$ (to the left) using waves with positive speed.
We introduce the fluxes F and $f^{\max}$ defined as follows (see Fig. 2.6):

- $F := R_f v_f(R_f) = \max_{\rho \in \Omega_f} \rho v_f(\rho) > \max_{(\rho,q)\in\Omega_c} \rho v_c(\rho, q)$ is the maximal flux supported by the road;
- for $\mathbf{u}_{j,0} \in \Omega_c$, $f^{\max} := f^{\max}(\mathbf{u}_{j,0}) = \rho^{\max} v_c(\rho^{\max}, q^{\max})$, where $\rho^{\max}$ is the bigger root of the equation

$$\left(1 - \frac{\rho^{\max}}{R}\right)\left(Q + \frac{Q_+ - Q}{R}\rho^{\max}\right) = \rho^{\max} v_c(\rho_{j,0}, q_{j,0})\,,$$

  and $q^{\max} = Q + \rho^{\max}(Q_+ - Q)/R$.

The sets of reachable fluxes are given by

$$\mathcal{O}_j = \begin{cases} [0, F] & \text{if } \mathbf{u}_{j,0} \in \Omega_f\,, \\ [0, f^{\max}] & \text{if } \mathbf{u}_{j,0} \in \Omega_c\,, \end{cases} \tag{2.25}$$

for $j = n+1, \ldots, n+m$. Since the sets $\mathcal{O}_j$ are convex, the corresponding maximum fluxes are defined accordingly:

$$\gamma_j^{\max} = \begin{cases} F & \text{if } \mathbf{u}_{j,0} \in \Omega_f\,, \\ f^{\max} & \text{if } \mathbf{u}_{j,0} \in \Omega_c\,. \end{cases} \tag{2.26}$$

Proposition 2.5.4 *Given an initial datum $\mathbf{u}_{j,0}$ on an outgoing road and $\hat{\gamma} \in [0, \gamma_j^{max}]$, there exists a unique $\hat{\mathbf{u}}_j \in \mathcal{O}_j$ such that the Riemann problem $(\hat{\mathbf{u}}_j, \mathbf{u}_{j,0})$ is solved by waves with positive speed and $\mathbf{f}_1(\hat{\mathbf{u}}_j) = \hat{\gamma}$.*

2.5.4 The Riemann solver at junctions

We consider a Riemann solver similar to the one introduced in [36] for scalar equations. First, we need to define a suitable set of matrices. Consider the set

$$\mathcal{A} := \left\{ A = \{a_{ji}\}_{i=1,\dots,n,\ j=n+1,\dots,n+m} : \begin{array}{c} 0 < a_{ji} < 1\ \forall i,j, \\ \sum_{j=n+1}^{n+m} a_{ji} = 1\ \forall i \end{array} \right\}.$$

Let $\{e_1, \dots, e_n\}$ be the canonical basis of $\mathbb{R}^n$. For every $i = 1, \dots, n$, we denote $H_i = \{e_i\}^\perp$. If $A \in \mathcal{A}$, then we write, for every $j = n+1, \dots, n+m$, $a_j = (a_{j1}, \dots, a_{jn}) \in \mathbb{R}^n$ and $H_j = \{a_j\}^\perp$. Let $\mathcal{K}$ be the set of indices $\mathbf{k} = (k_1, ..., k_\ell)$, $1 \le \ell \le n-1$, such that $0 \le k_1 < k_2 < \cdots < k_\ell \le n+m$ and for every $\mathbf{k} \in \mathcal{K}$ define

$$H_{\mathbf{k}} = \bigcap_{h=1}^{\ell} H_{k_h}.$$

Writing $\mathbf{1} = (1, \dots, 1) \in \mathbb{R}^n$ and following [36] we define the set

$$\mathfrak{N} := \left\{ A \in \mathcal{A} : \mathbf{1} \notin H_{\mathbf{k}}^\perp \text{ for every } \mathbf{k} \in \mathcal{K} \right\}. \tag{2.27}$$

Notice that, if $n > m$, then $\mathfrak{N} = \emptyset$. This means that we cannot have more incoming that outgoing roads. The matrices of $\mathfrak{N}$ allow to define a unique solution to the Riemann problem at J.

1. Fix a matrix $A \in \mathfrak{N}$ and consider the closed, convex and not empty set

$$\Lambda = \left\{ (\gamma_1, \cdots, \gamma_n) \in \prod_{i=1}^{n} [0, \gamma_i^{\max}] : A \cdot (\gamma_1, \cdots, \gamma_n)^T \in \prod_{j=n+1}^{n+m} [0, \gamma_j^{\max}] \right\}.$$

2. Find the point $(\bar{\gamma}_1, \dots, \bar{\gamma}_n) \in \Lambda$ which maximizes the function

$$E(\gamma_1, \dots, \gamma_n) = \gamma_1 + \cdots + \gamma_n,$$

and define $(\bar{\gamma}_{n+1}, \dots, \bar{\gamma}_{n+m})^T := A \cdot (\bar{\gamma}_1, \dots, \bar{\gamma}_n)^T$. Since $A \in \mathfrak{N}$, the point $(\bar{\gamma}_1, \dots, \bar{\gamma}_n)$ is uniquely defined. In fact, by (2.27), $\nabla E = \mathbf{1}$ is not orthogonal to any nontrivial subspace contained in a supporting hyperplane of Λ.

3. For every $i \in \{1, \dots, n\}$, set $\hat{\mathbf{u}}_i$ either to $\mathbf{u}_{i,0}$ if $\mathbf{f}_1(\mathbf{u}_{i,0}) = \bar{\gamma}_i$, or to the solution to $\mathbf{f}_1(\mathbf{u}) = \bar{\gamma}_i$ given by Proposition 2.5.3. For every $j \in \{n+1, \dots, n+m\}$, set $\hat{\mathbf{u}}_j$ either to $\mathbf{u}_{j,0}$ if $\mathbf{f}_1(\mathbf{u}_{j,0}) = \bar{\gamma}_j$, or to the solution to $\mathbf{f}_1(\mathbf{u}) = \bar{\gamma}_j$ given by Proposition 2.5.4. Finally, set

$$\mathcal{R}_J(\mathbf{u}_{1,0}, \dots, \mathbf{u}_{n+m,0}) = (\hat{\mathbf{u}}_1, \dots, \hat{\mathbf{u}}_{n+m}).$$

It is easy to verify that $\mathcal{R}_J$ satisfies the consistency condition **(CC)**.

2.5.5 Existence of solutions on the whole network

To prove existence of solutions on the whole network, we first construct a sequence of approximate solutions via wave-front tracking (see [22] for the general theory and [66, § 4.3] in the case of networks) and then pass to the limit using a **BV** bound on the density flux.

Roughly speaking a wave-front tracking solution is constructed as follows: Fix an initial datum $\mathbf{u}_0 = (\mathbf{u}_{1,0}, \dots, \mathbf{u}_{N,0})$ with bounded total variation on the whole network. For every $\nu \in \mathbb{N}$, one first discretizes the initial datum using a piecewise constant approximation $\mathbf{u}_{\nu,0}$ with total variation bounded by the total variation of $\mathbf{u}_0$. Then Riemann problems on each road and at each junction of the network are solved, replacing rarefaction waves by a collection of small rarefaction shocks of size at most $1/\nu$. A solution is obtained, for small times, by piecing together the solution to Riemann problems and it is a weak solution up to the interaction of two waves or of a wave with a junction. Then a new Riemann problem is solved and so on.

To construct approximate solutions, one needs to bound the number of waves and of interactions. To assure this bounds, we rely on accurate estimates of waves number based on variation estimates. Since we obtain estimates on $\mathbf{f}_1(\mathbf{u}_\nu)$, we make the following assumption in order to provide the needed estimates on ρ_ν and q_ν:

(H) There exists a positive $\bar{v}$ such that the approximate solutions $\mathbf{u}_\nu = (\mathbf{u}_{1,\nu}, \dots, \mathbf{u}_{N,\nu})$ attain values in $\widetilde{\Omega} = \Omega_f \cup \{(\rho, q) \in \Omega_c \colon v_c(\rho, q) \geq \bar{v}\}$.

Assumption **(H)** is verified as long as the traffic keeps away from the complete congestion, which is the standard situation in, say, highway traffic.
It is easy to verify the following:

Proposition 2.5.5 *If assumption **(H)** holds, there exists $C = C(\bar{v})$ such that, for every $\mathbf{u}_1$, $\mathbf{u}_2 \in \widetilde{\Omega}$ belonging to the same phase, one has:*

$$|\rho_1 - \rho_2| \leq C\,|\mathbf{f}_1(\mathbf{u}_1) - \mathbf{f}_1(\mathbf{u}_2)|, \qquad |q_1 - q_2| \leq C\,|\mathbf{f}_1(\mathbf{u}_1) - \mathbf{f}_1(\mathbf{u}_2)|\,.$$

Therefore, under assumption **(H)**, a **BV** estimate on $\mathbf{f}_1(\mathbf{u}_{l,\nu})$, $l = 1, \dots, N$, ensures the estimates on the conserved variables, provided we give bounds on the number of phase boundaries in $\mathbf{u}_{l,\nu}$.

The strategy used to get a **BV** estimate on $\mathbf{f}_1(\mathbf{u}_{l,\nu})$ is the following: We determine three basic properties **(Pr1)**, **(Pr2)** and **(Pr3)** of the map $\mathcal{R}_J$, which guarantee the desired estimates. These properties can be verified as in [67].

Consider a wave front tracking approximate solution $\mathbf{u}_\nu$ and define the functionals

$$\begin{aligned} \Gamma_J(t) &:= \sum_{i \in Inc(J)} \mathbf{f}_1\left(\mathbf{u}_{i,\nu}(t, b_i-)\right) \\ TV_f(t) &:= \sum_{l=1}^{N} \mathbf{TV}\left(\mathbf{f}_1\left(\mathbf{u}_{l,\nu}(t,\cdot)\right)\right), \end{aligned}$$

where J is a given junction. These functionals are well defined for every positive time and can vary only when a wave reaches a junction or when two waves interact in a road. Thus, we easily derive for every $t \geq 0$ the bound

$$0 \leq \Gamma_J(t) \leq \#Inc(J)\ F,$$

where $\#Inc(J)$ is the cardinality of $Inc(J)$.

Definition 2.5.6 *Let $(\mathbf{u}_l, \mathbf{u}_r)$ be a wave interacting with J from I_i, $i \in Inc(J)$, then we say that the wave has **decreasing flux** if $\mathbf{f}_1(\mathbf{u}_l) < \mathbf{f}_1(\mathbf{u}_r)$ (i.e. the flux at the junction J from road I_i decreases because of the interaction).*

*Let $(\mathbf{u}_l, \mathbf{u}_r)$ be a wave interacting with J from I_j, $j \in Out(J)$, then we say that the wave has **decreasing flux** if $\mathbf{f}_1(\mathbf{u}_l) > \mathbf{f}_1(\mathbf{u}_r)$ (i.e. the flux at the junction J from road I_j decreases because of the interaction).*

Now I can state the three key properties of a Riemann solver at junctions, which ensures the necessary bounds on the approximate solutions.

Definition 2.5.7 *We say that a Riemann solver $\mathcal{R}_J$ at a junction J has property **(Pr1)** if the solution depends only on the values $\gamma_i^{\max}$, $i \in Inc(J)$, see (2.24), and $\gamma_j^{\max}$, $i \in Inc(J)$, see (2.26).*

*We say that a Riemann solver $\mathcal{R}_J$ has property **(Pr2)** if there exists $C > 0$ such that the following holds true. Assume $\mathbf{u}_0$ is an equilibrium at J, i.e. $\mathcal{R}_J(\mathbf{u}_0) = \mathbf{u}_0$, a wave is interacting with J and there is no other wave in the network. Denote with TV_f^-, resp. TV_f^+, the value of TV_f before, resp. after, the interaction, similarly for Γ_J, and set $\Delta\Gamma_J = \left|\Gamma_J^+ - \Gamma_J^-\right|$, then*

$$TV_f^+ - TV_f^- \leq C\ \min\left\{TV_f^-, \Delta\Gamma_J\right\}.$$

*We say that $\mathcal{R}_J$ has property **(Pr3)** if the following holds true. Assume $\mathbf{u}_0$ is an equilibrium, i.e. $\mathcal{R}_J(\mathbf{u}_0) = \mathbf{u}_0$, and a wave with decreasing flux is interacting with J. Denote with Γ_J^-, resp. Γ_J^+, the value of Γ_J before, respectively after, the interaction. Then,*

$$\Gamma_J^+ \leq \Gamma_J^-.$$

I can now state the existence result.

Theorem 2.5.8 *Consider a network $(\mathcal{I}, \mathcal{J})$, a Riemann solver $\mathcal{R}_J$ for every $J \in \mathcal{J}$ satisfying properties **(Pr1)**, **(Pr2)** and **(Pr3)**, an initial datum $\mathbf{u}_0$ on the network, with bounded total variation, and let $\mathbf{u}_\nu$ be a sequence of wave-front tracking approximate solutions. If **(H)** holds true, then there exists the limit $\mathbf{u}$ of $\mathbf{u}_\nu$ in L^1_{loc} and $\mathbf{u}$ is a weak entropic solution on each road of the network with $\mathbf{u}_0$ as initial datum. Moreover, for every $J \in \mathcal{J}$ and for a.e. $t > 0$:*

$$\mathcal{R}_J\left(\mathbf{u}_J(t)\right) = \mathbf{u}_J(t),$$

where $\mathbf{u}_J = (\mathbf{u}_i(t, b_i-), \mathbf{u}_j(t, a_j+))$ with i varying in $Inc(J)$ and j in $Out(J)$.

I refer the reader to [47, Sec. 6] for the technical details of the proof.

3

Numerical schemes

This chapter is devoted to the numerical approximation of the models with phase transitions presented in Chapter 2 and of the Aw-Rascle model [8]. This study has been done in collaboration with C. Chalons, and is detailed in [32, 31].

3.1 Numerical approximation of traffic flow models with phase transitions

In this section, I present a numerical strategy designed to cope with the difficulties arising in the approximation of solutions to (2.7) and (2.15).

From a numerical point of view, the presence of phase transitions makes standard numerical schemes useless. For example, it is easy to see that the classical Godunov method is not applicable due to the lack of convexity of the whole model phase space $\Omega = \Omega_f \cup \Omega_c$. Indeed, the latter turns out to be a disconnected set in $\mathbb{R}^2$, made of two connected components associated with the free and the congested domains, respectively. In the presence of phase transitions, the projection step taking place in the classical Godunov method can then give values that are not in the domain. This necessarily stops the procedure. We propose a new version of Godunov method, based on a modified averaging strategy and a sampling procedure. More precisely, we modify the mesh cells following the phase boundaries, so that the projection involves only values belonging to the same phase. In order to come back to the original cells, we complete the projection step with a Glimm-type sampling technique.

This scheme is essentially first order accurate, and hence introduces a considerable dissipation away from phase transitions. In order to improve accuracy, we have extended the method to second-order accuracy in space and time.

The averaging procedure on modified cells that we introduce has first been used (to the best of my knowledge) in [103], but in a different context and in a slightly different form. However, the idea of going back to the initial cells by means of a sampling procedure is new and allows to avoid dealing with moving meshes (as in [103]). It has been motivated by recent works proposed by Chalons for approximating nonclassical solutions arising in certain nonlinear hyperbolic equations (see [29], [29] and the references

therein), and very recently by Chalons and Coquel in [30] for computing sharp discrete shock profiles. Let me stress that the model studied here greatly differs from the one addressed in [103], since we are coupling systems of different dimensions. Moreover, we describe a higher order strategy adapted to our model.

The technique is described and tested for (2.7), but it applies without changes to models in [59, 68] (see also [19]).

3.1.1 Description of the method

We introduce a space step Δx and a time step Δt (for simplicity, both of them are assumed to be constant in the forthcoming developments). We set $\nu = \Delta t/\Delta x$. Then, we define the mesh interfaces $x_{j+1/2} = j\Delta x$ for $j \in \mathbb{Z}$ and the intermediate times $t^n = n\Delta t$ for $n \in \mathbb{N}$, and at each time t^n we seek an approximation $\mathbf{u}_j^n$ of the solution of (2.5)-(2.18) on the interval $[x_{j-1/2}, x_{j+1/2})$, $j \in \mathbb{Z}$. Therefore, a piecewise constant approximated solution $x \to \mathbf{u}_\nu(t^n, x)$ of the solution $\mathbf{u}$ is given by

$$\mathbf{u}_\nu(t^n, x) = \mathbf{u}_j^n \ \text{ for all } \ x \in C_j = [x_{j-1/2}; x_{j+1/2}), \ \ j \in \mathbb{Z}, \ \ n \in \mathbb{N}.$$

When $n = 0$, we set $x_j = 0.5 \cdot (x_{j-1/2} + x_{j+1/2})$ and

$$\mathbf{u}_j^0 = \mathbf{u}_0(x_j), \ \text{ for all } \ j \in \mathbb{Z}.$$

Note that the usual $\mathbf{L^2}$ projection is not adapted in the present context since, depending on the initial data, it could artificially introduce unphysical states which are not in the phase space at time $t = 0$ (recall that $\Omega = \Omega_f \cup \Omega_c$ is not connected).

Assuming that a sequence $(\mathbf{u}_j^n)_{j\in\mathbb{Z}}$ is given at time t^n, we propose a strategy to update at the next time t^{n+1}.

Step 1: Evolution in time.
In this first step, one solves the following Cauchy problem

$$\begin{cases} \partial_t \mathbf{v} + \partial_x \mathbf{f}(\mathbf{v}) = 0, \ \ x \in \mathbb{R}, \\ \mathbf{v}(0, x) = \mathbf{u}_\nu(t^n, x), \end{cases} \tag{3.1}$$

for times $t \in [0, \Delta t]$. Recall that $x \to \mathbf{u}_\nu(t^n, x)$ is piecewise constant. Then, under the usual CFL restriction

$$\frac{\Delta t}{\Delta x} \max_{\mathbf{v}} \{|\lambda_i(\mathbf{v})|, \ i = 1 \text{ if } \mathbf{v} \in \Omega_f, \ i = 1, 2 \text{ if } \mathbf{v} \in \Omega_c\} \leq \frac{1}{2}, \tag{3.2}$$

for all the $\mathbf{v}$ under consideration, the solution of (3.1) is known by gluing together the solutions of the Riemann problems set at each interface. More precisely

$$\mathbf{v}(t, x) = \mathcal{R}(\mathbf{u}_j^n, \mathbf{u}_{j+1}^n)\left((x - x_{j+1/2})/t\right) \ \text{ for all } \ (t, x) \in [0, \Delta t] \times [x_j, x_{j+1}], \tag{3.3}$$

where $(t,x) \to \mathcal{R}(\mathbf{u}_j^n, \mathbf{u}_{j+1}^n)\big((x-x_{j+1/2})/t\big)$ denotes the self-similar solution of the Riemann problem

$$\left\{ \begin{array}{l} \partial_t \mathbf{v} + \partial_x \mathbf{f}(\mathbf{v}) = 0, \;\; x \in \mathbb{R}, \;\; t \in \mathbb{R}^{+,\star} \\ \mathbf{v}(0,x) = \left\{ \begin{array}{ll} \mathbf{v}^l & \text{if} \quad x < 0, \\ \mathbf{v}^r & \text{if} \quad x > 0, \end{array} \right. \end{array} \right.$$

whatever $\mathbf{v}^l$ and $\mathbf{v}^r$ are in the phase space $\Omega_f \cup \Omega_c$ (see Sec. 2.2.1).

Step 2: Projection (modified).
In order to define a piecewise constant approximated solution on each cell $\mathcal{C}_j$ at time t^{n+1}, the Godunov scheme averages the solution $\mathbf{v}(\Delta t, x)$ given by (3.3) on each space cell, as expressed by the following update formula :

$$\mathbf{u}_j^{n+1} = \frac{1}{\Delta x} \int_{x_{j-1/2}}^{x_{j+1/2}} \mathbf{v}(\Delta t, x)\, dx, \;\; j \in \mathbb{Z}. \tag{3.4}$$

In order to overcome the difficulties mentioned above, we propose to average the solution on (possibly) modified cells constructed as follows. Let $(\sigma_{j+1/2}^n = \sigma(\mathbf{u}_j^n, \mathbf{u}_{j+1}^n))_{j\in\mathbb{Z}}$ be a sequence of characteristic speeds of propagation at the interfaces $(x_{j+1/2})_{j\in\mathbb{Z}}$ such that:
- if $\mathbf{u}_j^n$ and $\mathbf{u}_{j+1}^n$ are not in the same phase (free or congested), then $\sigma_{j+1/2}^n$ coincides with the speed of propagation of the phase transition in the Riemann solution $\mathcal{R}(\mathbf{u}_j^n, \mathbf{u}_{j+1}^n)$,
- if $\mathbf{u}_j^n$ and $\mathbf{u}_{j+1}^n$ belong to the same phase, then $\sigma_{j+1/2}^n = 0$.
Then, assuming that for all $j \in \mathbb{Z}$ the interface $x_{j+1/2}$ moves at velocity $\sigma_{j+1/2}^n$ between times t^n and $t^{n+1} = t^n + \Delta t$, we define the new interface $\overline{x}_{j+1/2}^n$ at time t^{n+1} setting

$$\overline{x}_{j+1/2}^n = x_{j+1/2} + \sigma_{j+1/2}^n \, \Delta t, \quad j \in \mathbb{Z}. \tag{3.5}$$

We also introduce the new space step

$$\overline{\Delta x}_j^n = \overline{x}_{j+1/2}^n - \overline{x}_{j-1/2}^n, \quad j \in \mathbb{Z}.$$

The modified cells $\overline{\mathcal{C}}_j^n = [\overline{x}_{j-1/2}^n, \overline{x}_{j+1/2}^n)$ may be either smaller or larger than the original ones $\mathcal{C}_j^n$, depending on the signs of the velocities $\sigma_{j+1/2}^n$, $j \in \mathbb{Z}$. This is illustrated in Fig. 3.1. The advantage is that on $\overline{\mathcal{C}}_j^n$ the solution $x \to \mathbf{v}(x, \Delta t)$ given by (3.3) is fully either in the free phase or in the congested phase. Then, averaging this solution on the cells $\overline{\mathcal{C}}_j^n$ provide us with a piecewise constant approximated solution $\overline{\mathbf{u}}_\nu(x, t^{n+1})$ on a non uniform mesh defined by

$$\overline{\mathbf{u}}_\nu(t^{n+1}, x) = \overline{\mathbf{u}}_j^{n+1} \;\text{ for all }\; x \in \overline{C}_j^n, \;\; j \in \mathbb{Z}, \;\; n \in \mathbb{N},$$

with

$$\overline{\mathbf{u}}_j^{n+1} = \frac{1}{\overline{\Delta x}_j^n} \int_{\overline{x}_{j-1/2}^n}^{\overline{x}_{j+1/2}^n} \mathbf{v}(\Delta t, x)\, dx, \;\; j \in \mathbb{Z}.$$

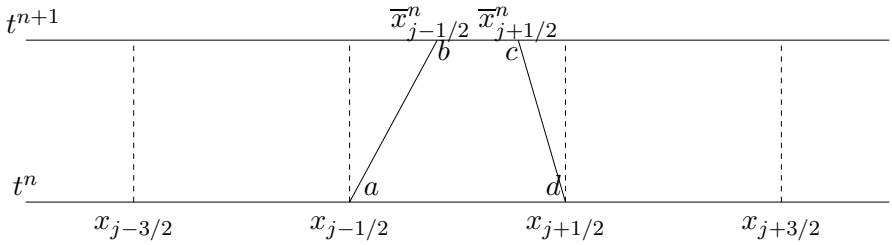

Figure 3.1: An example of averaging element in the modified Godunov method

Even in this case, a simpler formula is obtained for $\overline{\mathbf{u}}_j^{n+1}$ by integrating equation (3.1) over the element $\overline{E} = (abcd)$ defined by :

$$\overline{E} = \{(t,x)\colon t \in [0,\Delta t] \text{ and } x_{j-1/2} + \sigma^n_{j-1/2}\, t \leq x \leq x_{j+1/2} + \sigma^n_{j+1/2}\, t\}$$

(see again Fig. 3.1). Applying Green's theorem on E, we get

$$\overline{\mathbf{u}}_j^{n+1} = \frac{\Delta x}{\overline{\Delta x}_j^n}\mathbf{u}_j^n - \frac{\Delta t}{\overline{\Delta x}_j^n}\left(\overline{\mathbf{f}}^-(\mathbf{u}_j^n,\mathbf{u}_{j+1}^n) - \overline{\mathbf{f}}^+(\mathbf{u}_{j-1}^n,\mathbf{u}_j^n)\right) \text{ for all } j \in \mathbb{Z}, \tag{3.6}$$

with numerical fluxes

$$\overline{\mathbf{f}}^{\pm}(\mathbf{u}_j^n,\mathbf{u}_{j+1}^n) = \mathbf{f}(\mathcal{R}(\mathbf{u}_j^n,\mathbf{u}_{j+1}^n)(\sigma^{n,\pm}_{j+1/2})) - \sigma^n_{j+1/2}\mathcal{R}(\mathbf{u}_j^n,\mathbf{u}_{j+1}^n)(\sigma^{n,\pm}_{j+1/2}) \text{ for all } j \in \mathbb{Z}. \tag{3.7}$$

Let me notice that if $\mathbf{u}_j^n$ and $\mathbf{u}_{j+1}^n$ are in the same phase, then $\mathcal{R}(\mathbf{u}_j^n,\mathbf{u}_{j+1}^n)(\sigma^{n,-}_{j+1/2})$ and $\mathcal{R}(\mathbf{u}_j^n,\mathbf{u}_{j+1}^n)(\sigma^{n,+}_{j+1/2})$ also does. The conservation property

$$\begin{array}{c} \mathbf{f}(\mathcal{R}(\mathbf{u}_j^n,\mathbf{u}_{j+1}^n)(\sigma^{n,-}_{j+1/2})) - \sigma^n_{j+1/2}\mathcal{R}(\mathbf{u}_j^n,\mathbf{u}_{j+1}^n)(\sigma^{n,-}_{j+1/2}) \\ = \\ \mathbf{f}(\mathcal{R}(\mathbf{u}_j^n,\mathbf{u}_{j+1}^n)(\sigma^{n,+}_{j+1/2})) - \sigma^n_{j+1/2}\mathcal{R}(\mathbf{u}_j^n,\mathbf{u}_{j+1}^n)(\sigma^{n,+}_{j+1/2}) \end{array} \tag{3.8}$$

then remains valid thanks to Rankine-Hugoniot conditions. Actually, note that in such a situation $\sigma^n_{j+1/2} = 0$ by definition. If $\mathcal{R}(\mathbf{u}_j^n,\mathbf{u}_{j+1}^n)(\sigma^{n,-}_{j+1/2})$ and $\mathcal{R}(\mathbf{u}_j^n,\mathbf{u}_{j+1}^n)(\sigma^{n,+}_{j+1/2})$ are not in the same phase, equality (3.8) makes sense only for the first component associated with the mass conservation.

Step 3: Sampling.
In order to avoid dealing with moving meshes, we complete the projection step defining a new approximation $\mathbf{u}_j^{n+1}$ of the solution at time t^{n+1} on the original cells $\mathcal{C}_j$, $j \in \mathbb{Z}$. To this aim, for all $j \in \mathbb{Z}$, we propose to pick up randomly on the cell $\mathcal{C}_j$ a value between $\overline{\mathbf{u}}_{j-1}^{n+1}$, $\overline{\mathbf{u}}_j^{n+1}$ and $\overline{\mathbf{u}}_{j+1}^{n+1}$, in agreement with their rate of presence in the cell. More precisely, given an equidistributed random sequence (a_n) within interval $(0,1)$, we set :

$$\mathbf{u}_j^{n+1} = \begin{cases} \overline{\mathbf{u}}_{j-1}^{n+1} & \text{if} \quad a_{n+1} \in (0, \frac{\Delta t}{\Delta x}\max(\sigma^n_{j-1/2}, 0)), \\ \overline{\mathbf{u}}_j^{n+1} & \text{if} \quad a_{n+1} \in [\frac{\Delta t}{\Delta x}\max(\sigma^n_{j-1/2}, 0), 1 + \frac{\Delta t}{\Delta x}\min(\sigma^n_{j+1/2}, 0)), \\ \overline{\mathbf{u}}_{j+1}^{n+1} & \text{if} \quad a_{n+1} \in [1 + \frac{\Delta t}{\Delta x}\min(\sigma^n_{j+1/2}, 0), 1), \end{cases} \tag{3.9}$$

for all $j \in \mathbb{Z}$.
Following a proposal by Collela [38], we consider the van der Corput random sequence (a_n) defined by

$$a_n = \sum_{k=0}^{m} i_k 2^{-(k+1)}, \tag{3.10}$$

where $n = \sum_{k=0}^{m} i_k 2^k$, $i_k = 0, 1$, denotes the binary expansion of the integers $n = 1, 2, ...$ This sequence is often used in the context of Glimm scheme because it leads to very good results in the smooth parts of the solutions (see for instance [38, 33] for illustration).

It is worth noting that, due to the sampling procedure, the algorithm proposed is not "strictly" conservative in the classical sense of finite volumes methods. However, the numerical tests presented in Sec. 4.6.3 show that the scheme is "weakly" conservative in the sense that phase transitions propagate with the right speeds (given by the Rankine-Hugoniot condition) and conservation errors seem to tend to zero with the mesh size.

Remark. Of course, the random choice method (Glimm scheme) can be applied successfully to compute solutions of (2.5). Nevertheless, our method doesn't need to compute all the values in the Riemann solution, but only the values on both sides of the phase transition. Moreover, the algorithm coincides with the classical Godunov scheme, and hence it is conservative, away from phase transitions.

3.1.2 Higher order extension of the method in space and time

We have proposed a both space and time second-order extension of the modified Godunov scheme presented in Sec. 3.1.1. Our strategy relies on the very popular MUSCL approach for the space accuracy and on a Runge-Kutta technique for the time accuracy. As usual, the second-order accuracy is obtained for smooth solutions only, even if better numerical results are expected also when discontinuities (or non smooth regions) are present. In our context, it is important to notice that smooth solutions exist, but, necessarily, take values in a fixed phase (free or congested) since phase changes are always associated with discontinuities. As a consequence, the resulting procedure has to be considered second-order accurate away from phase transitions. For this reason, I will focus on the first part of the projection step only, the sampling procedure being kept unchanged.

Below, I first address the space accuracy and show how to obtain a MUSCL scheme which is stable in the $\mathbf{L^1}$ sense. Then, I deal with the time accuracy and show how to apply a second-order Runge-Kutta technique.

Accuracy in space
I begin by briefly recalling the MUSCL method for obtaining the second-order accuracy in space. For more details, I refer the reader to [99, 69, 97, 17] and the references therein. Assume that there exists a change of variables $\mathbf{u} \to \mathbf{U} = \varphi(\mathbf{u})$ from Ω onto some set

$\Omega_{\mathbf{U}}$. The starting point of the method consists in replacing at each time t^n and on each cell C_j the constant values $\mathbf{u}_j^n$ by means of φ and a linear reconstruction of $\mathbf{U}$. We set

$$\mathbf{u}^n(x) = \varphi^{-1}(\mathbf{U}^n(x))$$

for $x \in C_j = [x_{j-1/2}; x_{j+1/2})$, with

$$\mathbf{U}^n(x) = \mathbf{U}_j^n + s_j^n \frac{(x - x_j)}{\Delta x}, \quad \mathbf{U}_j^n = \varphi(\mathbf{u}_j^n),\ j \in \mathbb{Z}.$$

Above, x_j represents the center of the cell C_j, $x_j = \frac{1}{2}(x_{j-1/2} + x_{j+1/2})$, and s_j^n is the slope of the linear reconstruction. The choice of the reconstructed variable $\mathbf{U}$ generally depends on the system under consideration. In the present study, in order to ensure the $\mathbf{L^1}$ stability of the method, the reconstruction can be performed on the conservative variable for the scalar equation modeling the free flow ($\mathbf{U} = \mathbf{u}$), while the Riemann variables $\mathbf{U} = (w_1, w_2)$ turn out to be more adapted for the congested phase.
We denote $\mathbf{u}_j^{n,\pm}$ and $\mathbf{U}_j^{n,\pm}$ the values at the edges $x = x_{j\pm1/2}$ of $\mathbf{u}^n$ and $\mathbf{U}^n$ respectively:

$$\mathbf{u}_j^{n,\pm} = \varphi^{-1}(\mathbf{U}_j^{n,\pm}), \qquad \mathbf{U}_j^{n,\pm} = \mathbf{U}_j^n \pm \frac{1}{2} s_j^n.$$

Then we replace the couple $(\mathbf{u}_j^n, \mathbf{u}_{j+1}^n)$ with $(\mathbf{u}_j^{n,+}, \mathbf{u}_{j+1}^{n,-})$ in the evaluation of the numerical fluxes $\overline{\mathbf{f}}_{j+1/2}^{n,\pm}$ at each interface $x_{j+1/2}$. More precisely, we consider $\overline{\mathbf{f}}^{\pm}(\mathbf{u}_j^{n,+}, \mathbf{u}_{j+1}^{n,-})$ instead of $\overline{\mathbf{f}}^{\pm}(\mathbf{u}_j^n, \mathbf{u}_{j+1}^n)$ in (3.7).

As far as the choice of the reconstructed variable $\mathbf{U}$ and the slopes s_j^n is concerned, it is well-known that these have to be carefully determined for stability reasons. Once $\mathbf{U}$ is chosen, an usual choice for s_j^n is given by a slope-limiter procedure with for instance the so-called minmod limiter:

$$s_j^n = \text{minmod}(\mathbf{U}_{j+1}^n - \mathbf{U}_j^n, \mathbf{U}_j^n - \mathbf{U}_{j-1}^n), \tag{3.11}$$

where the minmod function is defined by

$$\text{minmod}(a, b) = \begin{cases} \text{sgn}\,(a)\ \min(|a|, |b|) & \text{if } ab \geq 0, \\ 0 & \text{otherwise,} \end{cases}$$

for two scalar quantities a and b. In (3.11), minmod is applied component by component.

In the rest of this section, in order to simplify the notations, I will assume that the three states $\mathbf{U}_{j-1}^n$, $\mathbf{U}_j^n$ and $\mathbf{U}_{j+1}^n$ in (3.11) belong to the same phase. Otherwise, if $\mathbf{U}_{j-1}^n$ and/or $\mathbf{U}_{j+1}^n$ are not in the same phase of $\mathbf{U}_j^n$, they are replaced by $\varphi(\mathbf{u}_+(\mathbf{u}_{j-1}^n, \mathbf{u}_j^n))$ and/or $\varphi(\mathbf{u}_-(\mathbf{u}_j^n, \mathbf{u}_{j+1}^n))$, where $\mathbf{u}_\pm(\mathbf{u}_j^n, \mathbf{u}_{j+1}^n)$ represent for all j the values on both sides of the phase transition in the Riemann solution associated with initial states $\mathbf{u}_j^n$ and $\mathbf{u}_{j+1}^n$. Then, by definition $\varphi(\mathbf{u}_+(\mathbf{u}_{j-1}^n, \mathbf{u}_j^n))$, $\mathbf{u}_j^n$ and $\varphi(\mathbf{u}_-(\mathbf{u}_j^n, \mathbf{u}_{j+1}^n))$ belong to the same phase.

The objective is guaranteeing the $\mathbf{L^1}$ stability of the reconstruction procedure, i.e., $\mathbf{u}_j^{n,\pm}$ to necessarily belong to the phase space Ω. This relies on a suitable choice of $\mathbf{U}$.

If $\mathbf{u}_j^n \in \Omega_f$, we consider a conservative reconstruction: $\mathbf{U} = \mathbf{u}$. Since q always equals ρV in the free phase, the constraint $\mathbf{u}_j^{n,\pm} \in \Omega_f$ reads

$$V_f \leq v_f(\rho_j^{n,\pm}),$$

which by definition of v_f is equivalent to

$$0 \leq \rho_j^{n,\pm} \leq R\left(1 - \frac{V_f}{V}\right).$$

Since the above set is convex, we can take

$$s_j^n = \text{minmod}(\rho_{j+1}^n - \rho_j^n, \rho_j^n - \rho_{j-1}^n).$$

If $\mathbf{u}_j^n \in \Omega_c$, the constraints $\mathbf{u}_j^{n,\pm} \in \Omega_c$ are equivalent to

$$\left\{ \begin{array}{l} 0 \leq w_1(\rho_j^{n,\pm}, q_j^{n,\pm}) \leq V_c, \\ W_2^- \leq w_2(\rho_j^{n,\pm}, q_j^{n,\pm}) \leq W_2^+. \end{array} \right. \tag{3.12}$$

We set $\mathbf{U} = (w_1(\rho, q), w_2(\rho, q))$, where w_1, w_2 denote the Riemann invariants defined in (2.9), and define

$$\left\{ \begin{array}{l} (w_1)_j^{n,\pm} = (w_1)_j^n \pm \frac{1}{2}\text{minmod}((w_1)_{j+1}^n - (w_1)_j^n, (w_1)_j^n - (w_1)_{j-1}^n), \\ (w_2)_j^{n,\pm} = (w_2)_j^n \pm \frac{1}{2}\text{minmod}((w_2)_{j+1}^n - (w_2)_j^n, (w_2)_j^n - (w_2)_{j-1}^n), \end{array} \right.$$

which is easily seen to imply the last two constraints in (3.12) by definition of the minmod function (and since $\mathbf{u}_{j-1}^n$ and $\mathbf{u}_{j+1}^n$ are also assumed to be in Ω_c).

Accuracy in time

In order to have second-order accuracy in time in smooth regions and away from phase transitions, we propose a simple numerical time integration that is equivalent, away from phase transitions, to the well-known RK2 method (2nd order Runge-Kutta, or Heun).

The MUSCL scheme obtained above writes

$$\overline{\mathbf{u}}_j^{n+1} - \mathbf{u}_j^n = \frac{\Delta x - \overline{\Delta x}_j^n}{\overline{\Delta x}_j^n}\mathbf{u}_j^n - \frac{\Delta t}{\overline{\Delta x}_j^n}(\overline{\mathbf{f}}^-(\mathbf{u}_j^{n,+}, \mathbf{u}_{j+1}^{n,-}) - \overline{\mathbf{f}}^+(\mathbf{u}_{j-1}^{n,+}, \mathbf{u}_j^{n,-})).$$

From this formula and the approximated values $(\mathbf{u}_j^n)_{j\in\mathbb{Z}}$ on the cells $\mathcal{C}_j$, we then define a first approximation $\overline{\mathbf{u}}_j^{n+1=}$ of the updated value on the cell $\overline{\mathcal{C}}_j^n$ by

$$\overline{\mathbf{u}}_j^{n+1=} - \mathbf{u}_j^n = \frac{\Delta x - \overline{\Delta x}_j^n}{\overline{\Delta x}_j^n}\mathbf{u}_j^n - \frac{\Delta t}{\overline{\Delta x}_j^n}(\overline{\mathbf{f}}^-(\mathbf{u}_j^{n,+}, \mathbf{u}_{j+1}^{n,-}) - \overline{\mathbf{f}}^+(\mathbf{u}_{j-1}^{n,+}, \mathbf{u}_j^{n,-})).$$

Then, another one denoted $\overline{\mathbf{u}}_j^{n+1-}$ is obtained from the first approximations $(\overline{\mathbf{u}}_j^{n+1=})_{j\in\mathbb{Z}}$:

$$\overline{\mathbf{u}}_j^{n+1-} - \mathbf{u}_j^{n+1=} = \frac{\Delta x - \overline{\Delta x}_j^n}{\overline{\Delta x}_j^n}\overline{\mathbf{u}}_j^{n+1=} - \frac{\Delta t}{\overline{\Delta x}_j^n}(\overline{\mathbf{f}}^-(\mathbf{u}_j^{n+1=,+}, \mathbf{u}_{j+1}^{n+1=,-}) - \overline{\mathbf{f}}^+(\mathbf{u}_{j-1}^{n+1=,+}, \mathbf{u}_j^{n+1=,-})).$$

Finally, $\overline{\mathbf{u}}_j^{n+1}$ is defined from these two approximations setting

$$\overline{\mathbf{u}}_j^{n+1} = \mathbf{u}_j^n + \frac{1}{2}[(\overline{\mathbf{u}}_j^{n+1=} - \mathbf{u}_j^n) + (\overline{\mathbf{u}}_j^{n+1-} - \overline{\mathbf{u}}_j^{n+1=})],$$

which equivalently recasts as

$$\begin{aligned}\overline{\mathbf{u}}_j^{n+1} = \mathbf{u}_j^n \quad &+ \quad \frac{\Delta x - \overline{\Delta x}_j^n}{2\overline{\Delta x}_j^n}(\mathbf{u}_j^n + \overline{\mathbf{u}}_j^{n+1=}) \\ &- \quad \frac{\Delta t}{2\overline{\Delta x}_j^n}(\overline{\mathbf{f}}^-(\mathbf{u}_j^{n,+}, \mathbf{u}_{j+1}^{n,-}) - \overline{\mathbf{f}}^+(\mathbf{u}_{j-1}^{n,+}, \mathbf{u}_j^{n,-})) \\ &- \quad \frac{\Delta t}{2\overline{\Delta x}_j^n}(\overline{\mathbf{f}}^-(\mathbf{u}_j^{n+1=,+}, \mathbf{u}_{j+1}^{n+1=,-}) - \overline{\mathbf{f}}^+(\mathbf{u}_{j-1}^{n+1=,+}, \mathbf{u}_j^{n+1=,-})).\end{aligned}$$

Note that, away from phase transitions, we have $\overline{\Delta x}_j^n = \Delta x$ and the numerical fluxes coincide with the ones of the usual Godunov method. In this case we get

$$\begin{aligned}\overline{\mathbf{u}}_j^{n+1} = \mathbf{u}_j^n \quad &- \quad \frac{\Delta t}{2\Delta x}\big(\mathbf{f}(\mathcal{R}(\mathbf{u}_j^{n,+}, \mathbf{u}_{j+1}^{n,-})(0)) - \mathbf{f}(\mathcal{R}(\mathbf{u}_{j-1}^{n,+}, \mathbf{u}_j^{n,-})(0))\big) \\ &- \quad \frac{\Delta t}{2\Delta x}\big(\mathbf{f}(\mathcal{R}(\mathbf{u}_j^{n+1=,+}, \mathbf{u}_{j+1}^{n+1=,-})(0)) - \mathbf{f}(\mathcal{R}(\mathbf{u}_{j-1}^{n+1=,+}, \mathbf{u}_j^{n+1=,-})(0))\big),\end{aligned}$$

and we recover the classical method consisting in a RK2 time integration together with a MUSCL reconstruction strategy for the space discretization. The scheme is then second-order accurate in both space and time in smooth regions.

3.1.3 Numerical experiments

In [32] we have tested the algorithm on several cases. Here, I present the results obtained on three Riemann problems leading to solutions involving phase transitions. The parameters of the model are: $R = 1,\ V = 2,\ V_f = 1,\ V_c = 0.85,\ Q = 0.5,\ Q^- = 0.25,\ Q^+ = 1.5$. The numerical solutions are represented by the density and velocity profiles, and are compared to the exact solutions. Solutions computed by the second-order extension of the method are also showed.

For **Test A**, we consider $\rho^l = 0.7,\ \rho^l v^l = 0.3$ in the congested phase and $\rho^r = 0.3$ in the free phase, leading to a solution made of a rarefaction in the congested phase, followed by a phase transition to a free state, itself followed by a rarefaction wave in the free phase. The solutions are plotted on Fig. 3.2 at time $T_f = 0.5$. For this test case, we have used a mesh containing 500 points ($\Delta x = 0.002$).

For **Test B**, we choose $\rho^l = 0.35$ in the free phase and $\rho^r = 0.6,\ \rho^r v^r = 0.25$, in the congested phase. The corresponding solution is a shock-like phase transition followed by a contact discontinuity. Fig. 3.3 plots the solution at time $T_f = 0.6$ with $\Delta x = 0.002$.

For **Test C**, we take $\rho^l = 0.215$ in the free phase and $\rho^r = 0.7$, $\rho^r v^r = 0.2$, in the congested phase, leading a solution composed of a phase transition followed by a rarefaction wave, and a contact discontinuity propagating with positive speed. In this case the congested state of the phase transition is very difficult to capture properly, due to the numerical diffusion of the scheme, which is present in the rarefaction wave. Note that this state is always over-estimated from the proposed averaging strategy. However, we observe a good agreement between the numerical solution and the exact solution, and the numerical solution becomes closer to the exact one when the order of accuracy of the method is higher, as it is illustrated on Fig. 3.4, where we have taken $\Delta x = 0.005$ and $T_f = 0.8$.

Conservation error. Due to the random sampling in *Step 3*, the method does not strictly conserve the mass ρ. We measure the conservation error on the piecewise constant numerical solution ρ_ν defined as

$$\rho_\nu(t,x) = \rho_j^n \quad \text{if} \quad (t,x) \in [t^n, t^{n+1}) \times [x_{j-1/2}, x_{j+1/2}),$$

between times $t = 0$ and $t = T$, for some $T > 0$. In the computational domain $[-0.5, 0.5]$, we compare with 0 the function $E : T \in \mathbb{R}^+ \to E(T) \in \mathbb{R}$ with $E(T)$ defined by

$$\int_{x_0}^{x_1} \rho_\nu(T,x)\ dx \quad \times \quad E(T) = \int_{x_0}^{x_1} \rho_\nu(T,x)\ dx - \int_{x_0}^{x_1} \rho_\nu(0,x)\ dx + \int_0^T \{\rho v_c(\rho,q)\}_\nu(t,x_1)\ dt - \int_0^T \{\rho v_c(\rho,q)\}_\nu(t,x_0)\ dt.$$

Recall that $q = \rho V$ in the free phase. $E(T)$ represents the relative conservation error of ρ_ν at time T on the interval $[x_0, x_1]$. In the next table, we give for the **Tests A, B, C** the values of the $\mathbf{L^1}$ norm $\frac{1}{T_f}||E||_{\mathbf{L^1}(0,T_f)}$ of E, namely

$$\frac{1}{T_f}||E||_{\mathbf{L^1}(0,T_f)} = \frac{1}{T_f}\int_0^{T_f} |E(T)|dT = \sum_{t^n=0}^{t^{n+1}=T_f} \frac{(t^{n+1}-t^n)}{T_f}|E(t^n)|,$$

where T_f is the final time of the corresponding simulations. We observe that the conservation errors are very small and decrease with the mesh size.

# of points	**Test A**	**Test B**	**Test C**
100	0.44%	0.64%	0.91%
500	0.16%	0.17%	0.22%
1000	0.094%	0.095%	0.11%
2000	0.051%	0.057%	0.052%

Table 3.1: Conservation errors (first-order scheme).

# of points	**Test A**	**Test B**	**Test C**
100	0.25%	0.23%	0.87%
500	0.054%	0.071%	0.21%
1000	0.030%	0.044%	0.11%
2000	0.016%	0.031%	0.052%

Table 3.2: Conservation errors (second-order scheme).

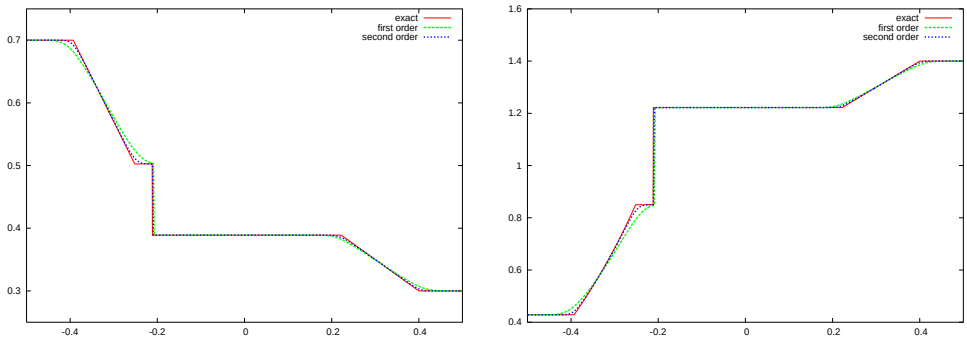

Figure 3.2: **Test A**: ρ (Left) and v (Right)

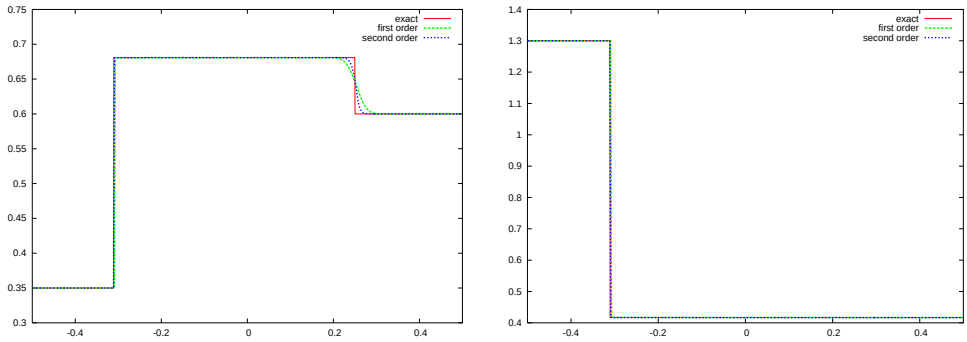

Figure 3.3: **Test B**: ρ (Left) and v (Right)

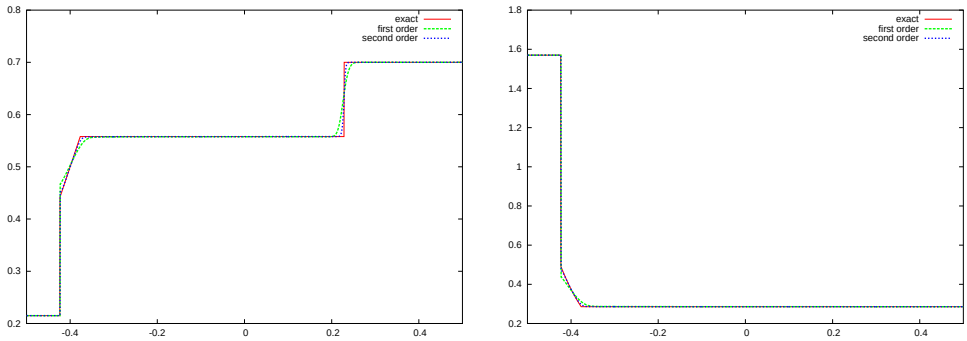

Figure 3.4: **Test C**: ρ (Left) and v (Right)

3.2 Numerical approximation of the Aw-Rascle model

In this section, I present a numerical scheme designed to capture the contact discontinuities in the Aw-Rascle model of traffic flow

$$\begin{cases} \partial_t \rho + \partial_x (\rho v) = 0 \,, \\ \partial_t y + \partial_x (y v) = 0 \,, \end{cases} \qquad t > 0, \;\; x \in \mathbb{R} \,, \tag{3.13}$$

that has been already surveyed in Sec. 2.3. The system under consideration is strictly hyperbolic for $\rho > 0$, with a genuinely nonlinear and a linearly degenerate characteristic field. The latter is associated with the faster eigenvalue, which is equal to v, and develops discontinuous waves, the so-called contact discontinuities, along which the speed of propagation is constant and given by v. I will focus on the numerical approximation of these contact discontinuities.

In the past decade, the numerical approximation of contact discontinuities received a lot of attention in the context of compressible multicomponent (or multifluid) flows. Indeed, when the flow is made of several species, it is observed that classical conservative schemes (like Godunov's scheme) generate important nonphysical oscillations near the material fronts, eventually leading to numerical solutions that are not precise (at least for realistic meshes). The same pathologies also exist for single fluid computations, and they are going to appear for system (3.13). Several corrections have been proposed in the literature, see for instance [78, 79, 1, 94, 62, 2, 12] and the references therein. Roughly speaking, the common idea is to keep on using a classical conservative scheme far from the material interfaces and to introduce a *non conservative* modification in the regions where the problem occurs, in order to preserve constant pressure and velocity. Note however that the threshold technique often attached to the local treatment prevents the methods from strictly preserving isolated contact discontinuities. The resulting *non conservative* schemes give good results and seem to be numerically converging. In addition, these strategies are usually designed for models involving at least two fluids,

and then two pressure laws. As a consequence, it seems difficult to apply them to our "single fluid" system (3.13).

The algorithm presented here is based on the *Transport-Equilibrium* approach recently introduced by Chalons in [28]. The idea of the Transport-Equilibrium schemes lies on the following observation. On one side, classical Godunov-type schemes are cheap and give good approximations of smooth solutions. On the other side, Glimm scheme works well for discontinuities, but it requires the computation of the solution to the Riemann problem at each mesh interface, being in general very expensive. Hence the idea is to construct an hybrid method based on a Godunov type technique, but using a random strategy near the discontinuities we are interested for. These schemes require two steps: a Transport step to localize the discontinuity and make it move by a random sampling, and an Equilibrium step to take into account the regular parts by introducing a suitable numerical flux. I would like to underline here that the Transport-Equilibrium method was originally designed for scalar conservations laws with non classical shocks. On the contrary in this case it is applied to a 2×2 system. It allows to remove the spurious oscillations generated by the Godunov scheme near the contact discontinuities. As expected, the algorithm is *non conservative* but numerical experiments give very accurate numerical solutions with *sharp* (without numerical diffusion) contact discontinuities and very small conservation errors that decrease with the mesh size. Moreover, we are able to prove that the method enjoys important stability properties like strong consistency and a maximum principle on the two Riemann invariants of system (3.13), see Theorems 3.2.1 and 3.2.2 in Sec. 3.2.2. Note also that the algorithm is free of threshold techniques. As a consequence of all these properties, contact discontinuities are *always* computed without oscillations.

To conclude, I wish to mention that the same difficulties related to the numerical computation of contact discontinuities are expected to occur for the second-order model proposed by Colombo [39], that has a linearly degenerate field. Moreover, the techniques presented in this section can be easily adapted and used for models with phase transitions (2.7), (2.15), in combination with the numerical scheme described in the previous section.

In the following sections, I will use the notations introduced in Sec. 3.1.1.

3.2.1 Failure of Godunov scheme in properly capturing contact discontinuities

I begin recalling that the self-similar solution to the general Riemann problem for (3.13), i.e.

$$\begin{cases} \partial_t \mathbf{u} + \partial_x \mathbf{f}(\mathbf{u}) = 0, \\ \mathbf{u}(0,x) = \begin{cases} \mathbf{u}^l & \text{if } x < 0, \\ \mathbf{u}^r & \text{if } x > 0, \end{cases} \end{cases} \tag{3.14}$$

is made of one Lax wave (shock or rarefaction) moving with negative and/or positive speeds, and a contact discontinuity always moving with positive speed $v = v^r$. For a more detailed description of the Riemann solver see [8]. Using the Riemann coordinates introduced in (2.16) and the property that w_1 (respectively w_2) is constant across the

waves of the first (respectively second) family, the intermediate state $\mathbf{u}^\star(\mathbf{u}^l, \mathbf{u}^r)$ in the Riemann solution is easily computed :

$$\left\{ \begin{array}{l} w_1^\star = w_1^l = v^l + p(\rho^l), \\ w_2^\star = w_2^r = v^r, \end{array} \right. \quad \Longrightarrow \quad \left\{ \begin{array}{l} \rho^\star = \rho^l \exp\left(\dfrac{v^l - v^r}{v_{ref}}\right), \\ y^\star = \rho^\star(v^r + p(\rho^\star)). \end{array} \right.$$

Note that $v^\star := v(\mathbf{u}^\star(\mathbf{u}^l, \mathbf{u}^r)) = v^r$.

Let us consider the Riemann problem (3.14) with $\mathbf{u}^l = (\rho^l, y^l)$ and $\mathbf{u}^r = (\rho^r, y^r)$ such that $\rho^l > 0$, $\rho^r > 0$, $\rho^l \neq \rho^r$ but $v^l = v^r > 0$. In this case, the solution simply consists in a contact discontinuity propagating at speed $v_0 := v^l = v^r$:

$$\mathbf{u}(t,x) = \left\{ \begin{array}{lll} \mathbf{u}^l & \text{if} & x < v_0 t, \\ \mathbf{u}^r & \text{if} & x > v_0 t. \end{array} \right.$$

The first time step:
The discretization of the initial data gives

$$\mathbf{u}_j^0 = \left\{ \begin{array}{lll} \mathbf{u}^l & \text{if} & j \leq 0, \\ \mathbf{u}^r & \text{if} & j > 0. \end{array} \right.$$

Due to the CFL restriction (3.2) and the assumption $v_0 > 0$, only the cell $\mathcal{C}_1$ may be affected by the update formula (3.4) in the first time step. In other words,

$$\mathbf{u}_j^1 = \mathbf{u}_j^0 \quad \text{for all} \quad j \neq 1.$$

For $j = 1$, (3.4) is equivalent to

$$\rho_1^1 = \overline{\rho} \quad \text{and} \quad y_1^1 = \overline{y},$$

where we have used the notation

$$\overline{\alpha} = \frac{1}{\Delta x} \int_0^{\Delta x} \alpha(\Delta t, x)\ dx.$$

We observe that

$$\overline{y} = \frac{1}{\Delta x} \int_0^{\Delta x} y(\Delta t, x)\ dx = \frac{1}{\Delta x} \int_0^{\Delta x} (\rho v + \rho p(\rho))(\Delta t, x)\ dx.$$

Since the velocity remains constant across a contact discontinuity, we have

$$\overline{y} = v_0 \frac{1}{\Delta x} \int_0^{\Delta x} \rho(\Delta t, x)\ dx + \frac{1}{\Delta x} \int_0^{\Delta x} (\rho p(\rho))(\Delta t, x)\ dx = v_0 \overline{\rho} + \overline{\rho p(\rho)}.$$

On the contrary, if we calculate v_1^1 from $\overline{\rho}$ and $\overline{y}$, we get

$$v_1^1 = \frac{\overline{y}}{\overline{\rho}} - p(\overline{\rho}) = v_0 + \frac{\overline{\rho p(\rho)} - \overline{\rho} p(\overline{\rho})}{\overline{\rho}}.$$

We observe that the function $\rho \to \rho p(\rho)$ is convex. By Jensen's inequality, we deduce $\overline{\rho p(\rho)} \geq \overline{\rho}\, p(\overline{\rho})$ and then

$$v_1^1 \geq v_0,$$

with strict inequality generally speaking. This means that after the first time iteration, the velocity no longer equals v_0 everywhere. We conclude that the Godunov method is not able to keep constant the velocity profile and then to properly capture contact discontinuities. In Sec. 3.2.3, numerical tests show that the non physical values created by the Godunov method around contact discontinuities may significantly damage the numerical solution.

Remark. (i) The failure that I have just underlined is due to the fact that Godunov method does not obey to a maximum principle property on the velocity v. The algorithm proposed in the next section verifies the maximum principle on the Riemann invariants v and $v + p(\rho)$, see Theorem 3.2.2.

(ii) It is important to notice that if we consider an isolated 1-wave between $\mathbf{u}^l$ and $\mathbf{u}^r$, the Godunov method actually keeps constant the Riemann invariant $v + p(\rho)$. If we set $C_0 := v^l + p(\rho^l) = v^r + p(\rho^r)$, we have indeed

$$(v + p(\rho))_1^1 = (\frac{y}{\rho})_1^1 = \frac{\overline{y}}{\overline{\rho}} = \frac{\overline{\rho(v + p(\rho))}}{\overline{\rho}} = C_0 \frac{\overline{\rho}}{\overline{\rho}} = C_0.$$

This property is very interesting and means in particular that all the points in a numerical 1-wave profile associated with Godunov's method belong to the same 1-wave curve for all the possible choices of $p(\rho)$. This property is also satisfied by our method (see Theorems 3.2.1 (iii) and 3.2.2).

3.2.2 A Transport-Equilibrium scheme

In [31], we have proposed an algorithm that allows to avoid the spurious oscillations generated near the contact discontinuities by the classical Godunov method. The basic idea is to treat in a different way contact discontinuities on one side, and other waves (shock and rarefaction waves) on the other side. We keep on using Godunov method for shocks and rarefactions (since it works well and it is conservative), and we propose a particular treatment for contact discontinuities, which make use of a (Glimm's) random sampling strategy.

We set

$$\mathbf{g}(\mathbf{u}^l, \mathbf{u}^r) = \mathbf{f}(\mathcal{R}(\mathbf{u}^l, \mathbf{u}^r)(0-)),$$

so that the numerical flux of the Godunov method writes $\mathbf{f}_{j+1/2}^n = \mathbf{g}(\mathbf{u}_j^n, \mathbf{u}_{j+1}^n)$ for all $j \in \mathbb{Z}$. Recall that $\mathbf{u}^\star(\mathbf{u}^l, \mathbf{u}^r)$ is the intermediate state in the Riemann solution $\mathbf{u_r}(\cdot; \mathbf{u}^l, \mathbf{u}^r)$ (between the 1-wave and the 2-contact discontinuity). See Fig. 3.5.

The method is made of two steps. On each interval $[x_j, x_{j+1}]$, $j \in \mathbb{Z}$, the first step takes into account only the contact discontinuity in the Riemann solution $\mathcal{R}(\mathbf{u}_j^n, \mathbf{u}_{j+1}^n)$, while the second step focuses on the 1-wave. Our procedure may be viewed as a waves

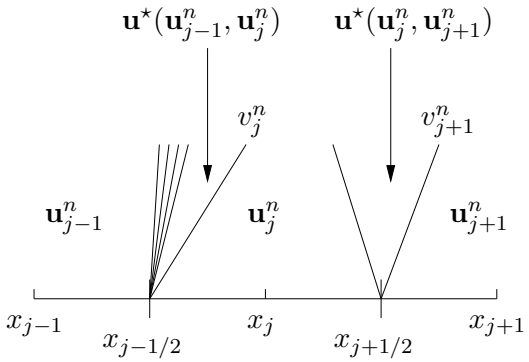

Figure 3.5: Notations used in Sec. 3.2.2.

splitting strategy, performed locally around each interface $x_{j+1/2}$ where a Riemann problem is set.

Assuming as given $\mathbf{u}^n_{j-1}$, $\mathbf{u}^n_j$ and $\mathbf{u}^n_{j+1}$, we show now how to define $\mathbf{u}^{n+1}_j$. Note that, under the CFL condition (3.2), it is sufficient to focus on the interval $[x_{j-1}, x_{j+1}]$, since the Riemann problems set at other interfaces are not expected to influence the definition of $\mathbf{u}^{n+1}_j$. See Fig. 3.5.

Step 1: Propagation of contact discontinuities ($t^n \to t^{n+1/2}$).
In this step, we focus on the dynamics of contact discontinuities. The Riemann problems at the interfaces $x_{j-1/2}$ and $x_{j+1/2}$ generally develop a 1-wave and a 2-contact discontinuity, the latter propagating at speed v^n_j and v^n_{j+1} respectively (see again Fig. 3.5). These velocities being nonnegative, the contact discontinuities only affect $[x_{j-1/2}, x_j)$ and $[x_{j+1/2}, x_{j+1}]$, but not $[x_{j-1}, x_{j-1/2})$ and $[x_j, x_{j+1/2})$. This means that the Riemann solutions $\mathcal{R}(\mathbf{u}^n_{j-1}, \mathbf{u}^n_j)$ and $\mathcal{R}(\mathbf{u}^n_j, \mathbf{u}^n_{j+1})$ can be replaced in this step with the following function

$$\tilde{\mathbf{v}}(t,x) = \begin{cases} \mathbf{u}^n_{j-1} & \text{if} \quad x \in [x_{j-1}, x_{j-1/2}), \\ \mathbf{u}^\star(\mathbf{u}^n_{j-1}, \mathbf{u}^n_j) & \text{if} \quad x \in [x_{j-1/2}, x_{j-1/2} + v^n_j(t-t^n)), \\ \mathbf{u}^n_j & \text{if} \quad x \in [x_{j-1/2} + v^n_j(t-t^n), x_{j+1/2}), \\ \mathbf{u}^\star(\mathbf{u}^n_j, \mathbf{u}^n_{j+1}) & \text{if} \quad x \in [x_{j+1/2}, x_{j+1/2} + v^n_{j+1}(t-t^n)), \\ \mathbf{u}^n_{j+1} & \text{if} \quad x \in [x_{j+1/2} + v^n_{j+1}(t-t^n), x_{j+1}], \end{cases}$$

on the whole interval (x_{j-1}, x_{j+1}), see Fig. 3.6. Of course, this function has to be considered as a substitute of function $\mathbf{v}$ in (3.3), where only contact discontinuities have been kept.

In order to properly capture contact discontinuities, we define $\tilde{\mathbf{v}}(t^{n+1/2}, x)$ as a piecewise constant function on each interval $[x_{j-1}, x_{j-1/2})$, $[x_{j-1/2}, x_{j+1/2})$ and $[x_{j+1/2}, x_{j+1}]$ (as $\tilde{\mathbf{v}}(t^n, x)$ is) by means of a Glimm's random sampling strategy. More precisely, we pick up randomly on the cell $[x_{j-1}, x_{j+1}]$ a value between $\mathbf{u}^n_{j-1}$, $\mathbf{u}^\star(\mathbf{u}^n_{j-1}, \mathbf{u}^n_j)$, $\mathbf{u}^n_j$, $\mathbf{u}^\star(\mathbf{u}^n_j, \mathbf{u}^n_{j+1})$ and $\mathbf{u}^n_{j+1}$ in agreement with their rate of presence in the corresponding interval, or equivalently in agreement with the definition of the function $x \to \tilde{\mathbf{v}}(t^n + \Delta t, x)$. Given an

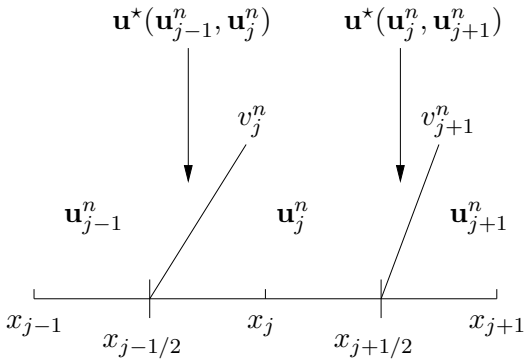

Figure 3.6: Function $\tilde{\mathbf{v}}$.

equidistributed random sequence (a_n) within interval $(0,1)$, it amounts to set :

$$\tilde{\mathbf{v}}(t^{n+1/2},x)=\left\{\begin{array}{cc}\mathbf{u}^n_{j-1} & \text{if} \quad x\in[x_{j-1},x_{j-1/2})\\ \mathbf{u}^{n+1/2}_j & \text{if} \quad x\in[x_{j-1/2},x_{j+1/2})\\ \mathbf{u}^{n+1/2}_{j+1,L} & \text{if} \quad x\in[x_{j+1/2},x_{j+1}]\end{array}\right.$$

with

$$\mathbf{u}^{n+1/2}_j=\left\{\begin{array}{cc}\mathbf{u}^\star(\mathbf{u}^n_{j-1},\mathbf{u}^n_j) & \text{if} \quad a_{n+1}\in(0,\frac{\Delta t}{\Delta x}v^n_j),\\ \mathbf{u}^n_j & \text{if} \quad a_{n+1}\in[\frac{\Delta t}{\Delta x}v^n_j,1),\end{array}\right. \tag{3.15}$$

and

$$\mathbf{u}^{n+1/2}_{j+1,L}=\left\{\begin{array}{cc}\mathbf{u}^\star(\mathbf{u}^n_j,\mathbf{u}^n_{j+1}) & \text{if} \quad a_{n+1}\in(0,\frac{2\Delta t}{\Delta x}v^n_j),\\ \mathbf{u}^n_{j+1} & \text{if} \quad a_{n+1}\in[\frac{2\Delta t}{\Delta x}v^n_j,1).\end{array}\right. \tag{3.16}$$

See Fig. 3.7. We will consider the van der Corput random sequence (a_n) defined by (3.10).

Remark. It is worth noticing from now on that if both $\mathbf{u}^n_{j-1}$ and $\mathbf{u}^n_j$ on one hand and $\mathbf{u}^n_j$ and $\mathbf{u}^n_{j+1}$ on the other hand can be connected by a 1-wave, then $\tilde{\mathbf{v}}(t^{n+1/2},x)=\tilde{\mathbf{v}}(t^n,x)$. Then, the first step is transparent when no contact discontinuity is present.

Step 2 : Account for the dynamics of shock and rarefaction waves ($t^{n+1/2}\to t^{n+1}$). Let us first consider the Riemann problem set at the interface $x_{j+1/2}$ for which only the part of the solution located on the left of the contact discontinuity may enter the cell $\mathcal{C}_j=[x_{j-1/2},x_{j+1/2})$ (see Fig. 3.5). We propose to take it into account by simply averaging $\mathcal{R}(\mathbf{u}^{n+1/2}_j,\mathbf{u}^{n+1/2}_{j+1,L})$ on $(x_j,x_{j+1/2})$. Then we set

$$\begin{array}{rcl}\mathbf{u}^{n+1}_{j+1/2,L} & = & \dfrac{2}{\Delta x}\displaystyle\int_{x_j}^{x_{j+1/2}}\mathcal{R}(\mathbf{u}^{n+1/2}_j,\mathbf{u}^n_{j+1})((x-x_{j+1/2})/\Delta t)\;dx\\ & = & \mathbf{u}^{n+1/2}_j-\frac{2\Delta t}{\Delta x}(\mathbf{g}(\mathbf{u}^{n+1/2}_j,\mathbf{u}^n_{j+1})-\mathbf{f}(\mathbf{u}^{n+1/2}_j)).\end{array} \tag{3.17}$$

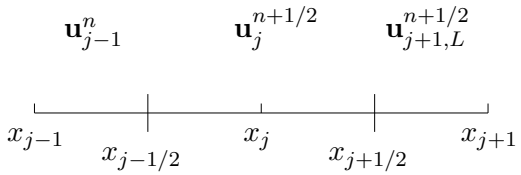

Figure 3.7: Function $\tilde{\mathbf{v}}(t^{n+1/2}, x)$.

Let us now focus on the Riemann problem set at the interface $x_{j-1/2}$ for which both parts of the solution located on the left and on the right of the contact discontinuity may enter the cell $\mathcal{C}_j$ depending on the sense of propagation of the 1-wave (see again Fig. 3.5). There are two possibilities:

- $\mathbf{u}_j^{n+1/2} = \mathbf{u}_j^n$: it corresponds to the case where the random sampling "decided" that the (possibly present) contact discontinuity of $\mathcal{R}(\mathbf{u}_{j-1}^n, \mathbf{u}_j^n)$ do not yet enter the cell $\mathcal{C}_j$. Then we only have to account for:
  - the right part of the contact discontinuity in $\mathcal{R}(\mathbf{u}_{j-1}^n, \mathbf{u}_j^n)$ (*i.e.* $\mathbf{u}_j^n = \mathbf{u}_j^{n+1/2}$) *if a contact discontinuity is actually present* in $\mathcal{R}(\mathbf{u}_{j-1}^n, \mathbf{u}_j^n)$, that is if $\mathbf{u}^\star(\mathbf{u}_{j-1}^n, \mathbf{u}_j^n) \neq \mathbf{u}_j^n$. This is simply done by replacing $\mathbf{u}_{j-1}^n$ and $\mathbf{u}_j^n$ with $\mathbf{u}_j^{n+1/2} = \mathbf{u}_j^n$ in $\mathcal{R}(\mathbf{u}_{j-1}^n, \mathbf{u}_j^n)$;
  - the part of the solution $\mathcal{R}(\mathbf{u}_{j-1}^n, \mathbf{u}_j^n)$ entering $\mathcal{C}_j$ *if no contact discontinuity is present* in $\mathcal{R}(\mathbf{u}_{j-1}^n, \mathbf{u}_j^n)$, that is if $\mathbf{u}^\star(\mathbf{u}_{j-1}^n, \mathbf{u}_j^n) = \mathbf{u}_j^n$.

- $\mathbf{u}_j^{n+1/2} = \mathbf{u}^\star(\mathbf{u}_{j-1}^n, \mathbf{u}_j^n) \neq \mathbf{u}_j^n$: it corresponds to the case where the random sampling makes the contact discontinuity of $\mathcal{R}(\mathbf{u}_{j-1}^n, \mathbf{u}_j^n)$ enter the cell $\mathcal{C}_j$. Then we also have to account for the part of the solution $\mathcal{R}(\mathbf{u}_{j-1}^n, \mathbf{u}_j^n)$ located on the left of the contact discontinuity and entering the cell $\mathcal{C}_j$, that is equivalently the part of the solution $\mathcal{R}(\mathbf{u}_{j-1}^n, \mathbf{u}_j^{n+1/2})$ entering the cell $\mathcal{C}_j$.

Thus, since the condition $\mathbf{u}^\star(\mathbf{u}_{j-1}^n, \mathbf{u}_j^n) \neq \mathbf{u}_j^n$ is equivalent to $\mathbf{u}^\star(\mathbf{u}_{j-1}^n, \mathbf{u}_j^{n+1/2}) \neq \mathbf{u}_j^{n+1/2}$ when $\mathbf{u}_j^{n+1/2} = \mathbf{u}_j^n$, we average on $[x_{j-1/2}, x_j)$ setting

$$\begin{aligned} \mathbf{u}_{j-1/2,R}^{n+1} &= \frac{2}{\Delta x} \int_{x_{j-1/2}}^{x_j} \mathcal{R}(\mathbf{u}_{j-1}^n, \mathbf{u}_j^{n+1/2})((x - x_{j-1/2})/\Delta t)\ dx \\ &= \mathbf{u}_j^{n+1/2} - \frac{2\Delta t}{\Delta x}(\mathbf{f}(\mathbf{u}_j^{n+1/2}) - \mathbf{g}(\mathbf{u}_{j-1}^n, \mathbf{u}_j^{n+1/2})) \end{aligned}$$

if $\mathbf{u}^\star(\mathbf{u}_{j-1}^n, \mathbf{u}_j^{n+1/2}) = \mathbf{u}_j^{n+1/2}$,

$$\mathbf{u}_{j-1/2,R}^{n+1} = \frac{2}{\Delta x} \int_{x_{j-1/2}}^{x_j} \mathcal{R}(\mathbf{u}_j^{n+1/2}, \mathbf{u}_j^{n+1/2})((x - x_{j-1/2})/\Delta t)\ dx = \mathbf{u}_j^{n+1/2}$$

otherwise. We get the following update formula:

$$\mathbf{u}_j^{n+1} = \frac{1}{2}(\mathbf{u}_{j+1/2,L}^{n+1} + \mathbf{u}_{j-1/2,R}^{n+1}) = \mathbf{u}_j^{n+1/2} - \frac{\Delta t}{\Delta x}(\mathbf{g}_{j+1/2}^{n+1/2,L} - \mathbf{g}_{j-1/2}^{n+1/2,R}) \text{ for all } j \in \mathbb{Z}, \tag{3.18}$$

where the left and right numerical flux functions $\mathbf{g}_{j+1/2}^{n+1/2,L}$ and $\mathbf{g}_{j-1/2}^{n+1/2,R}$ are defined according to

$$\begin{aligned} \mathbf{g}_{j+1/2}^{n+1/2,L} &= \mathbf{g}(\mathbf{u}_j^{n+1/2}, \mathbf{u}_{j+1}^n), \\ \text{and} & \\ \mathbf{g}_{j-1/2}^{n+1/2,R} &= \begin{cases} \mathbf{g}(\mathbf{u}_{j-1}^n, \mathbf{u}_j^{n+1/2}) & \text{if} \quad \mathbf{u}^\star(\mathbf{u}_{j-1}^n, \mathbf{u}_j^{n+1/2}) = \mathbf{u}_j^{n+1/2}, \\ \mathbf{f}(\mathbf{u}_j^{n+1/2}) & \text{otherwise.} \end{cases} \end{aligned} \tag{3.19}$$

The description of the method is now completed. Stability properties enjoyed by this algorithm are proposed below (see [31] for the proof).

Remark. (i) Putting the first and the second step together, we note that the definition of $\mathbf{u}_j^{n+1}$ only depends on $\mathbf{u}_{j-1}^n$, $\mathbf{u}_j^n$ and $\mathbf{u}_{j+1}^n$.

(ii) For numerical reasons, the test $\mathbf{u}^\star(\mathbf{u}_j^n, \mathbf{u}_{j+1}^{n+1/2}) = \mathbf{u}_{j+1}^{n+1/2}$ in (3.19) is replaced with $|\mathbf{u}^\star(\mathbf{u}_j^n, \mathbf{u}_{j+1}^{n+1/2}) - \mathbf{u}_{j+1}^{n+1/2}| \leq \varepsilon$, with for instance $\varepsilon = 1.e^{-12}$.

Theorem 3.2.1 (Consistency) *Under the CFL restriction* (3.2)*, the scheme defined by* (3.15)-(3.18)-(3.19) *is consistent with* (3.13) *in the following sense :*
(i) Constant state : Assume that $\mathbf{u} := \mathbf{u}_{j-1}^n = \mathbf{u}_j^n = \mathbf{u}_{j+1}^n$*, then* $\mathbf{u}_j^{n+1} = \mathbf{u}$*.*
(ii) Isolated contact discontinuity : Let $\mathbf{u}^l$ *and* $\mathbf{u}^r$ *be two distinct constant states that can be connected by a contact discontinuity. Set* $v := v^l = v^r$*. Assume that* $\mathbf{u}_j^0 = \mathbf{u}^l$ *if* $j \leq 0$ *and* $\mathbf{u}_j^0 = \mathbf{u}^r$ *if* $j > 0$*. Then the scheme* (3.15)-(3.18)-(3.19) *is equivalent to Glimm's random choice scheme and then converges to the solution of* (3.14) *given by* $\mathbf{u}(t,x) = \mathbf{u}^l$ *if* $x < vt$ *and* $\mathbf{u}(t,x) = \mathbf{u}^r$ *otherwise. In particular, we have* $\mathbf{u}_j^n \in \{\mathbf{u}^l, \mathbf{u}^r\}$ $\forall\ j\ \in \mathbb{Z}$ *and* $\forall\ n\ \in \mathbb{N}$ *so that the velocity profile remains constant :* $v_j^n = v\ \forall\ j\ \in \mathbb{Z}$ *and* $\forall\ n\ \in \mathbb{N}$*.*
(iii) Isolated 1-wave : Let us assume that $\mathbf{u}_{j-1}^n$ *and* $\mathbf{u}_j^n$ *can be connected by a 1-wave* ($\mathbf{u}^\star(\mathbf{u}_{j-1}^n, \mathbf{u}_j^n) = \mathbf{u}_j^n$)*. Then the definition* $\mathbf{u}_j^{n+1}$ *of the scheme* (3.15)-(3.18)-(3.19) *coincides with the one of the Godunov scheme.*

Theorem 3.2.2 (Maximum principle) *Under the CFL restriction* (3.2)*, the scheme defined by* (3.15)-(3.18)-(3.19) *satisfies the following maximum principle property for all* $j\ \in \mathbb{Z}$ *and all* $n \in \mathbb{N}$ *:*

$$\begin{cases} \inf\limits_{j\in\mathbb{Z}} v_j^0 \leq v_j^n \leq \sup\limits_{j\in\mathbb{Z}} v_j^0\,, \\ \inf\limits_{j\in\mathbb{Z}} (v_j^0 + p(\rho_j^0)) \leq v_j^n + p(\rho_j^n) \leq \sup\limits_{j\in\mathbb{Z}} (v_j^0 + p(\rho_j^0))\,. \end{cases}$$

3.2.3 Numerical experiments

In this section, I take $p(\rho) = V_{ref} \ln(\rho/R)$, $R = 1$ and $V_{ref} = 1.4427$. In order to test the proposed scheme, we have considered three Riemann problems leading to three

solutions of interest: an isolated contact discontinuity (**Test 1**), a shock wave followed by a contact discontinuity (**Test 2**) and a sonic rarefaction wave followed by a contact discontinuity (**Test 3**). In each case, the method is first evaluated by means of a qualitative comparison with the exact solution: the ρ, v and $v + p(\rho)$ profiles are shown on Figs. 3.8, 3.9 and 3.10. For several mesh sizes, a quantitative evaluation through the $\mathbf{L^1}$ norm (of the difference between the exact and the numerical solutions) is then made, as well as a measure of the conservation errors on both ρ and y. They are given on Tables 3.3, 3.4, 3.5 : E^{ρ}_{cons} and E^{y}_{cons} denote the conservation errors on ρ and y, and $E^{\rho}_{\mathbf{L^1}}$ and $E^{v}_{\mathbf{L^1}}$ denote the $\mathbf{L^1}$ errors on ρ and v. The $\mathbf{L^1}$ norm errors are computed in a very classical way. For the sake of completeness, I give the precise meaning of E^{ρ}_{cons} and E^{y}_{cons} in our computations (see [2, 28, 29] for more details on these formulas): denoting $[x_0, x_1] = [-0.25, 0.75]$ the computational domain of our simulations and T_f the corresponding final time, we first set for all $n \geq 0$

$$\begin{aligned} E^{\mathbf{u}}(t^n) &= \begin{pmatrix} E^{\rho}(t^n) \\ E^{y}(t^n) \end{pmatrix} \\ &= \frac{\displaystyle\int_{x_0}^{x_1} \mathbf{u}_\nu(t^n, x)dx - \int_{x_0}^{x_1} \mathbf{u}_\nu(0, x)dx + \int_0^{t^n} \mathbf{f}(\mathbf{u}_\nu(s, x_1))ds - \int_0^{t^n} \mathbf{f}(\mathbf{u}_\nu(s, x_0))ds}{\displaystyle\int_{x_0}^{x_1} \mathbf{u}_\nu(t^n, x)dx}, \end{aligned}$$

where the ratio has to be understood component by component, and then

$$E^{\mathbf{u}}_{cons} = \begin{pmatrix} E^{\rho}_{cons} \\ E^{y}_{cons} \end{pmatrix} = \frac{1}{T_f} \sum_{n=0}^{N} \Delta t |E^{\mathbf{u}}(t^n)| \qquad \text{with } N = T_f/\Delta t.$$

Note that $E^{\mathbf{u}}_{cons}$ corresponds to the sum of the absolute value of the relative conservation errors made at each intermediate time t^n. In other words, the possible compensation effects are not taken into account here.

Initial states are chosen as follows:

Test 1		
$\mathbf{u}^l$:	$\rho^l = 0.9$	$v^l = 1.$
$\mathbf{u}^r$:	$\rho^r = 0.1$	$v^r = 1.$

Test 2		
$\mathbf{u}^l$:	$\rho^l = 0.1$	$v^l = 1.8$
$\mathbf{u}^r$:	$\rho^r = 0.2$	$v^r = 1.6$

Test 3		
$\mathbf{u}^l$:	$\rho^l = 0.5$	$v^l = 1.2$
$\mathbf{u}^r$:	$\rho^r = 0.1$	$v^r = 1.6$

The qualitative results are presented on a mesh made of 100 points per unit interval.

We observe, as predicted above, that the classical Godunov method develops spurious oscillations near the contact discontinuities, that strongly affect the whole numerical solutions. On the contrary, our algorithm removes them and provides numerical solutions in full agreement with exact ones, with sharp contact discontinuities. As far as the conservation errors and the $\mathbf{L^1}$ errors are concerned, they decrease with the mesh size, which proves numerically the convergence of the method. Moreover, we see that the $\mathbf{L^1}$ errors between the numerical and exact solutions are really lower for our scheme compared with the Godunov method.

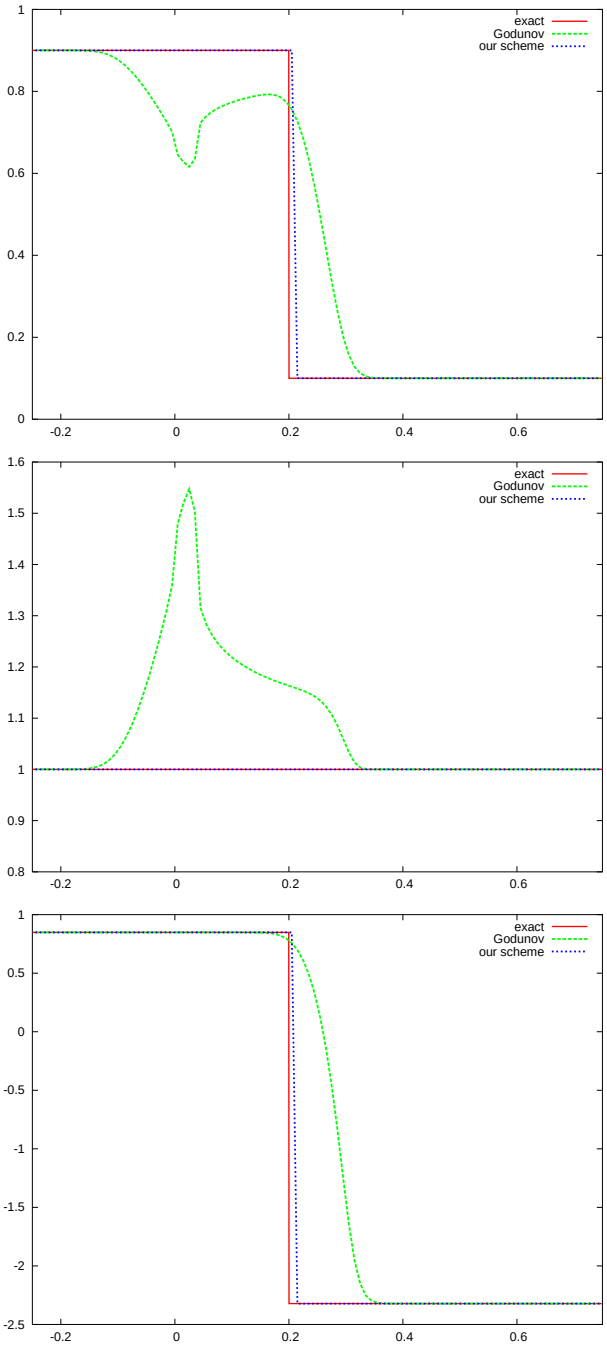

Figure 3.8: **Test 1**: ρ (top), v (middle) and $v + p(\rho)$ (bottom) at time $T_f = 0.2$.

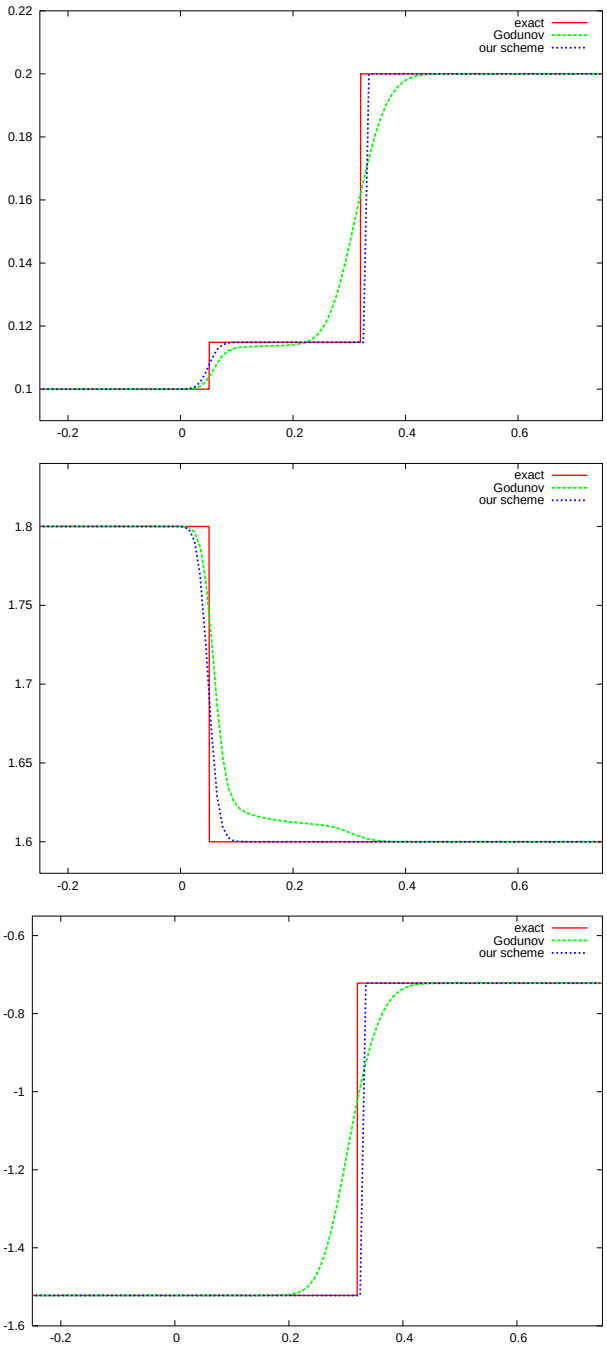

Figure 3.9: **Test 2**: ρ (top), v (middle) and $v + p(\rho)$ (bottom) at time $T_f = 0.2$.

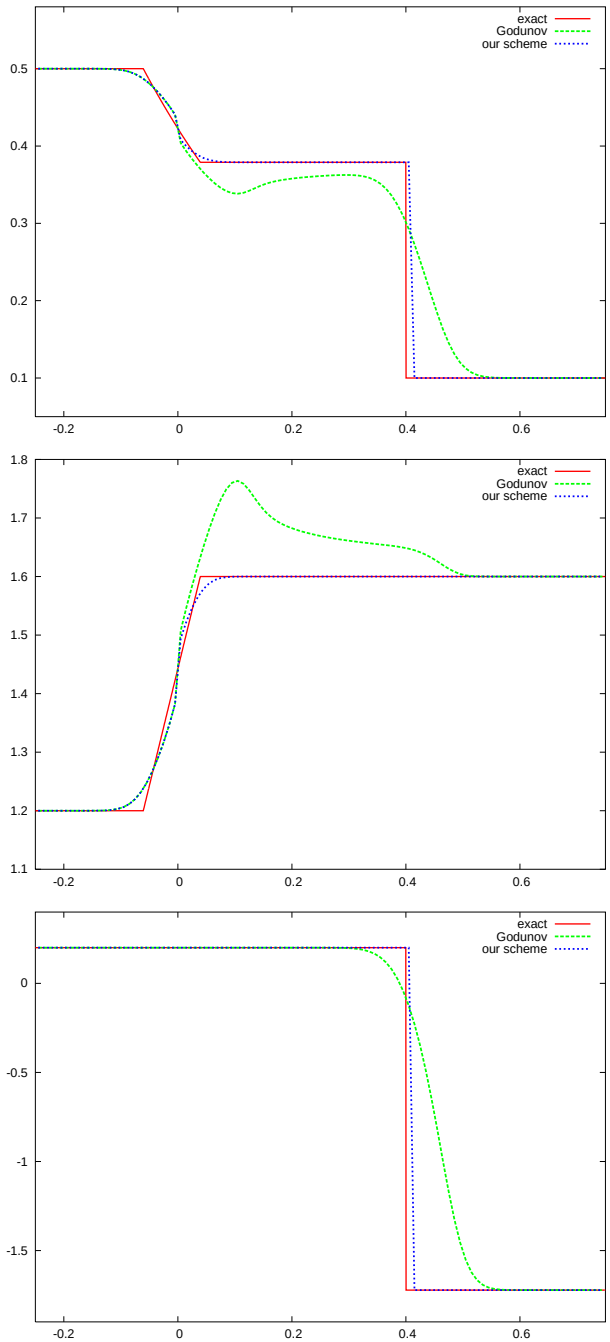

Figure 3.10: **Test 3**: ρ (top), v (middle) and $v + p(\rho)$ (bottom) at time $T_f = 0.25$.

# of points	E^{ρ}_{cons}	E^{y}_{cons}	$E^{\rho}_{L^1}$	$E^{v}_{L^1}$
100	0.	0.	$8.39e^{-2}$	$8.68e^{-2}$
500	0.	0.	$4.26e^{-2}$	$3.83e^{-2}$
1000	0.	0.	$3.06e^{-2}$	$2.66e^{-2}$
2000	0.	0.	$2.18e^{-2}$	$1.85e^{-2}$

# of points	E^{ρ}_{cons}	E^{y}_{cons}	$E^{\rho}_{L^1}$	$E^{v}_{L^1}$
100	1.52%	7.74%	$8.e^{-3}$	0.
500	0.32%	1.83%	$1.6e^{-3}$	0.
1000	0.16%	0.94%	$8.e^{-4}$	0.
2000	0.08%	0.47%	$4.e^{-4}$	0.

Table 3.3: **Test 1**: Godunov scheme (top) and our scheme (bottom).

# of points	E^{ρ}_{cons}	E^{y}_{cons}	$E^{\rho}_{L^1}$	$E^{v}_{L^1}$
100	0.	0.	$3.2e^{-3}$	$6.55e^{-3}$
500	0.	0.	$1.47e^{-3}$	$2.76e^{-3}$
1000	0.	0.	$1.03e^{-3}$	$1.78e^{-3}$
2000	0.	0.	$7.3e^{-4}$	$1.22e^{-3}$

# of points	E^{ρ}_{cons}	E^{y}_{cons}	$E^{\rho}_{L^1}$	$E^{v}_{L^1}$
100	0.35%	0.14%	$1.02e^{-3}$	$2.3e^{-3}$
500	0.07%	0.03%	$2.19e^{-4}$	$6.47e^{-4}$
1000	0.04%	0.02%	$1.09e^{-4}$	$3.26e^{-4}$
2000	0.03%	0.01%	$9.72e^{-5}$	$1.63e^{-4}$

Table 3.4: **Test 2**: Godunov scheme (top) and our scheme (bottom).

# of points	E^{ρ}_{cons}	E^{y}_{cons}	$E^{\rho}_{L^1}$	$E^{v}_{L^1}$
100	0.	0.	$2.12e^{-2}$	$3.8e^{-2}$
500	0.	0.	$9.82e^{-3}$	$1.68e^{-2}$
1000	0.	0.	$6.98e^{-3}$	$1.17e^{-2}$
2000	0.	0.	$4.94e^{-3}$	$8.22e^{-3}$

# of points	E^{ρ}_{cons}	E^{y}_{cons}	$E^{\rho}_{L^1}$	$E^{v}_{L^1}$
100	0.81%	6.04%	$3.82e^{-3}$	$3.36e^{-3}$
500	0.17%	1.14%	$9.41e^{-4}$	$1.25e^{-3}$
1000	0.08%	0.57%	$5.17e^{-4}$	$7.78e^{-4}$
2000	0.04%	0.28%	$2.84e^{-4}$	$4.72e^{-4}$

Table 3.5: **Test 3**: Godunov scheme (top) and our scheme (bottom).

4

Conservation laws with variable unilateral constraints

This chapter is devoted to scalar constrained Cauchy problems of the form

$$\partial_t u + \partial_x f(u) = 0, \qquad t > 0,\ x \in \mathbb{R}, \tag{4.1}$$

$$u(0,x) = u_0(x), \qquad x \in \mathbb{R}, \tag{4.2}$$

$$f(u(t,0)) \leq F(t), \qquad t > 0. \tag{4.3}$$

This problem was originally motivated by the modeling of a toll gate along a road, but it tuns out to be useful for other applications in traffic flow modelling such as traffic lights [5] or pedestrian motion through a door [49]. The results about the existence and stability of solutions to (4.1)-(4.3) have been obtained in collaboration with R.M. Colombo and are published in [46]. The construction and analysis of a class of corresponding finite volume schemes have been addressed in collaboration with B. Andreianov and N. Seguin in [5].

In the following sections, I will assume that the flux function $f : [0,1] \to \mathbb{R}$ is Lipschitz continuous with Lipschitz constant L and satifies

$$f(u) \geq 0,\ f(0) = f(1) = 0,\ f'(u)(\bar{u} - u) > 0 \quad \text{for a.e. } u \in [0,1] \setminus \{\bar{u}\}, \tag{4.4}$$

for some $\bar{u} \in (0,1)$. I will also assume that $F \in \mathbf{L}^\infty(\mathbb{R}^+; [0, f(\bar{u})])$ and $u_0 \in \mathbf{L}^\infty(\mathbb{R}; [0,1])$.

4.1 The Constrained Riemann Solver

This section is devoted to the Riemann problem for (4.1)-(4.3), i.e. we take

$$u_0 = \begin{cases} u^l \text{ if } x < 0, \\ u^r \text{ if } x > 0, \end{cases} \tag{4.5}$$

and $F(t) \equiv F$ constant.

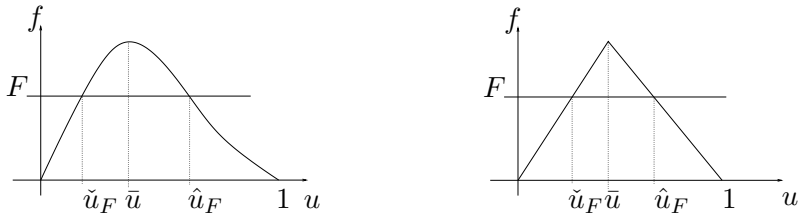

Figure 4.1: Examples of fundamental diagrams considered here.

We denote below by $\mathcal{R}$ the standard (i.e. without the constraint (4.3)) Lax [83] or Liu [87] Riemann solver for (4.5), i.e. the map $(t,x) \mapsto \mathcal{R}(u^l,u^r)(x/t)$ is the standard weak entropy solution to (4.1)-(4.5).

Definition 4.1.1 *A Riemann solver $\mathcal{R}^F : (u^l,u^r) \mapsto \mathcal{R}^F(u^l,u^r)$ for (4.1)-(4.3) is defined as follows.*
If $f\left(\mathcal{R}(u^l,u^r))(0)\right) \leq F$, then $\mathcal{R}^F(u^l,u^r) = \mathcal{R}(u^l,u^r)$.
Otherwise, $\mathcal{R}^F(u^l,u^r)(\lambda) = \begin{cases} \mathcal{R}(u^l,\hat{u}_F)(\lambda) \text{ if } \lambda < 0\,, \\ \mathcal{R}(\check{u}_F,u^r)(\lambda) \text{ if } \lambda > 0\,. \end{cases}$

Above, $\check{u}_F \leq \hat{u}_F$ are the solutions to $f(u) = F$, see Fig. 4.1. Note that when the constraint is enforced, a non classical shock arises at $x = 0$. The solution so obtained is a weak solution to (4.1) but it violates the entropy condition as soon as $F < f(\bar{u})$.

The Riemann solver $\mathcal{R}^F$ generates a semigroup $\mathcal{S}^F$ whose orbits are solutions to Cauchy problems. A necessary condition for the $\mathbf{L^1}$ continuity of $\mathcal{S}^F$ is the consistency of $\mathcal{R}^F$, see Definition 2.2.2. It is easy to verify the following:

Proposition 4.1.2 *The Riemann Solver defined by Definition 4.1.1 enjoys the following properties, for all $u^l, u^r \in [0,1]$.*

(RS1) $(t,x) \mapsto \left(\mathcal{R}^F(u^l,u^r)\right)(x/t)$ is a self similar weak solution to (4.1)-(4.5);

(RS2) $\mathcal{R}^F(u^l,u^r) \in \mathbf{BV}\left(\mathbb{R};[0,1]\right)$ for all $t > 0$;

(RS3) $\mathcal{R}^F(u^l,u^r)$ satisfies the constraint (4.3) in the sense that for all $t > 0$

$$\lim_{x\to 0-} f\left(\mathcal{R}^F(u^l,u^r)(x/t)\right) \leq F \text{ and } \lim_{x\to 0+} f\left(\mathcal{R}^F(u^l,u^r)(x/t)\right) \leq F\,;$$

(RS4) $\mathcal{R}^F$ is consistent in the sense of Definition 2.2.2.

Moreover, the map $\mathcal{R}^F\colon [0,1]^2 \mapsto \mathbf{L^1_{loc}}(\mathbb{R};\mathbb{R})$ is uniformly continuous for all $t > 0$.

4.2 Entropy solutions

The non-classical problem (4.1)-(4.3) can be viewed as a singular limit of a classical Cauchy problem with discontinuous flux function. Fix $\varepsilon > 0$ and consider the problem

$$\begin{cases} \partial_t u^\varepsilon + \partial_x \left(k_\varepsilon(t,x)\, f(u^\varepsilon)\right) = 0, \\ u^\varepsilon(0,x) = u_0(x), \end{cases} \qquad k_\varepsilon(t,x) = \begin{cases} 1 & |x| > \varepsilon, \\ \dfrac{F(t)}{f(\bar{u})} & |x| \leq \varepsilon. \end{cases} \tag{4.6}$$

(I refer the reader to [46] for the rigorous formalization of limit procedure.) The above equation fits in the framework provided by [77, Theorems 4.5, 5.5 and 6.5], see also [37, 76]. The associated entropy formulation (see for instance [98, 76, 77]) is

$$\int_0^{+\infty}\int_{\mathbb{R}}(|u^\varepsilon(t,x)-\kappa|\ \partial_t+\Phi(u^\varepsilon(t,x),\kappa)\partial_x)\ \varphi(t,x)\ dx\ dt + \int_{\mathbb{R}}|u_0(x)-\kappa|\ \varphi(0,x)\ dx + \int_0^{+\infty}\left(1-\frac{F(t)}{f(\bar u)}\right)f(\kappa)\ (\varphi(t,-\varepsilon)+\varphi(t,\varepsilon))\ dt\geq 0,$$

for all $\kappa\in[0,1]$ and $\varphi\in\mathbf{C_c^1}(\mathbb{R}^+\times\mathbb{R};\mathbb{R}^+)$, where I have set $\Phi(a,b)=\operatorname{sgn}(a-b)(f(a)-f(b))$. Note that the solution u^ε satisfies the constraint $f(u^\varepsilon(t,x))\leq F(t)$ for a.e. $|x|<\varepsilon$.
We are led to formulate the following definition for (4.1)-(4.3).

Definition 4.2.1 *A function $u\in\mathbf{L}^\infty(\mathbb{R}^+\times\mathbb{R};[0,1])$ is a weak entropy solution of* (4.1)-(4.3) *if*
(i) it satisfies the following entropy inequalities: for every $\varphi\in\mathbf{C_c^1}(\mathbb{R}^+\times\mathbb{R};\mathbb{R}^+)$ and all $\kappa\in[0,1]$,

$$\int_0^{+\infty}\int_{\mathbb{R}}(|u(t,x)-\kappa|\partial_t+\Phi(u(t,x),\kappa)\partial_x)\ \varphi(t,x)\ dx\ dt + \int_{\mathbb{R}}|u_0(x)-\kappa|\ \varphi(0,x)\ dx+2\int_0^{+\infty}\left(1-\frac{F(t)}{f(\bar u)}\right)f(\kappa)\ \varphi(t,0)\ dt\geq 0, \quad (4.7)$$

(ii) it verifies the constraint:

$$f((\gamma^l u)(t))=f((\gamma^r u)(t))\leq F(t)\quad \text{for a.e. } t>0, \quad (4.8)$$

where $\gamma^{l,r}$ denote the operators of left- and right-side strong traces on $\{x=0\}$.

Remark. Taking $\kappa=0$ and $\kappa=1$ in the above formulation, from the condition $u(t,x)\in[0,1]$ a.e. we deduce that u is a weak solution of equation (4.1) (i.e., solution in the sense of distributions).

It is worth noting that the traces $\gamma^{l,r}u$ exist a.e. since we are dealing with a flux function such that the measure of the set $\{s\in[0,1], f'(s)=0\}$ is zero (by assumption (4.4)), as shown by Panov [89] (see also Vasseur [100] in the case of smooth non linear flux functions).

Remark. Definition 4.2.1 selects the *maximal* solution, for a non classical stationary shock at $x=0$ separating states u_2 and u_1 with $u_1<u_2$ and $f(u_1)=f(u_2)<F(t)$ turns out to be non entropic.

Even if the above definition appears to be the natural one with respect to the approximation problem (4.6), its formulation is not easy to manipulate when dealing with wave-front traking or finite volume approximations, because of the explicit constraint on the traces of the flux in (4.8). Therefore, I introduce an (equivalent) entropy condition. Let me first define the following sets:

- $\mathcal{G}_1(F) = \{(c_l, c_r) \in [0,1]^2; c_l > c_r, f(c_l) = f(c_r) = F\}$,
- $\mathcal{G}_2(F) = \{(c, c) \in [0,1]^2; f(c) \leq F\}$,
- $\mathcal{G}_3(F) = \{(c_l, c_r) \in [0,1]^2; c_l < c_r, f(c_l) = f(c_r) \leq F\}$,

and denote

$$\mathcal{G}(F) = \mathcal{G}_1(F) \cup \mathcal{G}_2(F) \cup \mathcal{G}_3(F).$$

Remark that $\mathcal{G}_1(F) = \{(\hat{u}_F, \check{u}_F)\}$ is a singleton, uniquely defined by the conditions

$$f(\hat{u}_F) = f(\check{u}_F) = F, \qquad \hat{u}_F \geq \check{u}_F.$$

Using the ideas of [10, 6, 27], we propose in [5] a new definition of solutions based on the comparison of the solution with functions c defined by

$$c(x) = \begin{cases} c_l & \text{if } x < 0, \\ c_r & \text{if } x > 0, \end{cases} \tag{4.9}$$

with $(c_l, c_r) \in [0,1]^2$.

Definition 4.2.2 *A function $u \in \mathbf{L}^\infty(\mathbb{R}^+ \times \mathbb{R}; [0,1])$ is a weak entropy solution of* (4.1)-(4.3) *if there exists $M > 0$ such that for every $\varphi \in \mathbf{C}^\mathbf{1}_\mathbf{c}(\mathbb{R}^+ \times \mathbb{R}; \mathbb{R}^+)$ and all c defined by* (4.9) *with $(c_l, c_r) \in [0,1]^2$,*

$$\int_0^{+\infty} \int_{\mathbb{R}} (|u(t,x) - c(x)|\partial_t + \Phi(u(t,x), c(x))\partial_x)\ \varphi(t,x)\ dx\ dt$$
$$+ \int_{\mathbb{R}} |u_0(x) - c(x)|\ \varphi(0,x)\ dx + M \int_0^{+\infty} \operatorname{dist}\left((c_l, c_r), \mathcal{G}(F(t))\right)\ \varphi(t,0)\ dt \geq 0. \tag{4.10}$$

In (4.10) "dist" indicates a distance function on $\mathbb{R}^2$. I refer the reader to [5] for a detailed derivation of this condition, and the proof of equivalence between Definitions 4.2.1 and 4.2.2. Here I just want to point out that the two definitions are linked by a third formulation of the entropy condition, which gives accurate informations on the traces of the flux at $x = 0$ and hence turns out to be useful in the sequel when applied in standard techniques a la Kružkov.

Definition 4.2.3 *A function $u \in \mathbf{L}^\infty(\mathbb{R}^+ \times \mathbb{R}; [0,1])$ is a weak entropy solution of* (4.1)-(4.3) *if*

(i) it is a Kružkov entropy solution for $x < 0$ and $x > 0$: for all $\varphi \in \mathbf{C^1_c}(\mathbb{R}^+ \times \mathbb{R} \setminus \{0\}; \mathbb{R}^+)$ and all $\kappa \in [0,1]$,

$$\int_0^{+\infty} \int_{\mathbb{R}} (|u(t,x) - \kappa| \ \partial_t + \Phi(u(t,x), \kappa) \ \partial_x) \ \varphi(t,x) \ dx \ dt \\ + \int_{\mathbb{R}} |u_0(x) - \kappa| \ \varphi(0,x) \ dx \geq 0,$$

(ii) for a.e. $t > 0$,

$$((\gamma^l u)(t), (\gamma^r u)(t)) \in \mathcal{G}(F(t)). \tag{4.11}$$

The equivalence of the three definitions relies on the *dissipativity* and *maximality* properties of the admissibility germ $\mathcal{G}(F)$.

Lemma 4.2.4
(i) If $(b_l, b_r) \in \mathcal{G}(F)$, then

$$\forall (c_l, c_r) \in \mathcal{G}(F), \quad \Phi(b_l, c_l) \geq \Phi(b_r, c_r). \tag{4.12}$$

(ii) The converse is true, under the following form:

$$\begin{array}{l} \textit{if } (4.12) \textit{ holds and the Rankine-Hugoniot condition} \\ f(b_l) = f(b_r) \textit{ is satisfied, then } (b_l, b_r) \in \mathcal{G}(F). \end{array} \tag{4.13}$$

4.3 Well posedness in the BV setting

Fist of all, observe that the constraint (4.3) and the consequent Definition 4.1.1 may cause sharp increases in $\mathbf{TV}(u(t,\cdot))$. The simplest example is provided by a constant initial datum $u_0(x) = \bar{u}$ and a constraint

$$F(t) = \begin{cases} f(\bar{u}) & \text{if } t < 1 \\ \frac{1}{2} f(\bar{u}) & \text{if } t > 1 \,. \end{cases}$$

At time $t = 1$, two shocks arise from $x = 0$ and the total variation jumps from 0 to $2(\hat{u} - \check{u})$, where $\check{u} < \hat{u}$ and $f(\hat{u}) = f(\check{u}) = \frac{1}{2} f(\bar{u})$.

To overcome this difficulty, following [37, 95], we use the nonlinear mapping

$$\Psi(u) = \operatorname{sgn}(u - \bar{u}) \ (f(\bar{u}) - f(u)) \tag{4.14}$$

and bound the total variation of $\Psi \circ u$. In fact, Ψ is one-to-one, but possibly singular at $u = \bar{u}$. Indeed, it is immediate to see that if $u \in \mathbf{BV}(\mathbb{R}; \mathbb{R})$, then $\mathbf{TV}(\Psi \circ u) \leq \|f'\|_{\mathbf{C^0}} \cdot \mathbf{TV}(u)$, while $\mathbf{TV}(u)$ may well be infinite with $\mathbf{TV}(\Psi \circ u)$ finite, as in the case of $f(u) = u(1-u)$, $\bar{u} = 1/2$ and $u = \dfrac{1}{2} + \displaystyle\sum_{n=3}^{+\infty} \frac{1}{n} \chi_{\left[\frac{1}{n+1/2}, \frac{1}{n}\right[}$.

To state the well posedness result, it is useful to introduce the translation $\mathcal{T}_t$ by $(\mathcal{T}_t F)(\tau) = F(\tau + t)$. Below we introduce a map $\mathcal{S}^F \colon \mathbb{R}^+ \times \mathcal{D} \mapsto \mathcal{D}$, $\mathcal{D}$ being a suitable subset of $\mathbf{L^1}(\mathbb{R}; [0,1])$ containing the initial datum (4.2). We then denote by $\bar{\mathcal{S}}^F$ the map $\bar{\mathcal{S}}^F \colon \mathbb{R}^+ \times \bar{\mathcal{D}} \mapsto \bar{\mathcal{D}}$ defined by $\bar{\mathcal{S}}^F_t(u, F) = (\mathcal{S}^F_t u, \mathcal{T}_t F)$ with $\bar{\mathcal{D}} = \mathcal{D} \times \mathbf{BV}$.

Theorem 4.3.1 *Let* (4.4) *hold. Then, for every constraint* $F \in \mathbf{BV}\left(\mathbb{R}^+; [0, f(\bar{u})]\right)$ *there exists a map* $\mathcal{S}^F \colon \mathbb{R}^+ \times \mathcal{D} \mapsto \mathcal{D}$ *such that*

(CRS1) $\mathcal{D} \supseteq \left\{u \in \mathbf{L^1}\left(\mathbb{R}; [0,1]\right) : \Psi(u) \in \mathbf{BV}(\mathbb{R}; \mathbb{R})\right\}$*;*

(CRS2) $\bar{\mathcal{S}}^F$ *is a semigroup, i.e.* $\bar{\mathcal{S}}^F_0 = \mathrm{Id}$ *and* $\bar{\mathcal{S}}^F_{t_1} \circ \bar{\mathcal{S}}^F_{t_2} = \bar{\mathcal{S}}^F_{t_1+t_2}$*;*

(CRS3) $\mathcal{S}^F$ *is non expansive in* u*, i.e. for all* $u_1, u_2 \in \mathcal{D}$

$$\left\|\mathcal{S}^F_t u_1 - \mathcal{S}^F_t u_2\right\|_{\mathbf{L^1}} \leq \|u_1 - u_2\|_{\mathbf{L^1}}\,;$$

(CRS4) if u_0 *and* F *are piecewise constant, then for* t *sufficiently small,* $\mathcal{S}^F_t u_0$ *coincides with the gluing of the solutions to standard Riemann problems centered at the points of jump of* u_0 *and to* (4.1),(4.3) *and* (4.5) *at* $x = 0$*;*

(CRS5) for all $u_0 \in \mathcal{D}$*, the orbit* $t \mapsto \mathcal{S}^F_t u_0$ *yields a weak entropy solution to* (4.1)-(4.3)*, according to Definitions 4.2.1 or 4.2.2.*

The above statements *(CRS1)–(CRS4)* are clearly modeled on the definition of *Standard Riemann Semigroup*, see [22, Def. 9.1] and provide an analogue to it in the present constrained (and non autonomous) setting. The Lipschitz estimate *(CRS3)* is proved with suitable modifications of the techniques in [82].

Sketch of the proof. The proof uses the standard technique of wave front tracking and is detailed in [46, Sec. 4.3].
Fix a positive $n \in \mathbb{N}$, $n > 0$ and introduce in $[0,1]$ the mesh $\mathcal{M}_n$ by

$$\mathcal{M}_n = f^{\leftarrow}(2^{-n}\mathbb{N})\,.$$

Let $\mathbf{PLC}_n$ be the set of piecewise linear and continuous functions defined on $[0,1]$ whose derivatives exist in $[0,1] \setminus \mathcal{M}_n$. Let $f^n \in \mathbf{PLC}_n$ coincide with f on $\mathcal{M}_n$. Clearly, if f satisfies (4.4), then also f^n satisfies (4.4).

Similarly, introduce $\mathbf{PC}_n$, respectively $\mathbf{PC}^+_n$, as the set of piecewise constant functions defined on $\mathbb{R}$, respectively $\mathbb{R}^+$, with values in $\mathcal{M}_n$, respectively in $f(\mathcal{M}_n)$. Let $F^n \in \mathbf{PC}^+_n$ coincide with F on $f(\mathcal{M}_n)$. Note that if $F \in \mathbf{BV}(\mathbb{R}^+; [0,1])$, then so does F^n. We write

$$\begin{array}{rcll} u^n & = & \displaystyle\sum_\alpha u^n_\alpha\, \chi_{]x_{\alpha-1}, x_\alpha]} & \text{with } u^n_\alpha \in \mathcal{M}_n, \\ F^n & = & F^n_0\, \chi_{[0,t_1]} + \displaystyle\sum_{\beta \geq 1} F^n_\beta\, \chi_{]t_\beta, t_{\beta+1}]} & \text{with } F^n_\beta \in 2^{-n}\mathbb{N}, \end{array} \tag{4.15}$$

and we agree that for $\alpha = 0$, $x_\alpha = 0$. Both the approximations above are meant in the strong $\mathbf{L^1}$ topology: $\lim_{n\to+\infty} \|F^n - F\|_{\mathbf{L^1}(\mathbb{R})} = 0$ and $\lim_{n\to+\infty} \|u^n - u\|_{\mathbf{L^1}(\mathbb{R})} = 0$.

Let $\mathcal{D}_n = \{u \in \mathbf{PC}_n \colon \Psi(u) \in \mathbf{BV}(\mathbb{R}; \mathbb{R})\}$ and $\bar{\mathcal{D}}_n = \mathcal{D}_n \times \mathbf{PC}^+_n$. On any $(u^n, F^n) \in \bar{\mathcal{D}}_n$, written as in (4.15), we define the Glimm type functional Υ as

$$\Upsilon(u^n, F^n) = \sum_\alpha \left|\Psi(u^n_{\alpha+1}) - \Psi(u^n_\alpha)\right| + 5 \sum_{t_\beta \geq 0} \left|F^n_{\beta+1} - F^n_\beta\right| + \gamma\,, \tag{4.16}$$

where γ is defined by

$$\gamma = \begin{cases} 0 & \text{if } (u^n(0-), u^n(0+)) \in \mathcal{G}_1(F^n(0))\,, \\ 4\,(f(\bar{u}) - F^n(0)) & \text{otherwise.} \end{cases}$$

For small times, an approximate solution $u^n = u^n(t,x)$ to (4.1)-(4.3) is constructed by piecing together the solutions to the Riemann problems

$$\begin{cases} \partial_t u + \partial_x \left(f^n(u)\right) = 0 \\ u(0,x) = \begin{cases} u_{0,0} \text{ if } x < 0 \\ u_{0,1} \text{ if } x > 0 \end{cases} \\ f\left(u(t,0)\right) \leq F_0^n, \end{cases} \qquad \begin{cases} \partial_t u + \partial_x \left(f^n(u)\right) = 0 \\ u(0,x) = \begin{cases} u_{0,\alpha} & \text{if } x < x_\alpha \\ u_{0,\alpha+1} \text{ if } x > x_\alpha \end{cases} \\ \alpha \neq 0\,. \end{cases} \tag{4.17}$$

Note that the solutions to the Riemann problem (4.17), left, is constructed by means of $\mathcal{R}^F$, whereas the solutions to (4.17), right, by means of $\mathcal{R}$. In both cases, for fixed t, the solutions are piecewise constant in x. Their juxtaposition yields a well defined (exact) weak entropy solution u^n to

$$\begin{cases} \partial_t u^n + \partial_x \left(f^n(u^n)\right) = 0 \\ u^n(0,x) = u_0^n(x) \\ f(u^n(t,0)) \leq F^n(t), \end{cases} \tag{4.18}$$

as long as either two discontinuities collide, or the value of the constraint changes. In both cases, a new Riemann problem arises and its solution, obtained in the former case with $\mathcal{R}$ and in the latter with $\mathcal{R}^F$, allows to extend u^n further in time.

The following lemma guarantees that the total number of interactions is finite and the procedure allows to construct a global approximate solution.

Lemma 4.3.2 *For any $n \in \mathbb{N}$ and $(u_0^n, F^n) \in \bar{\mathcal{D}}_n$, at any interaction, the map $t \mapsto \Upsilon(t) = \Upsilon\left(u^n(t,\cdot)\right)$*

either *decreases by at least 2^{-n},*

or *remains constant and the number of waves does not increase.*

A standard procedure based on Helly's Compactness Theorem, see [22, Theorem 2.4] allows to exhibit a weak solution to (4.1)-(4.3). Passing to the limit in (4.10), we easily see that the limit is also an entropy solution. □

4.4 Well posedness in the $\mathbf{L}^\infty$ setting

For the extension to $\mathbf{L}^\infty$, we follow the classical way. As mentionned above, assumption (4.4) is sufficient for the existence of strong traces of the solution and therefore, to extend the result of uniqueness for **BV** solutions of [46]. Besides, the existence result for initial data and constraint in **BV** can be extended to $\mathbf{L}^\infty$ by the use of mollifiers and of the $\mathbf{L}^\mathbf{1}_\mathbf{loc}$ contraction with respect to the initial data and to the constraint.

Proposition 4.4.1 *Assume* $F^1, F^2 \in \mathbf{L}^\infty(\mathbb{R}^+; [0, f(\bar{u})])$, *and* $u_0^1, u_0^2 \in \mathbf{L}^\infty(\mathbb{R}, [0,1])$ *such that* $(u_0^1 - u_0^2) \in \mathbf{L^1}(\mathbb{R})$. *Assume that* u^1, u^2 *are entropy solutions of* (4.1)-(4.3), *corresponding to the initial data* u_0^1, u_0^2 *and to the constraints* F^1, F^2, *respectively. Then, for a.e.* $T > 0$, *we have*

$$\int_{\mathbb{R}} |u^1 - u^2|(T,x)\, dx \;\leq\; 2\int_0^T |F^1 - F^2|(t)\, dt \;+\; \int_{\mathbb{R}} |u_0^1 - u_0^2|(x)\, dx. \tag{4.19}$$

The proof mimics the standard Kružkov doubling of variables technique, with suitable test functions. It is detailled in [5, Sec. 6].

Combining the estimate (4.19) with a truncature and a density argument, we deduce the following generalization of Theorem 4.3.1.

Theorem 4.4.2 *For any* $u_0 \in \mathbf{L}^\infty(\mathbb{R}; [0,1])$ *and* $F \in \mathbf{L}^\infty(\mathbb{R}^+; [0, f(\bar{u})])$ *there exists one and only one entropy solution to Problem* (4.1)-(4.3) *(in the sense of Definitions 4.2.1 and 4.2.2).*

Proof. The uniqueness claim is contained in Proposition 4.4.1. Let us prove the existence. Take the truncations $u_0(x)\mathbb{1}_{\{|x|<n\}}$, $F(t)\mathbb{1}_{\{0<t<n\}}$ and regularize them by convolution with a standard sequence of mollifiers $(\rho_n)_{n\in\mathbb{N}}$. Denote by u_0^n, F^n the data obtained in this way; these data are of bounded variation. By Theorem 4.3.1, there exists a unique entropy solution u^n of (4.1) with initial datum u_0^n and constraint F^n. In particular, it verifies condition (4.10). Clearly,

$$u_0^n \to u_0 \text{ in } \mathbf{L^1_{loc}}(\mathbb{R}) \text{ and a.e.}; \quad F^n \to F \text{ in } \mathbf{L^1_{loc}}(\mathbb{R}^+) \text{ and a.e.}. \tag{4.20}$$

Combining (4.19) and (4.20) with the finite speed of propagation, we infer that the sequence $(u^n)_{n\in\mathbb{N}}$ is a Cauchy sequence in $\mathbf{L^1_{loc}}(\mathbb{R}^+ \times \mathbb{R})$. Further, notice that for all $(c_l, c_r) \in [0,1]^2$, for a.e. $t > 0$ we have

$$\operatorname{dist}\left((c_l, c_r),\, \mathcal{G}(F^n(t))\right) \longrightarrow \operatorname{dist}\left((c_l, c_r), \mathcal{G}(F(t))\right) \quad \text{as } n \to +\infty.$$

Indeed, this follows from the explicit description of $\mathcal{G}(F)$, from (4.20) and from the continuity of the map $F \mapsto (\hat{u}_F, \check{u}_F)$, which stems from the continuity of the two branches of f^{-1}:

$$f_-^{-1} : [0, f(\bar{u})] \longrightarrow [0, \bar{u}] \quad \text{and} \quad f_+^{-1} : [0, f(\bar{u})] \longrightarrow [\bar{u}, 1].$$

Passing to the limit in the "global" entropy formulation (4.10) written for u^n, we infer that the $\mathbf{L^1_{loc}}$ limit u of $(u^n)_{n\in\mathbb{N}}$ is an entropy solution of (4.1)-(4.3) associated with u_0 and F. □

4.5 Entropy process solutions

We now look at more general solutions, that are entropy process solutions. They are based on an $\mathbf{L}^\infty$ representation of Young measures via their distribution function (see

Eymard, Gallouët and Herbin [61]). Entropy process solutions are very useful since they are a natural tool to investigate the limit of numerical schemes for which enough compactness (we mean in particular **BV** bounds) cannot be proved. Besides, when the initial datum is a usual initial condition $u_0 \in \mathbf{L}^\infty(\mathbb{R})$, entropy process solutions coincide with entropy solutions; this is the reduction principle for entropy process solutions. The reduction principle guarantees the convergence (in the $\mathbf{L}^{\mathbf{p}}_{\mathbf{loc}}$ norm, for all $1 \leq p < \infty$) of the discrete solutions, obtained by numerical schemes, to the unique entropy solution.

Observe that it is difficult to generalize Definition 4.2.1 of entropy solutions, because the condition (4.8) requires the existence of strong one-sided traces $\gamma^{l,r}u$ of u on the interface $\{x = 0\}$. In the case of entropy process solutions, only weak traces of the mean entropy fluxes $\displaystyle\int_0^1 \Phi(\mu(\cdot,\alpha),\kappa)\, d\alpha$ are clearly available; fortunately the "traceless" Definition 4.2.2 can be adapted in a straightforward way.

Definition 4.5.1 *Let $u_0 \in \mathbf{L}^\infty(\mathbb{R},[0,1])$ and $F \in \mathbf{L}^\infty(\mathbb{R}^+,[0,f(\bar u)])$. Let $\mu \in \mathbf{L}^\infty(\mathbb{R}^+ \times \mathbb{R} \times (0,1);[0,1])$. Then μ is a $\mathcal{G}$-entropy process solution to* (4.1)-(4.3) *if there exists $M > 0$ such that for all test functions $\varphi \in \mathbf{C}^{\mathbf{1}}_{\mathbf{c}}(\mathbb{R}^+ \times \mathbb{R};\mathbb{R}^+)$ and all c defined by (4.9) with $(c_l,c_r) \in [0,1]^2$,*

$$\int_0^{+\infty}\int_{\mathbb{R}}\int_0^1 \left(|\mu(t,x,\alpha)-c(x)|\ \partial_t + \Phi(\mu(t,x,\alpha),c(x))\ \partial_x\right)\ \varphi(t,x)\ dx\ dt\ d\alpha$$
$$+\int_{\mathbb{R}} |u_0(x)-c(x)|\ \varphi(0,x)\ dx + M\int_0^{+\infty} \mathrm{dist}\left((c_l,c_r),\mathcal{G}(F(t))\right)\ \varphi(t,0)\ dt \geq 0. \quad (4.21)$$

It is not clear whether $\mathcal{G}$-entropy process solutions are "intrinsically" unique. Indeed, we lack an explicit description, of the kind (4.11), for the traces of $\mathcal{G}$-entropy process solutions. This prevents us from mimicking the proof of uniqueness of entropy solutions; as a matter of fact, we are unable to give a sign to the term coming from the comparison of two $\mathcal{G}$-entropy process solutions at the interface $\{x = 0\}$. However, *because we know the existence of an entropy solution*, we can compare a $\mathcal{G}$-entropy process solution with an entropy solution of (4.1)-(4.3), and thus deduce the uniqueness and the reduction principle for $\mathcal{G}$-entropy solutions:

Proposition 4.5.2 *Let $u_0 \in \mathbf{L}^\infty(\mathbb{R};[0,1])$ and $F \in \mathbf{L}^\infty(\mathbb{R}^+,[0,f(\bar u)])$. If u is the entropy solution to* (4.1)-(4.3) *and if μ is a $\mathcal{G}$-entropy process solution associated with the same initial datum u_0 and the same constraint F, then they coincide almost everywhere, i.e.,*

$$\mu(t,x,\alpha) = u(t,x) \quad \text{for a.e. } \alpha \in (0,1) \text{ and a.e.} (t,x) \in \mathbb{R}^+ \times \mathbb{R}. \quad (4.22)$$

Proof. We use the Kružkov doubling of variables method with test functions $\varphi \in \mathbf{C}^{\mathbf{1}}_{\mathbf{c}}(\mathbb{R}^+ \times \mathbb{R}\backslash\{x=0\};\mathbb{R}^+)$. We obtain

$$\int_0^1\int_{\mathbb{R}^+}\int_{\mathbb{R}\backslash\{0\}} \left(|\mu(t,x,\alpha)-u(t,x)|\ \partial_t + \Phi(\mu(t,x,\alpha),u(t,x))\ \partial_x\right)\ \varphi(t,x)\ dx\ dt\ d\alpha \geq 0.$$

Choosing φ as a sequence of approximations of the characteristic function of the set $\{t \in (0,T), 0 < |x| < R + L(T-t)\}$ with $R,\ T > 0$, from the previous inequality we deduce that

$$-\int_0^1 \int_{-R}^{R} |\mu(T,x,\alpha) - u(T,x)|\ dx\ d\alpha + \int_0^T \left(\gamma_w^r \left[\int_0^1 \Phi(\mu(\cdot,\alpha),u(\cdot))\ d\alpha\right]\right)(t)\ dt - \int_0^T \left(\gamma_w^l \left[\int_0^1 \Phi(\mu(\cdot,\alpha),u(\cdot))\ d\alpha\right]\right)(t)\ dt \geq 0. \quad (4.23)$$

The existence of the above weak traces follows from the previous inequality in the way of [34]. Moreover, the traces $\gamma^{l,r}u$ being strong, we have the identification

$$\gamma_w^{l,r}\left[\int_0^1 \Phi(\mu(\cdot,\alpha),u(\cdot))\ d\alpha\right] \equiv \gamma_w^{l,r}\left[\int_0^1 \Phi(\mu(\cdot,\alpha),\gamma^{l,r}u)\ d\alpha\right]. \quad (4.24)$$

Notice that $(\gamma^l u(t), \gamma^r u(t)) \in \mathcal{G}(F(t))$. Then we can use the fact that the weak traces of a $\mathcal{G}$-entropy process solution satisfy for a.e. $t > 0$ the inequalities

$$\gamma_w^l\left[\int_0^1 \Phi(\mu(\cdot,\alpha),c_l)\ d\alpha\right](t)\ \geq\ \gamma_w^r\left[\int_0^1 \Phi(\mu(\cdot,\alpha),c_r)\ d\alpha\right](t) \quad (4.25)$$

for all $(c_l,c_r) \in \mathcal{G}(F(t))$. The above property is stated and proved in [5, Proposition 3.1]. From (4.23), we then recover

$$\text{for all } R > 0 \text{ and for a.e. } T > 0 \quad \int_0^1 \int_{-R}^{R} |\mu(T,x,\alpha) - u(T,x)|\ dx\ d\alpha \leq 0.$$

□

4.6 Finite volume schemes

In this section, I describe the construction of a finite volume scheme to approximate (4.1)-(4.3), and analyze its convergence.

I start defining the mesh:

Definition 4.6.1 *An* admissible mesh $\mathcal{I}$ *of* $\mathbb{R}$ *is given by an increasing sequence of real values* $(x_{i+1/2})_{i\in\mathbb{Z}}$*, such that* $\mathbb{R} = \cup_{i\in\mathbb{Z}}[x_{i-1/2}, x_{i+1/2}]$ *and* $x_{1/2} = 0$*. The mesh* $\mathcal{I}$ *is the set* $\mathcal{I} = \{K_i, i \in \mathbb{Z}\}$ *of subsets of* $\mathbb{R}$ *defined by* $K_i = (x_{i-1/2}, x_{i+1/2})$ *for all* $i \in \mathbb{Z}$*. The length of* K_i *is denoted by* h_i *(the so-called* space step*), so that* $h_i = x_{i+1/2} - x_{i-1/2}$ *for all* $i \in \mathbb{Z}$*. We assume that* $h = size(\mathcal{I}) = \sup_{i\in\mathbb{Z}} h_i$ *is finite and that, for some* $\alpha \in \mathbb{R}_+^*$*,* $\alpha h \leq \inf_{i\in\mathbb{Z}} h_i$*.*

The finite volume approximation of the initial datum u_0 is

$$u_i^0 = \frac{1}{h_i}\int_{K_i} u_0(x)\ dx, \quad i \in \mathbb{Z}.$$

We aim at defining a sequence $(u_i^n)_{i\in\mathbb{Z},n\in\mathbb{N}}$ which approximates the solution u of (4.1)-(4.3) in the sense

$$u_i^n \approx \frac{1}{h_i}\int_{K_i} u(nk,x)\ dx, \quad i\in\mathbb{Z}, n>0,$$

where the *time step* k is a positive constant (which will be prone to a CFL condition in the sequel). The finite volume scheme which is presented in this section can be written under the form

$$u_i^{n+1} = u_i^n - \lambda_i(g(u_i^n, u_{i+1}^n, F_{i+1/2}^n) - g(u_{i-1}^n, u_i^n, F_{i-1/2}^n)) \tag{4.26}$$

where $\lambda_i = k/h_i$. The sequence $(F_{i+1/2}^n)_i$ is given by

$$F_{i+1/2}^n = \begin{cases} (1/k)\ \int_{nk}^{(n+1)k} F(s)\ ds & \text{if } i=0, \\ f(\bar{u}) & \text{if } i\neq 1. \end{cases} \tag{4.27}$$

Note that any approximation of F which strongly converges in $\mathbf{L^1_{loc}}$ can be chosen to define $F_{1/2}^n$.

The numerical flux g is defined by

$$g(u,v,f) = \min(h(u,v), f), \tag{4.28}$$

where h is a classical numerical flux, i.e. it obeys the three classical properties:

- Regularity: h is Lipschitz continuous, with L as Lipschitz constant.
- Consistency: $h(s,s) = f(s)$ for any $s\in[0,1]$.
- Monotonicity: h is nondecreasing with respect to (w.r.t.) its first argument and nonincreasing w.r.t. its second argument.

I will also employ the notation

$$u_i^{n+1} = \mathcal{G}_{\lambda_i}(u_{i-1}^n, u_i^n, u_{i+1}^n, F_{i-1/2}^n, F_{i+1/2}^n). \tag{4.29}$$

In the following sections, I give the results that we have obtained for this class of finite volume schemes.

4.6.1 *A priori* estimates and discrete entropy inequalities

The approximate solutions constructed by the numerical scheme (4.26)-(4.28) satisfy the following classical properties. (In the following, I adopt the notations: $a\perp b = \min(a,b)$ and $a\top b = \max(a,b)$.)

Lemma 4.6.2 ($\mathbf{L^\infty}$ estimates) *Assume that $u_0\in\mathbf{L}^\infty(\mathbb{R};[0,1])$. Then, under the CFL condition*

$$k \le \frac{\inf_i h_i}{2L}, \tag{4.30}$$

the functions $\mathcal{G}_{\lambda_i}$ are nondecreasing w.r.t. their three first arguments and the finite volume approximation (4.26) *satisfies*

$$0\le u_i^n \le 1, \quad \forall n\in\mathbb{N}, \forall i\in\mathbb{Z}. \tag{4.31}$$

Lemma 4.6.3 (Weak BV estimates) *Let $\xi \in (0,1)$ and $\mathcal{I}$ be an admissible mesh. Let $T > k$ and $R > h$ be two positive constants and denote I_0, I_1 and N the indices such that $-R \in \overline{K}_{I_0}$, $R \in \overline{K}_{I_1}$ and $T \in (Nk, (N+1)k]$. Then, if the time step k satisfies the CFL condition*

$$k \leq (1-\xi)\frac{\inf_{i\in\mathbb{Z}} h_i}{2L}, \tag{4.32}$$

there exists a positive constant C only depending on T, R, ξ, α, f and u_0 such that

$$\begin{aligned} k\sum_{n=0}^{N}\sum_{\substack{i=I_0\\ i\neq 0,1}}^{I_1} \Bigg(& \max_{(p,q)\in\ \mathbb{I}(u_i^n,u_{i+1}^n)} |h(p,q)-f(p)| \\ & + \max_{(p,q)\in\ \mathbb{I}(u_i^n,u_{i+1}^n)} |h(p,q)-f(q)| \Bigg) \leq C\ h^{-1/2}, \end{aligned} \tag{4.33}$$

where the set $\mathbb{I}(a,b)$ is defined as $\{(p,q) \in [a\perp b, a\top b], (q-p)(b-a) \geq 0\}$.

Lemma 4.6.4 (Discrete entropy inequalities) *Let $\kappa_i = c_l$ for $i \leq 0$ and $\kappa_i = c_r$ for $i > 0$, where $(c_l, c_r) \in [0,1]^2$. Then, the numerical scheme (4.26)-(4.28) fulfills the following inequalities:*

$$|u_i^{n+1} - \kappa_i| - |u_i^n - \kappa_i| + \lambda_i(G_{i+1/2}^n - G_{i-1/2}^n) - \lambda_i|H_i^n| \leq 0 \tag{4.34}$$

where

$$\begin{aligned} G_{i+1/2}^n &= g(u_i^n\top\kappa_i, u_{i+1}^n\top\kappa_{i+1}, F_{i+1/2}) - g(u_i^n\perp\kappa_i, u_{i+1}^n\perp\kappa_{i+1}, F_{i+1/2}), \\ H_i^n &= h(\kappa_i,\kappa_{i+1})\perp F_{i+1/2}^n - h(\kappa_{i-1},\kappa_i)\perp F_{i-1/2}^n, \end{aligned}$$

for all $n \in \mathbb{N}$ and $i \in \mathbb{Z}$.

The proofs of above lemmas are obtained as in the classical framework (see [61] for instance). The interested reader can find the details in [5]. Lemmas 4.6.2 and 4.6.3 will enable us to pass to the limit, using the nonlinear weak-$\star$ convergence (see Definition 4.6.5 below). The discrete entropy inequalities (4.34) will allow us to show that the limit is a $\mathcal{G}$-entropy process solution of (4.1-4.3).

4.6.2 Convergence

The convergence result is based on the notion of *nonlinear weak-$\star$ convergence*, defined in [61]:

Definition 4.6.5 *Let Ω be an open subset of $\mathbb{R}^N$, $N \geq 1$, $(u_m)_{m\in\mathbb{N}} \subset \mathbf{L}^\infty(\Omega)$ and $\mu \in \mathbf{L}^\infty(\Omega\times(0,1))$. The sequence $(u_m)_{m\in\mathbb{N}}$ converges to μ in the* nonlinear weak-$\star$ sense *if*

$$\int_\Omega \theta(u_m(y))\varphi(y)\ dy \xrightarrow[m\to\infty]{} \int_\Omega\int_0^1 \theta(\mu(y,\alpha))\varphi(y)\ dy\ d\alpha$$

for all $\varphi \in \mathbf{L^1}(\Omega)$ and all $\theta \in \mathbf{C}(\Omega)$.

This definition provides a useful interpretation of the convergence to Young's measures (as used by DiPerna in [58]). It enables to obtain the convergence of any sequence (up to a subsequence) just using a $\mathbf{L}^\infty(\Omega)$ bound:

Theorem 4.6.6 *Let Ω be an open subset of $\mathbb{R}^N$, $N \geq 1$. Consider a bounded sequence $(u_m)_{m\in\mathbb{N}}$ in $\mathbf{L}^\infty(\Omega)$. Then, one can extract a subsequence to $(u_m)_{m\in\mathbb{N}}$ which converges in the nonlinear weak-$\star$ sense.*

Moreover, the convergence is strong (in the $\mathbf{L}^\mathbf{1}_\mathbf{loc}(\Omega)$ sense) if and only if the nonlinear weak-$\star$ limit μ of $(u_m)_{m\in\mathbb{N}}$ is independent of α.

By Definition 4.6.5, in the situation of Theorem 4.6.6 the corresponding subsequence of $(\theta(u_m))_{m\in\mathbb{N}}$ converges weakly in $\mathbf{L}^\mathbf{1}_\mathbf{loc}(\Omega)$ to $\displaystyle\int_0^1 \theta(\mu(.,\alpha))\ d\alpha$, for all $\theta \in \mathbf{C}(\mathbb{R})$. In the sequel, I will not re-label the subsequences; the uniqueness of the entropy solution will ensure that all subsequences converge to the same limit, and the reduction of μ to an α-independent function will ensure that the convergence is strong.

Now, let me define the sequence of approximate solutions:

$$u_{\mathcal{I},k} = u_i^n \quad \text{for } x \in K_i \text{ and } t \in [nk,(n+1)k). \tag{4.35}$$

where $(u_i^n)_{i\in\mathbb{Z},n\in\mathbb{N}}$ is defined by the numerical scheme (4.26)-(4.28). Thanks to the *a priori* bounds and to the discrete entropy inequalities of Section 4.6.1, we can prove the following convergence result:

Proposition 4.6.7 *Let $\xi, \alpha \in (0,1)$. Consider a sequence of admissible meshes $\mathcal{I}_m$ and of time steps k_m satisfying the stability condition (4.30) for all $m \in \mathbb{N}$, such that size$(\mathcal{I}_m) \to 0$ as $m \to \infty$.*

Consider the sequence $(u_{\mathcal{I}_m,k_m})_{m\in\mathbb{N}}$, which is bounded in $\mathbf{L}^\infty(\mathbb{R}^+\times\mathbb{R})$. Then, there exists a subsequence, still noted $(u_{\mathcal{I}_m,k_m})_{m\in\mathbb{N}}$, and a function $\mu \in \mathbf{L}^\infty(\mathbb{R}^+\times\mathbb{R}\times(0,1))$ such that $(u_{\mathcal{I}_m,k_m})_m$ tends to μ in the nonlinear weak-$\star$ sense as $m \to +\infty$, and μ satisfies

$$\begin{aligned}\int_0^1\int_0^{+\infty}\int_{\mathbb{R}} \left(|\mu(t,x,\alpha)-c(x)|\ \partial_t + \Phi(\mu(t,x,\alpha),c(x))\partial_x\right)\ \varphi(t,x)\ dx\ dt\ d\alpha \\ + \int_{\mathbb{R}} |u_0(x)-c(x)|\ \varphi(0,x)\ dx \\ + 12L\int_0^{+\infty} \mathrm{dist}\left((c_l,c_r),\mathcal{G}_1(F(t))\cup\mathcal{G}_2(F(t))\right)\ \varphi(t,0)\ dt \geq 0, \end{aligned} \tag{4.36}$$

for all test functions $\varphi \in \mathbf{C}^\mathbf{1}_\mathbf{c}(\mathbb{R}^+\times\mathbb{R};\mathbb{R}^+)$ and all functions $c(x)$ given by (4.9) with $(c_l,c_r) \in [0,1]^2$.

Notice that the inequalities (4.36) seem weaker than the inequalities (4.21) in the definition of $\mathcal{G}$-entropy process solutions. In fact, it follows from Lemma 4.6.8 below that the two families of inequalities are equivalent.

Sketch of the proof. The convergence of the subsequence $(u_{\mathcal{I}_m,k_m})_m$ to μ follows by Lemma 4.6.2 and Theorem 4.6.6. We must now prove that μ satisfies (4.36).

Let $\varphi \in \mathbf{C_c^1}(\mathbb{R}^+ \times \mathbb{R}; \mathbb{R}^+)$ and two positive constants, T and R, be such that for all $t \geq T$ and $|x| \geq R$, $\varphi(t,x) = 0$ (we choose T and R sufficiently large w.r.t. h and k). Besides, let I_0, I_1 and N be the indices satisfying $-R \in \overline{K}_{I_0}$, $R \in \overline{K}_{I_1}$ and $T \in (Nk, (N+1)k]$.

We multiply the discrete entropy inequality (4.34) by $\int_{K_i} \varphi(nk,x)\ dx$ and sum for $n \in [0,N]$ and $i \in [I_0, I_1]$, which yields

$$A_h + B_h + C_h \leq 0, \tag{4.37}$$

where

$$\begin{aligned}
A_h &= \sum_{n=0}^{N} \sum_{i=I_0}^{I_1} (|u_i^{n+1} - \kappa_i| - |u_i^n - \kappa_i|) \int_{K_i} \varphi(nk,x)\ dx, \\
B_h &= \sum_{n=0}^{N} \sum_{i=I_0}^{I_1} \lambda_i (G_{i+1/2}^n - G_{i-1/2}^n) \int_{K_i} \varphi(nk,x)\ dx, \\
C_h &= -\sum_{n=0}^{N} \sum_{i=I_0}^{I_1} \lambda_i |H_i^n| \int_{K_i} \varphi(nk,x)\ dx.
\end{aligned}$$

We aim at passing to the limit $h \to 0$ in (4.37) and recover (4.36). The convergence of the terms A_h and B_h is achieved by standard procedures, as detailed in [5]. It gives:

$$\begin{aligned}
\lim_{h\to 0} A_h = &- \int_0^1 \int_0^\infty \int_{\mathbb{R}} |\mu(t,x,\alpha) - \kappa(x)| \partial_t \varphi\ dx\ dt\ d\alpha \\
&- \int_{\mathbb{R}} |u_0(x) - \kappa(x)| \varphi(0,x)\ dx,
\end{aligned} \tag{4.38}$$

and

$$\lim_{h\to 0} B_h = -\int_0^1 \int_0^\infty \int_{\mathbb{R}} \Phi(\mu(t,x,\alpha), \kappa(x)) \partial_x \varphi(t,x)\ dx\ dt\ d\alpha. \tag{4.39}$$

It remains to check that

$$\lim_{h\to 0} C_h = -12L \int_0^\infty \operatorname{dist}\left((c_l, c_r), \mathcal{G}_1(F(t)) \cup \mathcal{G}_2(F(t))\right)\ \varphi(t,0)\ dt. \tag{4.40}$$

By definition of H_i^n, we obtain

$$\begin{aligned}
C_h &= -\sum_{i=0}^{1} \frac{1}{h_i} \int_{K_i} \sum_{n=0}^{N} |H_i^n|\ k\ \varphi(nk,x)\ dx \\
&= -\frac{1}{h_0} \int_{K_0} \sum_{n=0}^{N} |h(c_l,c_r) \perp F^n - f(c_l)|\ k\ \varphi(nk,x)\ dx \\
&\quad - \frac{1}{h_1} \int_{K_1} \sum_{n=0}^{N} |f(c_r) - h(c_l,c_r) \perp F^n|\ k\ \varphi(nk,x)\ dx.
\end{aligned}$$

Since φ is smooth and F^n strongly converges to F, we obtain the limit

$$\lim_{h\to 0} C_h = -2\int_0^\infty D(c_l, c_r, F(t))\ \varphi(t,0)\ dt,$$

where

$$D(c_l, c_r, F) = |h(c_l, c_r)\perp F - f(c_l)| + |f(c_r) - h(c_l, c_r)\perp F|.$$

The function D is Lipschitz continuous with respect to c_l and c_r, with constant $6L$. Moreover, if $(c_l, c_r) \in \mathcal{G}_1(F) \cup \mathcal{G}_2(F)$, then $D(c_l, c_r, F) = 0$ (it is no longer true if $(c_l, c_r) \in \mathcal{G}_3(F)$, since a monotone scheme does not necessarily preserve stationary shock waves). Therefore

$$D(c_l, c_r, F) \le 6L \operatorname{dist}\left((c_l, c_r), \mathcal{G}_1(F) \cup \mathcal{G}_2(F)\right),$$

so that the limit verifies the entropy inequalities (4.36). □

It remains to prove that if inequalities (4.36) hold, then μ is a $\mathcal{G}$-entropy process solution. The proof of the equivalence between (4.21) and (4.36) is based on the following lemma.

Lemma 4.6.8 *Let $\eta \in \mathbf{L}^\infty(\mathbb{R}^+\times\mathbb{R}\times(0,1))$. Assume that the weak traces $\gamma_w^{l,r}\displaystyle\int_0^1 \Phi(\eta(\cdot,\alpha),\kappa)\ d\alpha$ exist. If for a.e. $t>0$, the inequality*

$$\left(\gamma_w^l \int_0^1 \Phi(\eta(\cdot,\alpha), c_l)\ d\alpha\right)(t) \ge \left(\gamma_w^r \int_0^1 \Phi(\eta(\cdot,\alpha), c_r)\ d\alpha\right)(t) \tag{4.41}$$

holds for all $(c_l, c_r) \in \mathcal{G}_1(F(t)) \cup \mathcal{G}_2(F(t))$, then it also holds for all $(c_l, c_r) \in \mathcal{G}_3(F(t))$.

Proof. Let $(c_l, c_r) \in \mathcal{G}_3$. Then,

$$\begin{aligned}
&\gamma_w^l \int_0^1 \Phi(\eta(t,\cdot,\alpha), c_l)\ d\alpha - \gamma_w^r \int_0^1 \Phi(\eta(t,\cdot,\alpha), c_r)\ d\alpha \\
&\quad = \gamma_w^l \int_0^1 \Phi(\eta(t,\cdot,\alpha), c_l)\ d\alpha - \gamma_w^l \int_0^1 \Phi(\eta(t,\cdot,\alpha), c_r)\ d\alpha \\
&\qquad + \gamma_w^l \int_0^1 \Phi(\eta(t,\cdot,\alpha), c_r)\ d\alpha - \gamma_w^r \int_0^1 \Phi(\eta(t,\cdot,\alpha), c_r)\ d\alpha \\
&\quad = \gamma_w^l \int_0^1 \left(\Phi(\eta(t,\cdot,\alpha), c_l) - \Phi(\eta(t,\cdot,\alpha), c_r)\right)\ d\alpha \\
&\qquad + \gamma_w^l \int_0^1 \Phi(\eta(t,\cdot,\alpha), c_r)\ d\alpha - \gamma_w^r \int_0^1 \Phi(\eta(t,\cdot,\alpha), c_r)\ d\alpha.
\end{aligned}$$

The first term in the right-hand side is nonnegative; indeed, the function $\tilde{u}(t,x) := c_l \mathbb{1}_{\{x<0\}} + c_r \mathbb{1}_{\{x>0\}}$ is a classical Kružkov stationary solution of (4.1), whereas $k = \eta(t,x,\alpha)$ can be seen as the constant in the Kružkov definition. The last line in the above inequality is nonnegative thanks to (4.41), because $(c_r, c_r) \in \mathcal{G}_2(F(t))$. □

Finally from Proposition 4.5.2, we obtain the final result:

Theorem 4.6.9 *Under the CFL condition* (4.30)*, the finite volume scheme* (4.26)-(4.28) *converges in* $\mathbf{L}^{\mathbf{p}}_{\mathbf{loc}}(\mathbb{R}^+ \times \mathbb{R})$ *for any* $1 \leq p < +\infty$ *to the unique entropy solution of* (4.1)-(4.3)*.*

4.6.3 Numerical results

I conclude this section by presenting some numerical experiments performed with the numerical scheme (4.26)-(4.28), using the Rusanov numerical flux [93]:

$$h(u,v) = \frac{f(u)+f(v)}{2} - \frac{\max(|f'(u)|,|f'(v)|)}{2}(v-u).$$

This numerical flux is consistent and monotone. The flux of the conservation law is given by $f(u) = u(1-u)$, so that the constraint $F(t)$ must belong to $[0, 1/4]$.

I report here a simple test case, corresponding to the simulation of the solution to a Riemann problem. Other studies are presented in [5].

The domain of computation is $[-1/2, 1/2]$ and the data are

$$u_0(x) = \begin{cases} 0.4 & \text{if } x < 0, \\ 0.5 & \text{if } x > 0, \end{cases} \quad \text{and} \quad F = 0.2\ .$$

The exact solution is composed of a classical shock wave with a negative speed, of a non-classical stationary shock wave at $x = 0$ satisfying the constraint, and of another classical shock wave with a positive speed. Fig. 4.2 shows the comparison between

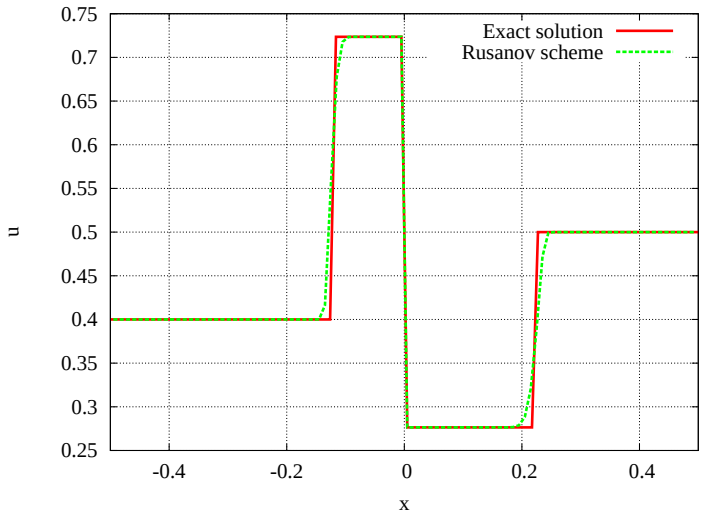

Figure 4.2: Comparison between the Rusanov scheme (100 cells, CFL=0.4) and the exact solution at time $t = 1$.

the numerical results provided by the "constrained" Rusanov scheme and the exact solution. The non-classical shock wave seems to be perfectly solved. An analysis of the convergence of the numerical scheme has been performed, as reported in Table 4.1:

Number of cells	$\mathbf{L^1}$-error	Rate of conv.
100	4.1938×10^{-3}	—
300	1.2356×10^{-3}	1.112
1000	3.7494×10^{-4}	0.990
3000	1.1864×10^{-4}	1.047
10000	3.6899×10^{-5}	0.970
30000	1.2945×10^{-5}	0.953
100000	3.6448×10^{-6}	1.053
300000	1.2199×10^{-6}	0.996

Table 4.1: Convergence analysis for Rusanov scheme.

Fig. 4.3 depicts the error with respect to the space step. We can easily see that the rate of convergence is 1, that is to say that the constraint does not affect the accuracy of the numerical scheme.

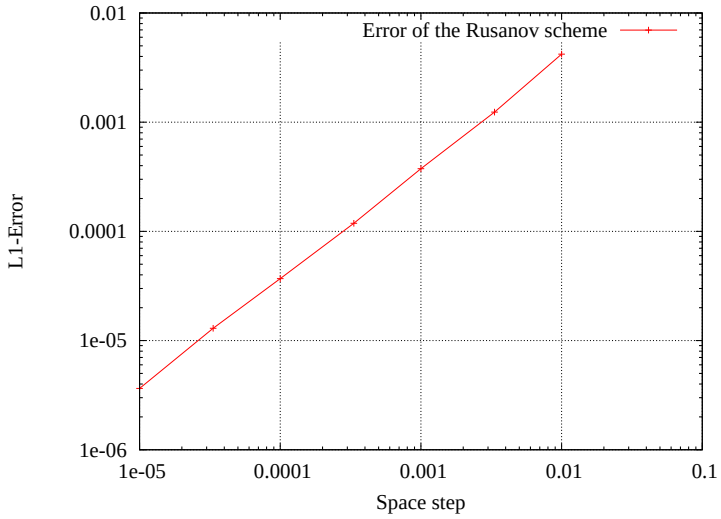

Figure 4.3: Convergence of the Rusanov scheme in the $\mathbf{L^1}$ norm.

Bibliography

[1] R. Abgrall. How to prevent pressure oscillations in multicomponent flow calculations: a quasi-conservative approach. *J. Comput. Phys.*, 125:150–160, 1996.

[2] R. Abgrall and S. Karni. Computations of compressible multifluids. *J. Comput. Phys.*, 169:594–623, 2001.

[3] Adimurthi, S. Mishra, and G. D. V. Gowda. Optimal entropy solutions for conservation laws with discontinuous flux-functions. *J. Hyperbolic Differ. Equ.*, 2(4):783–837, 2005.

[4] D. Amadori and R. M. Colombo. Continuous dependence for 2×2 conservation laws with boundary. *J. Differential Equations*, 138(2):229–266, 1997.

[5] B. Andreianov, P. Goatin, and N. Seguin. Finite volume schemes for locally constrained conservation laws. Preprint, 2009. Available at: `http://www.math.ntnu.no/conservation/2009/010.html`

[6] E. Audusse and B. Perthame. Uniqueness for scalar conservation laws with discontinuous flux via adapted entropies. *Proc. Roy. Soc. Edinburgh Sect. A*, 135(2):253–265, 2005.

[7] A. Aw, A. Klar, T. Materne, and M. Rascle. Derivation of continuum traffic flow models from microscopic follow-the-leader models. *SIAM J. Appl. Math.*, 63:259–278, 2002.

[8] A. Aw and M. Rascle. Resurrection of "second order" models of traffic flow. *SIAM J. Appl. Math.*, 60:916–938, 2000.

[9] P. Bagnerini, R. M. Colombo, and A. Corli. On the role of source terms in continuum traffic flow models. *Math. Comput. Modeling*, 44(9-10):917–930, 2006.

[10] P. Baiti and H. K. Jenssen. Well-posedness for a class of 2×2 conservation laws with L^∞ data. *J. Differential Equations*, 140(1):161–185, 1997.

[11] M. K. Banda, M. Herty, and A. Klar. Gas flow in pipeline networks. *Netw. Heterog. Media*, 1(1):41–56 (electronic), 2006.

[12] T. Barberon, P. Helluy, and S. Rouy. Practical computation of axisymmetrical multifluid flows. *International Journal of Finite Volumes*, 1:1–34, 2003. (electronic).

[13] G. Bastin and B. Haut. A second order model of road junctions in fluid models of traffic networks. *Netw. Heterog. Media*, 2(2):227–253 (electronic), 2007.

[14] A. M. Bayen, D. Sun, and I. S. Strub. Comparison of the performance of four Eulerian network flow models for strategic air traffic management. *Netw. Heterog. Media*, 2(4):569–595 (electronic), 2007.

[15] N. Bellomo, V. Coscia, and M. Delitala. On the mathematical theory of vehicular traffic flow I - fluid dynamic and kinetic modelling. *Math. Mod. Meth. Appl. Sci.*, 12:1801–1844, 2002.

[16] F. Berthelin and F. Bouchut. Weak solutions for a hyperbolic system with unilateral constraint and mass loss. *Ann. Inst. H. Poincaré Anal. Non Linéaire*, 20(6):975–997, 2003.

[17] C. Berthon. Why the MUSCL-Hancock scheme is L^1-stable. *Numer. Math.*, 104(1):27–46, 2006.

[18] S. Bianchini. The semigroup generated by a Temple class system with non-convex flux function. *Differential Integral Equations*, 13(10-12):1529–1550, 2000.

[19] S. Blandin, D. Work, P. Goatin, B. Piccoli, and A. Bayen. A general phase transition model for vehicular traffic. Preprint, 2009.

[20] A. Bressan. Global solutions of systems of conservation laws by wave-front tracking. *J. Math. Anal. Appl.*, 170(2):414–432, 1992.

[21] A. Bressan. The unique limit of the Glimm scheme. *Arch. Rational Mech. Anal.*, 130(3):205–230, 1995.

[22] A. Bressan. *Hyperbolic Systems of Conservation Laws*. Oxford University Press, 2000.

[23] A. Bressan and R. M. Colombo. The semigroup generated by 2×2 conservation laws. *Arch. Rational Mech. Anal.*, 133(1):1–75, 1995.

[24] A. Bressan, G. Crasta, and B. Piccoli. Well-posedness of the Cauchy problem for $n \times n$ systems of conservation laws. *Mem. Amer. Math. Soc.*, 146(694):viii+134, 2000.

[25] A. Bressan and P. Goatin. Stability of L^∞ solutions of Temple class systems. *Differential Integral Equations*, 13(10-12):1503–1528, 2000.

[26] R. Bürger, A. García, K. H. Karlsen, and J. D. Towers. A family of numerical schemes for kinematic flows with discontinuous flux. *J. Engrg. Math.*, 60(3-4):387–425, 2008.

[27] R. Bürger, K. H. Karlsen, and J. D. Towers. An Engquist-Oscher-type scheme for conservation laws with discontinuous flux adapted to flux connections. *SIAM J. Numer. Anal.* To appear.

[28] C. Chalons. Transport-equilibrium schemes for computing nonclassical shocks.Scalar conservation laws. To appear in Numer. Methods PDEs.

[29] C. Chalons. Numerical approximation of a macroscopic model of pedestrian flows. *SIAM J. Sci. Comput.*, 29:539–555, 2007.

[30] C. Chalons and F. Coquel. Capturing infinitely sharp discrete shock profiles with the godunov scheme. *Proceedings of the Eleventh International Conference on Hyperbolic Problems. Theory, Numerics, Applications*, 2007.

[31] C. Chalons and P. Goatin. Transport-equilibrium schemes for computing contact discontinuities in traffic flow modeling. *Commun. Math. Sci.*, 5(3):533–551, 2007.

[32] C. Chalons and P. Goatin. Godunov scheme and sampling technique for computing phase transitions in traffic flow modeling. *Interfaces and Free Boundaries*, 10(2):195–219, 2008.

[33] C. Chalons and P. G. LeFloch. Computing undercompressive waves with the random choice scheme. nonclassical shock waves. *Interfaces and Free Boundaries*, 5:129–158, 2003.

[34] G.-Q. Chen and H. Frid. Divergence-measure fields and hyperbolic conservation laws. *Arch. Ration. Mech. Anal.*, 147(2):89–118, 1999.

[35] Y. Chitour and B. Piccoli. Traffic circles and timing of traffic lights for cars flow. *Discrete Contin. Dyn. Syst. Ser. B*, 5(3):599–630, 2005.

[36] G. M. Coclite, M. Garavello, and B. Piccoli. Traffic flow on a road network. *SIAM J. Math. Anal.*, 36(6):1862–1886 (electronic), 2005.

[37] G. M. Coclite and N. H. Risebro. Conservation laws with time dependent discontinuous coefficients. *SIAM J. Math. Anal.*, 36(4):1293–1309 (electronic), 2005.

[38] P. Collela. Glimm's method for gas dynamics. *SIAM J. Sci. Stat. Comput.*, 3(2):76–110, 1982.

[39] R. M. Colombo. A 2×2 hyperbolic traffic flow model. *Math. Comput. Modeling*, 35(5-6):683–688, 2002. Traffic flow—modeling and simulation.

[40] R. M. Colombo. Hyperbolic phase transitions in traffic flow. *SIAM J. Appl. Math.*, 63(2):708–721, 2002.

[41] R. M. Colombo and A. Corli. Continuous dependence in conservation laws with phase transitions. *SIAM Journal Math. Anal.*, 31(1):34–62, 1999.

[42] R. M. Colombo and A. Corli. Sonic hyperbolic phase transitions and Chapman-Jouguet detonations. *J. Differential Equations*, 184(2):321–347, 2002.

[43] R. M. Colombo and A. Corli. On a class of hyperbolic balance laws. *J. Hyperbolic Differ. Equ.*, 1(4):725–745, 2004.

[44] R. M. Colombo and M. Garavello. A well posed Riemann problem for the p-system at a junction. *Netw. Heterog. Media*, 1(3):495–511 (electronic), 2006.

[45] R. M. Colombo and M. Garavello. On the Cauchy problem for the p-system at a junction. *SIAM J. Math. Anal.*, 39(5):1456–1471, 2008.

[46] R. M. Colombo and P. Goatin. A well posed conservation law with a variable unilateral constraint. *J. Differential Equations*, 234(234):654–675, 2007.

[47] R. M. Colombo, P. Goatin, and B. Piccoli. Road networks with phase transitions. Preprint, 2009. Available at: `http://www.dmf.unicatt.it/cgi-bin/preprintserv/semmat/Quad2009n08`

[48] R. M. Colombo, P. Goatin, and F. S. Priuli. Global well posedness of a traffic flow model with phase transitions. *Nonlinear Anal. Ser. A*, 66:2413–2426, 2007.

[49] R. M. Colombo, P. Goatin, and M. D. Rosini. Conservation laws with unilateral constraints in traffic modeling. *Communications to SIMAI Congress*, 3, 2009. To appear.

[50] R. M. Colombo and A. Groli. Minimising stop and go waves to optimise traffic flow. *Appl. Math. Lett.*, 17(6):697–701, 2004.

[51] R. M. Colombo and F. S. Priuli. Characterization of Riemann solvers for the two phase p-system. *Comm. Partial Differential Equations*, 28(7-8):1371–1390, 2003.

[52] C. M. Dafermos. Polygonal approximations of solutions of the initial value problem for a conservation law. *J. Math. Anal. Appl.*, 38:33–41, 1972.

[53] C. M. Dafermos. *Hyperbolic conservation laws in continuum physics*. Springer-Verlag, New York, first edition, 2000.

[54] C. F. Daganzo. Requiem for high-order fluid approximations of traffic flow. *Trans. Res.*, 29B(4):277–287, August 1995.

[55] C. D'Apice and R. Manzo. A fluid dynamic model for supply chains. *Netw. Heterog. Media*, 1(3):379–398 (electronic), 2006.

[56] C. D'apice, R. Manzo, and B. Piccoli. Packet flow on telecommunication networks. *SIAM J. Math. Anal.*, 38(3):717–740 (electronic), 2006.

[57] R. J. DiPerna. Global existence of solutions to nonlinear hyperbolic systems of conservation laws. *J. Differential Equations*, 20(1):187–212, 1976.

[58] R. J. DiPerna. Measure-valued solutions to conservation laws. *Arch. Rational Mech. Anal.*, 88(3):223–270, 1985.

[59] J. S. Drake, J. L. Schofer, and A. D. May. A statistical analysis of speed density hypotheses. *Highway Research Record*, 154:53–87, 1967.

[60] L. C. Edie. Car-following and steady-state theory for noncongested traffic. *Operations Research*, 9:66–76, 1961.

[61] R. Eymard, T. Gallouët, and R. Herbin. Finite volume methods. In *Handbook of numerical analysis, Vol. VII*, Handb. Numer. Anal., VII, pages 713–1020. North-Holland, Amsterdam, 2000.

[62] R. P. Fedkiw, T. Aslam, B. Merriman, and S. Osher. A non-oscillatory eulerian approach to interfaces in multimaterial flows (the ghost fluid method). *J. Comput. Phys.*, 152:457–492, 1999.

[63] M. Garavello, R. Natalini, B. Piccoli, and A. Terracina. Conservation laws with discontinuous flux. *Netw. Heterog. Media*, 2(1):159–179 (electronic), 2007.

[64] M. Garavello and B. Piccoli. Source-destination flow on a road network. *Commun. Math. Sci.*, 3(3):261–283, 2005.

[65] M. Garavello and B. Piccoli. Traffic flow on a road network using the Aw-Rascle model. *Comm. Partial Differential Equations*, 31(1-3):243–275, 2006.

[66] M. Garavello and B. Piccoli. *Traffic flow on networks*, volume 1 of *AIMS Series on Applied Mathematics*. American Institute of Mathematical Sciences (AIMS), Springfield, MO, 2006. Conservation laws models.

[67] M. Garavello and B. Piccoli. Conservation laws on complex networks. Preprint, 2008.

[68] P. Goatin. The Aw-Rascle traffic flow model with phase transition. *Math. Comput. Modeling*, 44:287–303, 2006.

[69] E. Godlewski and P.-A. Raviart. *Hyperbolic systems of conservation laws*, volume 3/4 of *Mathématiques & Applications (Paris) [Mathematics and Applications]*. Ellipses, Paris, 1991.

[70] S. Göttlich, M. Herty, and A. Klar. Network models for supply chains. *Commun. Math. Sci.*, 3(4):545–559, 2005.

[71] D. Helbing. Traffic and related self-driven many-particle systems. *Rev. Mod. Phys.*, 73:1067–1141, 2001.

[72] D. Helbing, J. Siegmeier, and S. Lämmer. Self-organized network flows. *Netw. Heterog. Media*, 2(2):193–210 (electronic), 2007.

[73] M. Herty, S. Moutari, and M. Rascle. Optimization criteria for modelling intersections of vehicular traffic flow. *Netw. Heterog. Media*, 1(2):275–294 (electronic), 2006.

[74] H. Holden and N. H. Risebro. A mathematical model of traffic flow on a network of unidirectional roads. *SIAM J. Math. Anal.*, 26(4):999–1017, 1995.

[75] H. Holden and N. H. Risebro. *Front tracking for hyperbolic conservation laws*, volume 152 of *Applied Mathematical Sciences*. Springer-Verlag, New York, 2002.

[76] K. H. Karlsen, N. H. Risebro, and J. D. Towers. L^1 stability for entropy solutions of nonlinear degenerate parabolic convection-diffusion equations with discontinuous coefficients. *Skr. K. Nor. Vidensk. Selsk.*, (3):1–49, 2003.

[77] K. H. Karlsen and J. D. Towers. Convergence of the Lax-Friedrichs scheme and stability for conservation laws with a discontinous space-time dependent flux. *Chinese Ann. Math. Ser. B*, 25(3):287–318, 2004.

[78] S. Karni. Multicomponent flow calculations by a consistent primitive algorithm. *J. Comput. Phys.*, 112(1):31–43, 1994.

[79] S. Karni. Hybrid multifluid algorithms. *SIAM J. Sci. Comput.*, 17:1019–1039, 1996.

[80] B. Kerner. *The physics of traffic*. Springer-Verlag, 2004.

[81] B. S. Kerner. Phase transitions in traffic flow. In D. Helbing, H. Hermann, M. Schreckenberg, and D. Wolf, editors, *Traffic and Granular Flow '99*, pages 253–283. Springer Verlag, 2000.

[82] S. N. Kružkov. First order quasilinear equations with several independent variables. *Mat. Sb. (N.S.)*, 81 (123):228–255, 1970.

[83] P. D. Lax. Hyperbolic systems of conservation laws. II. *Comm. Pure Appl. Math.*, 10:537–566, 1957.

[84] P. G. LeFloch and M. D. Thanh. Nonclassical Riemann solvers and kinetic relations. I. A nonconvex hyperbolic model of phase transitions. *Z. Angew. Math. Phys.*, 52(4):597–619, 2001.

[85] P. G. LeFloch and M. D. Thanh. Non-classical Riemann solvers and kinetic relations. II. An hyperbolic-elliptic model of phase-transition dynamics. *Proc. Roy. Soc. Edinburgh Sect. A*, 132(1):181–219, 2002.

[86] M. J. Lighthill and G. B. Whitham. On kinematic waves. II. A theory of traffic flow on long crowded roads. *Proc. Roy. Soc. London. Ser. A.*, 229:317–345, 1955.

[87] T. P. Liu. The Riemann problem for general systems of conservation laws. *J. Differential Equations*, 18:218–234, 1975.

[88] G. F. Newell. A simpified car-following theory: a lower order model. *Transport. Res. B*, 36(3):195–205, 2002.

[89] G. F. Panov. Existence of strong traces for quesi-solutions of multidimensional conservation laws. *J. Hyperbolic Differ. Equ.*, 4(4):729–770, 2007.

[90] H. J. Payne. Models of freeway traffic and control. In *Simulation Council Proc.28*, pages 51–61. Math. Models Publ. Sys., 1971.

[91] P. I. Richards. Shock waves on the highway. *Operations Res.*, 4:42–51, 1956.

[92] N. H. Risebro. A front-tracking alternative to the random choice method. *Proc. Amer. Math. Soc.*, 117(4):1125–1139, 1993.

[93] V. V. Rusanov. The calculation of the interaction of non-stationary shock waves with barriers. *Ž. Vyčisl. Mat. i Mat. Fiz.*, 1:267–279, 1961.

[94] R. Saurel and R. Abgrall. A simple method for compressible multifluid flows. *SIAM J. Sci. Comput.*, 21:1115–1145, 1999.

[95] B. Temple. Global solution of the Cauchy problem for a class of 2×2 nonstrictly hyperbolic conservation laws. *Adv. in Appl. Math.*, 3(3):335–375, 1982.

[96] B. Temple. Systems of conservation laws with coinciding shock and rarefaction curves. *Contemp. Math.*, 17:143–151, 1983.

[97] E. F. Toro. *Riemann solvers and numerical methods for fluid dynamics*. Springer-Verlag, Berlin, second edition, 1999. A practical introduction.

[98] J. D. Towers. Convergence of a difference scheme for conservation laws with a discontinuous flux. *SIAM J. Numer. Anal.*, 38(2):681–698 (electronic), 2000.

[99] B. van Leer. Towards the ultimate conservative difference scheme. V. A second-order sequel to Godunov's method. *J. Computational Phys.*, 32, 1979.

[100] A. Vasseur. Strong traces for solutions of multidimensional scalar conservation laws. *Arch. Ration. Mech. Anal.*, 160(3):181–193, 2001.

[101] G. B. Whitham. *Linear and Nonlinear Waves*. John Wiley and Sons, New York, 1999.

[102] H. M. Zhang and T. Kim. A car-following theory for multiphase vehicular traffic flow. *Transport. Res. B*, 39(5):385–399, 2005.

[103] X. Zhong, T. Y. Hou, and P. G. LeFloch. Computational methods for propagating phase boundaries. *J. Comput. Phys.*, 124:192–216, 1996.